LEVEL II

5

ANNUAL TECHNICAL REPORT

NO.2

1 OCTOBER 1980 TO 30 SEPTEMBER 1981

THE USE OF INTERMEDIATE AND LONG PERIOD SEISMIC WAVES FOR DISCRIMINATION AND YIELD DETERMINATION

1 NOVEMBER 1981

RONDOUT ASSOCIATES INCORPORATED
P.O. BOX 224
STONE RIDGE, NEW YORK 12484

Sponsored by
Advanced Research Projects Agency (DOD)
ARPA Order No. 3291-01
Monitored by AFOSR under Contract #F49620-80-C-0021

Unclassified

SECURITY CLASSIFICATION OF THIS PAGE (When Data Entered)

REPORT DOCUMENTATION PAGE

READ INSTRUCTIONS BEFORE COMPLETING FORM

1. REPORT NUMBER: AFOSR-TR- 81-0871
2. GOVT ACCESSION NO.: AD-A101847
3. RECIPIENT'S CATALOG NUMBER:

4. TITLE (and Subtitle): THE USE OF INTERMEDIATE AND LONG PERIOD SIESMIC WAVES FOR DISCRIMINATION AND YIELD DETERMINATION
5. TYPE OF REPORT & PERIOD COVERED: Annual Technical 1 Oct. 1980-30 Sept. 1981
6. PERFORMING ORG. REPORT NUMBER: 05-80-01

7. AUTHOR(s): Dr. Paul W. Pomeroy
8. CONTRACT OR GRANT NUMBER(s): F49620-80-C-0021

9. PERFORMING ORGANIZATION NAME AND ADDRESS: Rondout Associates, Incorporated, P.O. Box 224, Stone Ridge, New York 12484
10. PROGRAM ELEMENT, PROJECT, TASK AREA & WORK UNIT NUMBERS: 61102F, 2301/A9

11. CONTROLLING OFFICE NAME AND ADDRESS: Air Force Office of Scientific Research/NP, Building 410, Bolling Air Force Base, D.C. 20332
12. REPORT DATE: 1 November 1981
13. NUMBER OF PAGES: 106

14. MONITORING AGENCY NAME & ADDRESS (if different from Controlling Office):
15. SECURITY CLASS. (of this report): Unclassified
15a. DECLASSIFICATION/DOWNGRADING SCHEDULE:

16. DISTRIBUTION STATEMENT (of this Report)

Approved for public release; distribution unlimited.

17. DISTRIBUTION STATEMENT (of the abstract entered in Block 20, if different from Report)

18. SUPPLEMENTARY NOTES

19. KEY WORDS (Continue on reverse side if necessary and identify by block number)

Lg waves
Catskill Seismic Array
yield determination
HARZER
seismic noise characteristics
array calibration

20. ABSTRACT (Continue on reverse side if necessary and identify by block number)

This report, which is presented in four parts, deals with the following subjects:

(1) The use of Lg to determine yield for U.S. explosions as recorded by WWSSN stations in the United States;

(2) Analyses of seismic data from the HARZER nuclear explosion as recorded at the Catskill Seismic Array (CSA) in Stone Ridge, New York; (over)

DD FORM 1 JAN 73 1473 A

Unclassified

SECURITY CLASSIFICATION OF THIS PAGE (When Data Entered)

(cont'd)

(3) Seismic noise characteristics at the Catskill Seismic Array, and (CSA; and

(4) The calibration and response of the Catskill Seismic Array.

CSA,

Table of Contents

Introduction

This report deals with research carried out under Contract F49620-80-C-0021 between the Air Force Office of Scientific Research and Rondout Associates Incorporated. The title of this research program is "The Use of Intermediate and Long Period Seismic Waves for Discrimination and Yield Determination". The work statement of the contract is as follows:

Task I - Regional Seismic Wave Propagation

1. Investigate the presence-absence, frequency content and attenuation of regional seismic phases in the USSR and adjacent areas as a function of geographic location.
2. Investigate the three dimensional motion of Lg. Obtain Lg(T) to study high frequency higher mode Love wave content.
3. Investigate and evaluate the use of Lg(Z) as a depth discriminant through velocity filtering and frequency filtering. Evaluate the use of Lg/P amplitude ratios as a discriminant.

Task II - Operate and maintain the tri-partite broad band digital array being installed in the Stone Ridge, New York area under a cooperative program with the University of Nevada and use that data in the regional wave propagation investigations of Task I.

Task III - The Use of Long Period Seismic Waves for Yield Determination and Discrimination.

1. Evaluate the propagation characteristics of fundamental and higher mode surface waves on continental paths in the 2-12 second period range from underground explosion and earthquake sources and determine the discrimination capability of surface waves in this period range.
2. Using the full spectrum of Love and Rayleigh waves recorded from explosions of known yield, determine the relationships between the yield and both single period measurements and amplitude spectra.

This report is divided in four sections:

1. The use of Lg to determine yield for U.S. explosions as recorded by WWSSN stations in the United States. Task I.
2. Analyses of seismic data from the HARZER nuclear explosion as recorded at the Catskill Seismic Array (CSA) in Stone Ridge, New York. Task I and II.

3. Noise characteristics at the CSA. Task II.
4. Calibration and response of the CSA. Task II.

Work currently in progress on Task III will be reported in the following technical reports. The principal conclusions of each section are contained in the section executive summaries.

SECTION 1
THE USE OF Lg TO DETERMINE YIELD FOR U.S. EXPLOSIONS AS RECORDED BY WWSSN STATIONS IN THE UNITED STATES

Introduction

This study deals with the usefulness of Lg(Z, L or T) in evaluating yield from explosions detonated at the Nevada Test Site. The issues in this study are:

1. To evaluate the effect of tectonic strain release on Lg amplitudes for NTS events as recorded at U.S. WWSSN stations.
2. To establish amplitude-yield relationships for Lg(Z), Lg(L), and Lg(T).
3. To evaluate usefulness of Lg(Z) and/or Lg(T) as a measure of yield.
4. To study Lg attenuation characteristics.

To carry out this baseline study, Lg(Z, L and T) amplitudes from twelve (12) underground nuclear explosions are examined as recorded by most of the three component short period instruments of the WWSSN within the United States. The long period surface waves of these twelve explosions seem to have been contaminated to different degrees by tectonic strain release. Thus, by examining the recorded wave amplitudes, the issues outlined above may be resolved.

The resultant amplitude-yield curves were then used to evaluate the yields of three test events: SALMON, GASBUGGY and PILEDRIVER, all non-NTS (but continental U.S.) events.

Data

Source

The pertinent source data on the twelve (12) explosions utilized in this baseline study are listed in Table 1-1. Data on the test events is given in Table 1-2.

The nuclear explosions used in the baseline study were selected from the event set examined by Aki and Tsai (1972) in a paper entitled, "Mechanism of Love-wave excitation by explosive sources". In that paper, Aki and Tsai examined the amplitude ratios of long period ($T \gtrsim 10$ sec) Love waves to Rayleigh waves from 18 underground nuclear explosions at Yucca Flat on the Nevada Test Site. Finding variations among the amplitude ratios of the explosion ; they divided the explosions into three groups according to the different ratios: the strong-, intermediate-, and weak- exciters of Love waves. They also found a correlation between the efficiency of Love-wave excitation and the magnitude and/or the burial depth of the detonation. (Due to the strong correlation between source depth and source size, they were unable to separate the two effects.)

TABLE 1-1

DATA ON

U.S. NUCLEAR EVENTS

UTILIZED IN THIS STUDY

	NAME	DATE	ORIGIN TIME	DEPTH (M)	ANNOUNCED YIELD	LONG PERIOD LOVE WAVE EXCITATION
1.	CORDUROY	3 DEC. 1965	15:13:02	208	100	STRONG
2.	CUP	26 MAR. 1965	15:34:08	164	35	STRONG
3.	COMMODORE	20 MAY 1967	15:00:00	227	230	STRONG
4.	DUMONT	19 MAY 1966	13:56:28	205	190	STRONG
5.	BOURBON	20 JAN. 1967	17:40:03	171	29	INTERMEDIATE
6.	BUFF	16 DEC. 1965	19:15:00	152	36	INTERMEDIATE
7.	FORE	16 JAN. 1964	16:00:00	151	19	INTERMEDIATE
8.	TAN	3 JUNE 1966	14:00:00	171	140	INTERMEDIATE
9.	WAGTAIL	3 MAR. 1965	19:13:00	229	65	INTERMEDIATE
10.	AUK	2 OCT. 1964	20:03:00	138	12	WEAK
11.	CHARCOAL	10 SEPT.1965	17:12:00	139	20	WEAK
12.	PIRAHNA	13 MAY 1965	13:30:00	167	100	WEAK

TABLE 1-2

TEST EVENTS

	SALMON	GASBUGGY	PILEDRIVER
DATE	22 OCT. 1964	10 DEC. 1967	2 JUNE 1966
ORIGIN TIME	16:00:00 Z	19:30:00 Z	15:30:00 Z
LOCATION	NEAR HATTIESBURG, MISS.	DULCE, NM	CLIMAX NTS
BURIAL MEDIUM	SALT	SHALE	GRANITE
ANNOUNCED YIELD	5.3	29	56
SEISMIC YIELD FROM L_g (NUMBER OF POINTS)	5.0 ± 4.4 (11)	22.4 ± 17.8 (27)	61.5 ± 38.0 (32)

Thus, by using the body-wave magnitude of the event as the dependent variable, they were able to test whether the condition of different test sites affects the level of Love-wave excitation. The site conditions considered were: the depth of the water-table and alluvium-tuff interface and the distance between the shot point and the more competent basement rocks. The only satisfactory separation of these different groups is suggested by a plot of m_b of the event vs. testing date, about which Aki and Tsai state, "a magnitude threshold (or depth threshold, since we cannot separate the two factors) may exist for strong excitation of Love waves, and the threshold apparently increased with time during the periods 1962 to 1969". Based on this observation and other arguments, they came to the conclusion that a model of tectonic strain release following a trigger explosion offered the most satisfactory interpretation.

Since the objective in this study is to investigate the various aspects of short-period wave generation by underground nuclear explosions, the study by Aki and Tsai presents two desirable features. Firstly, the closely located events (the events selected for our study were confined within an area $\sim$11 X 6 km) providing an almost identical source-receiver geometry from the different explosions to a given station. The common propagation path (and the associated propagation effects) allows us to attribute the observed discrepancies at the station to source effects. Secondly, the study of Aki and Tsai succeeded in determining tectonic strain release as the causal mechanism for the anomalous excitation of long period Love waves at Yucca Flat, NTS. Our aim is to estimate the yield of an explosion from the amplitudes of the Lg wave which results from the superposition of higher-mode Love and Rayleigh waves. Hence, we are interested in knowing whether tectonic strain release has a correspondingly large effect on Lg, and if so, what relationship between the amplitudes of long period surface waves and those of Lg exists.

Receiver

Figure 1-1 shows the geographic distribution of the underground nuclear explosions, and the WWSSN stations used in this study and one interpretation of the tectonic provinces in the United States. Even though the WWSSN short period seismograph system has a response sharply peaked around 1 sec (T pendulum $\simeq$ 1.0 sec, T galvanometer $\simeq$ 0.75 sec), waves with periods ranging from 0.5 to 4 to 5 seconds can usually be observed on its seismograms. Furthermore, since NTS is located in a structurally complicated region, most of the great-circle paths traverse one or more tectonic provinces.

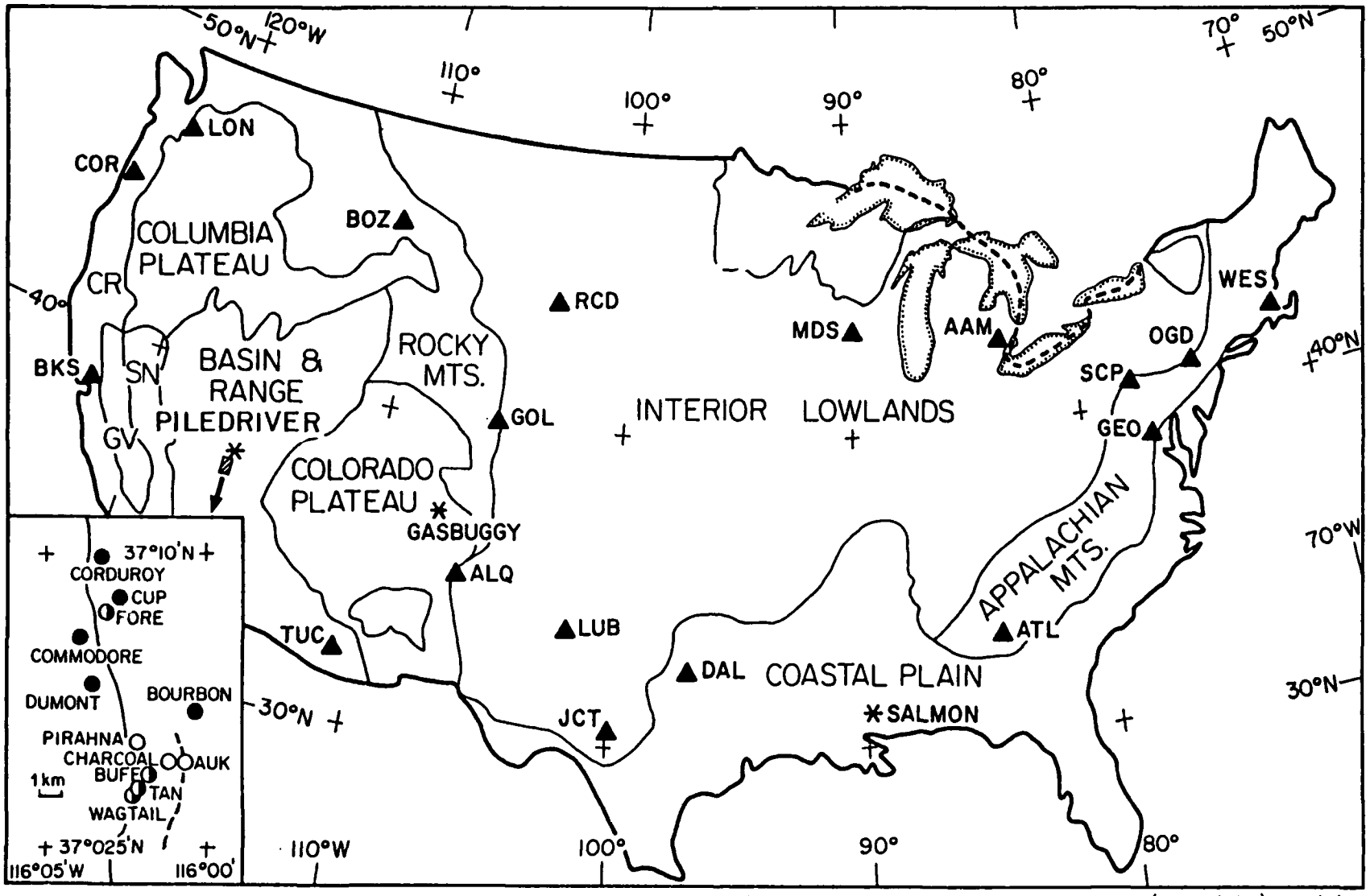

Figure 1-1. Location of the seismograph stations (solid triangles) and underground nuclear explosions (asterisks) used in in this study. The tectonic map is modified from that of King (1977). In the insert, solid, half-filled, and open circles represent strong-, intermediate-, and weak- exciters of Love waves (modified from Aki and Tsai, 1972). CR=Coastal Ranges, GV=Great Valley, SN=Sierra Nevada.

Measuring Procedure

The amplitudes used to derive the amplitude-yield relations and the attenuation coefficients were obtained in the following fashion. For P waves, the maximum peak-to-peak amplitude is measured from the initial three cycles. For Pg and Lg waves, the measuring scheme is slightly different. When the predominant period around the appropriate group-velocity (6.0 km/sec for Pg, 3.5 km/sec for Lg) is less or equal to 1.5 sec, the peak-to-peak amplitude of the third largest wavelet is measured; otherwise ($T > 1.5$ sec), the maximum amplitude is used. The underlying motives for this approach are: (1) to reduce the chance of measuring any spuriously large amplitude resulting from constructive interference, the occurrence of which is common at short periods, and (2) to obtain a representative value for the maximum amplitude of the coda. Adverse conditions such as missing or poorly-recorded seismograms, high magnification at nearby stations and vice versa, and noise (both electronic and natural) have reduced the number of usable seismograms at some stations.

Data Analysis and Discussion

In this section, we will discuss the applications of these amplitudes in estimating: (A) the relationship between the excitation of long- and short-period surface waves by tectonic strain release, (B) amplitude-yield relations, and (C) the excitation of Pg and Lg waves by explosive sources.

A. Effect of Tectonic Strain Release

All of the amplitudes measured from the seismograms were first corrected for instrument magnification to obtain the amplitudes of the ground motion. To estimate the effect of tectonic strain release on the short period Lg wave, we divided the Lg amplitudes on the transverse component by those on the vertical component. (When the horizontal component, NS or EW, lies within 30^{0} of the back azimuth to the source, it is referred to as the longitudinal component; and the other one, the transverse component. Otherwise, the horizontal components are labeled as NS or EW.) We then represented the quotient for strong-, intermediate-, and weak- exciters of Love waves by different symbols and plotted them versus distance (Figure 1-2). This figure shows three important features:

1. most of the data points have values greater than one, i.e. the amplitudes on the transverse component are greater than those on the vertical component

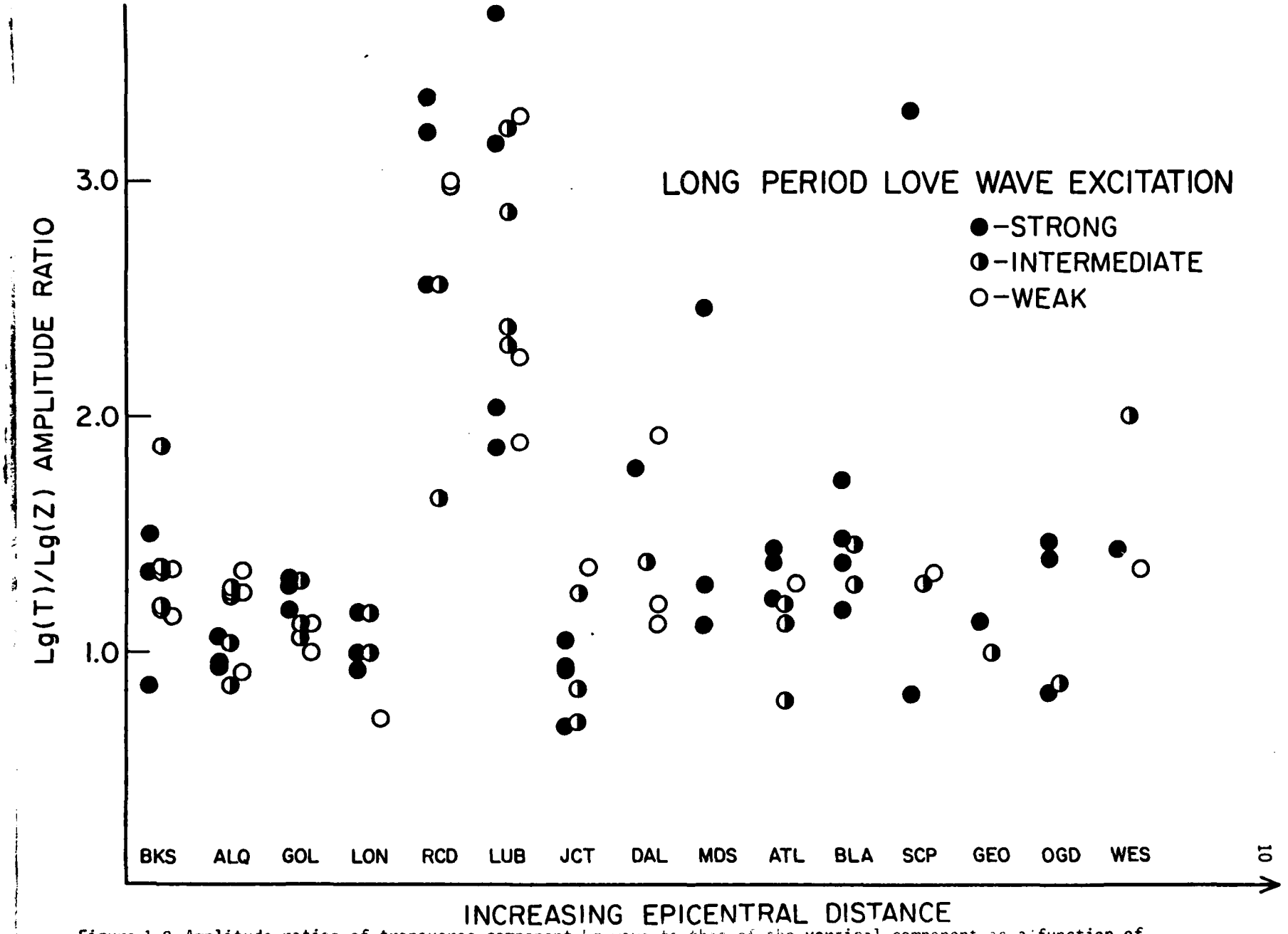

Figure 1-2. Amplitude-ratios of transverse-component Lg wave to that of the vertical component as a function of increasing epicentral distance.

2. at each station, no clear separation for the strong-, intermediate-, and weak- exciters of Love waves is discernible and
3. no simple distance dependence is noted.

The second characteristic implies that there is no observable correlation between the amplitude ratios of short period higher modes of Love waves to those of Rayleigh waves and their long period, fundamental-mode counterparts. Hence, recorded amplitudes of Lg waves from these events at these stations do not suffer any discernible amplitude change from the tectonic strain release.

This finding is not surprising in view of the long period nature generally associated with the process of tectonic strain release; as a result the tectonic strain release probably has little effect on the spectral level at short periods. The effect of tectonic strain release on P waveforms has been studied theoretically (Bache, 1976; Burdick and Helmberger, 1979); the results indicate that, unless the magnitude of the accompanying tectonic event is greater than that of the explosion, maximum amplitudes of the short period P waves will not be affected.

If the small differences in source location weaken the assumption of common path effects, factors such as scattering, mode-coupling between the Love- and Rayleigh-type higher modes, and differences in the attenuation rate for Love- and Rayleigh-type Lg waves, may become significant enough to mask the short period radiation from the tectonic event. As we shall find in a later section, attenuation rates for the vertical, transverse, and longitudinal components of Lg seem to be approximately equal. Consequently, they do not cause the lack of contamination of short period Lg by the tectonic release.

Although both mode-coupling and scattering interact with lateral heterogeneities, they do connote different physical processes. The former suggests a coherent process of energy exchange, and the latter, a random one. Their effects on wave-amplitude are usually difficult to distinguish. In the following paragraph, we will discuss the effect of mode-coupling and that of scattering.

Assuming that the higher-mode surface waves of the Rayleigh-type do couple or exchange energy with those of the Love-type at boundaries of lateral heterogeneities, then we would expect a homogenizing effect on the displacement vector as the number of boundaries increases. That is, the amplitudes of the different components would gradually become equal. The greater-than-unity amplitude ratios and the lack of any discernible distance dependence within the epicentral-distance range of 5^{o} to 35^{o}, however, implies that the effect of mode-coupling

is small if not negligible. Similarly, the roughly equivalent amplitude ratios at nearby and faraway stations indicate that scattering, however much it may affect the observed amplitudes, appears to have imposed equal influence on the different components of Lg amplitude. If this deduction is correct, then the observed amplitudes should reflect their source characteristics. But, as we have already noted, the amplitude ratios for strong exciters do not appear different from those for intermediate and weak exciters of Love waves; thus, there is no observable correlation between the excitation of higher-mode surface (or Rayliegh) waves at periods around 1 sec and that of fundamental-mode Love waves at periods greater than 10 sec. Consequently, the tectonic strain release which is interpreted as the causal mechanism of long period Love waves, does not seem to affect the amplitudes of short period surface waves. As a consequence, it appears valid to derive amplitude-yield relationships and to attempt to apply them to different geographic areas.

B. Amplitude-Yield of Relations

The previous section has shown that the amplitudes of short period Lg waves from underground nuclear explosions at NTS do not seem to be affected by the radiation from the accompanying tectonic event. This property of short period Lg waves is potentially useful for estimating the yields of underground nuclear explosions using Lg. An example of an amplitude-yield relation is:

$$\log A = m \log Y + \gamma\Delta + S$$

where A = amplitude of the ground motion,
Y = estimated yield of the explosion, estimated from a combination of radiochemistry and other means (Springer and Kinnaman, 1975),
m = slope of the log-amplitude vs. log-yield plots,
γ = attenuation rate, i.e. slope of log-amplitude vs. distance plots, and
S = correction for station response.

In this section, we will confine our attention to the determination of m for Lg waves. Since the attenuation term is a constant for a given source-receiver geometry, the second and third terms in expression (1) can be considered as one, and equation (1) can be reduced to

$$\log A = m \log Y + b$$

where $b = s + \gamma\Delta$. The value, besides being the y-axis intercept on a log Y- log A plot, has the physical significance of being the ground amplitude from a 1-kt explosion at the particular recording station.

The values of m and b for each recording station and wave-type (Lg(Z), Lg (L), Lg(T)) were determined separately by a least-squares regression analysis. Examples are plotted in Figures 1-3 and 1-4 for Lg waves at RCD and GOL, respectively. An examination of all of these plots after the initial regression reveals that the amplitudes from the 19-kt event, FORE, are consistently higher than the values predicted for the yield; consequently, the amplitudes of that event are not incorporated into the subsequent regression analysis.

Three patterns emerge from a careful inspection of all of these figures:

1. the scatter of the data points around the best-fitting line,
2. the difference in the values of m and b for different wave-types and stations, and
3. the distinction between well-correlated BKS, BOZ, GOL, JCT, LUB for Pg and Lg waves and poorly correlated ALQ, DAL for Pg wave amplitude-yield relations. Below, we will discuss each of these characteristics individually.

The scatter of the data points in all amplitude-yield plots can be explained several ways. Firstly, lack of correlation may result because the yield used to correlate with the wave amplitudes was derived from "radiochemistry and other means" (Springer and Kinnaman, 1975), and depending on the source configuration and site conditions, the value may not correspond to the seismic yield as reflected by the amplitudes of the seismic waves. Secondly, the measuring technique may not have adequately gauged the seismic yield of the underground nuclear explosions. Thirdly, the slight variations in the source location may be responsible for the observed scatter. Lastly, the source radiation may be anisotropic as a result of (a) interactions with near-source heterogeneities, (b) peculiar test configurations and/or nonlinear, inelastic response in the source region (Rodean, 1971), and (c) random, small-scale strain release in the inelastic zone of the explosion.

With regard to the first two possibilities, the excellent agreement between the ground amplitudes and the 'announced' yields at some of the stations seems to indicate that the yields estimated by AEC and our measuring technique can produce satisfactory results at these stations. On the other hand, the anomalously large amplitudes from FORE and the clear amplitude discrepancies between

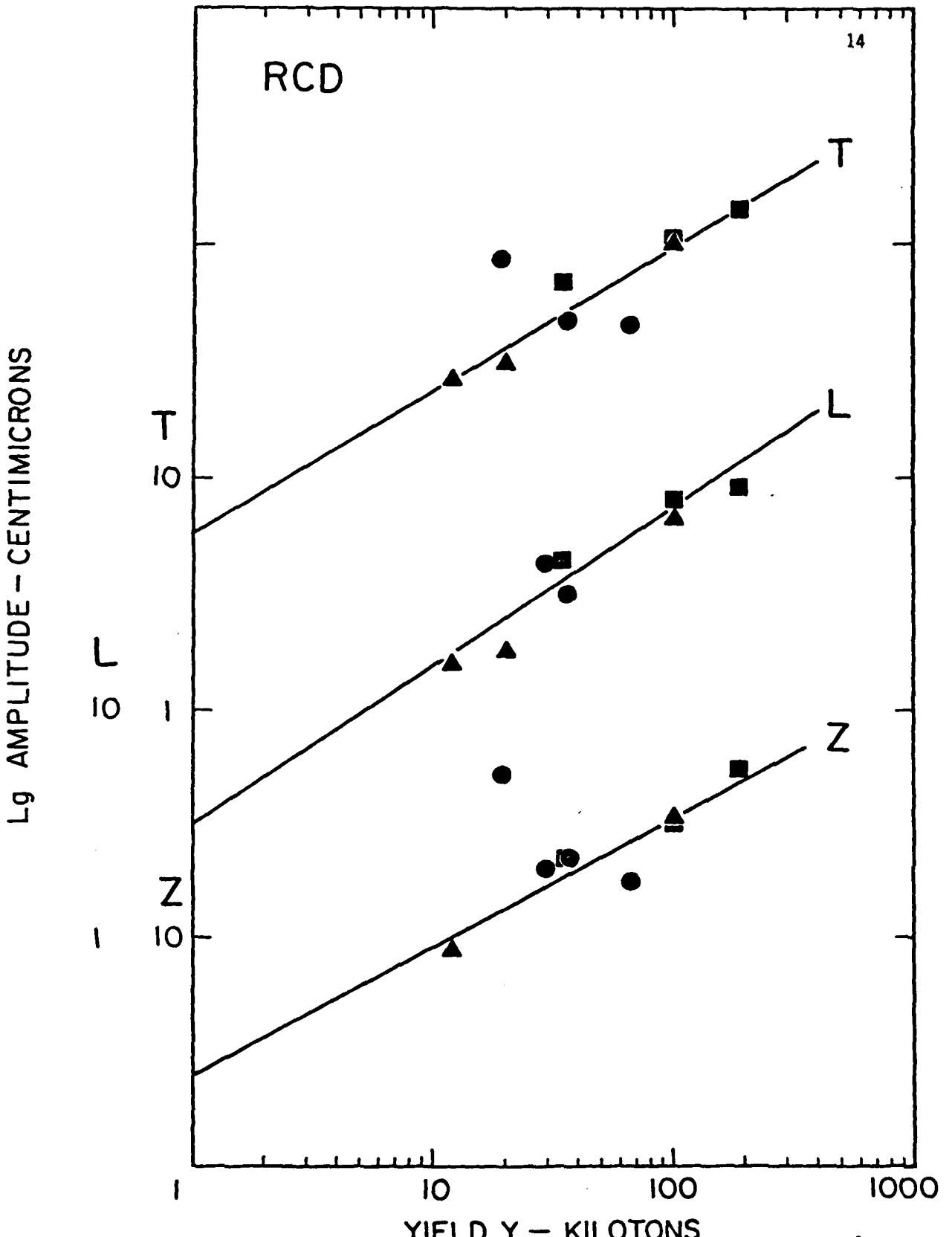

Figure 1-3. Log-log plots of Lg wave ground amplitude at RCD in centimicrons (10^{-8} m) vs. announced yield in kilotons. The squares, circles, and triangles represent strong, intermediate, and weak exciters of long-period Love waves, respectively.

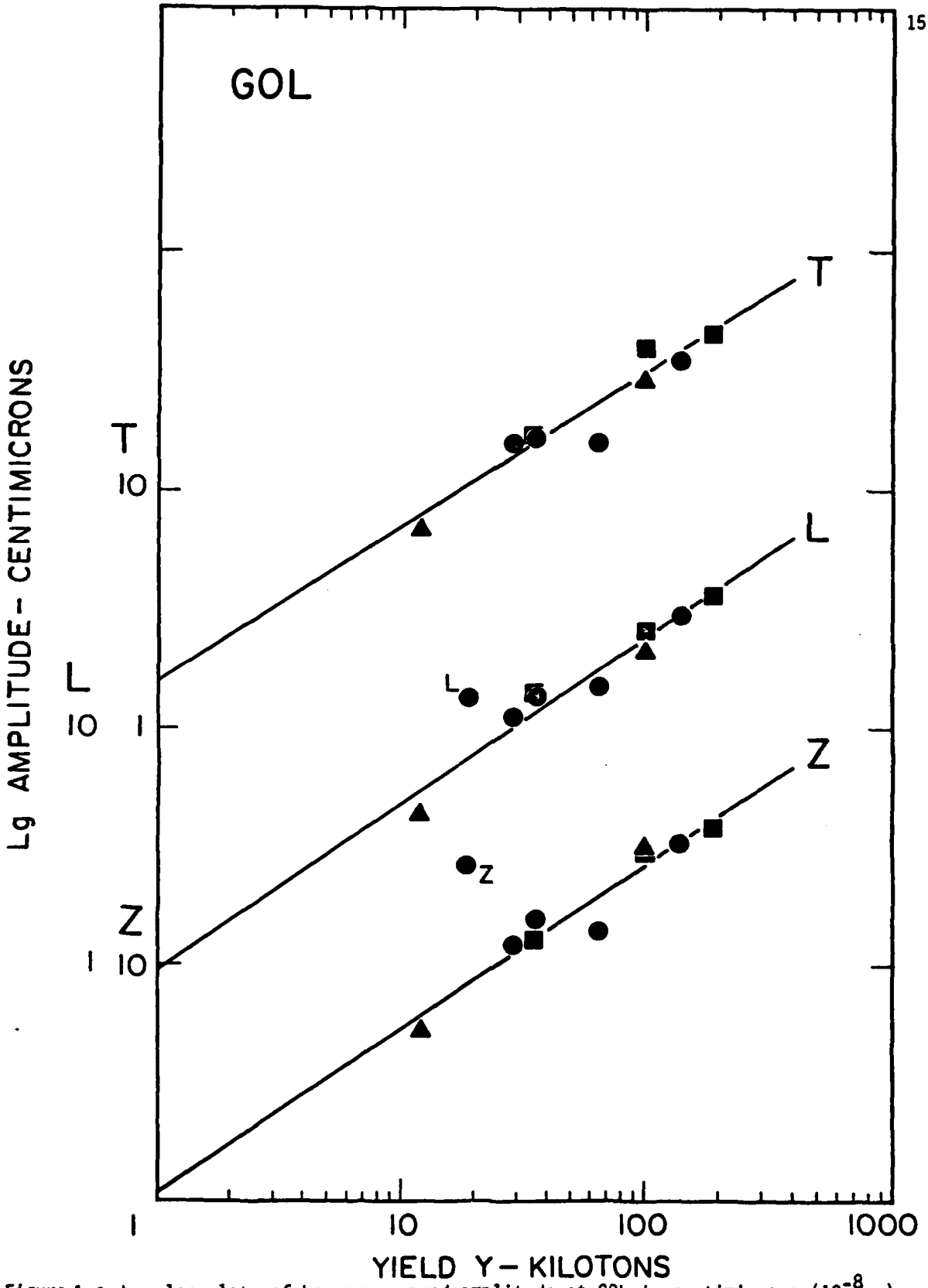

Figure 1-4. Log-log plots of Lg wave ground amplitude at GOL in centimicrons (10^{-8} m) vs. announced yield in kilotons. The squares, circles, and triangles represent strong, intermediate, and weak exciters of long-period Love waves, respectively.

the two 100-kt events: CORDUROY and PIRAHNA highlight the differences between the announced yield and the seismic yield estimated by us.

Our experience with correlating a large number (>100) of announced yields and their corresponding m_b (ISC) indicates that a spread of up to 0.8 magnitude-unit (an amplitude difference of~6X) exists at a given value of announced yield and that, on the average, the announced yield seems to correlate well with the seismic yield as determined from the amplitudes of seismic waves (Chen and Pomeroy, 1980). (Even with our nearly identical source-receiver geometry, an offset of ~ 0.6X of the predicted amplitude is to be expected.) Except for the period-dependent approach in measuring the amplitudes of Lg waves, our scheme is commensurate with the conventional procedure for magnitude-determination (Richter, 1935; Nuttli, 1973). Therefore, we believe that the measuring technique is valid, that the announced yields are also in general valid and that we must therefore examine the other two possibilities mentioned above.

With regards to the effects of scattering and anisotropic source, we tend to be more impressed with the importance of the former. For example, when looking at the relative proximity in epicentral distance and back azimuth to the source from three WWSSN stations in Texas: DAL ($\Delta \simeq 16.3^{o}$, azim. $\simeq 99.0^{o}$), JCT ($\Delta \simeq 15.0^{o}$, azim $\simeq 111.3^{o}$), and LUB ($\Delta \simeq 12.1^{o}$, azim. $\simeq 103^{o}$), one would expect the amplitude characteristics to be approximately equal. There are two marked differences among the amplitudes observed at these stations. Firstly, the observed amplitudes correlate quite well with the estimated yields at LUB and JCT, but not as well at DAL. Secondly, the average amplitudes for the ground motion at DAL are comparable to those at LUB when effects for attenuation and geometrical spreading are taken into account. The average amplitudes at JCT, on the other hand, are usually a factor of two or more smaller than those at DAL (and LUB), even though the epicentral distance to JCT is in between those to LUB and DAL. Although the effects of source and propagation path are difficult to separate, since the range of azimuth back from these three stations differs only by~12.3^{o} in this case, we suspect that the source radiation pattern which at short periods tend to be oval in shape (Cheng and Herrmann, 1980), could result in such a large change ($\gtrsim$ 2X) in amplitude. Sutton et al. (1967) showed anisotropic energy contours from an NTS event, HARDHAT, for Pg and Lg waves. Their results indicate a strong focusing effect to the SE direction; unfortunately, DAL, JCT, and LUB lie beyond the extent of their contour map, and hence direct comparison between their findings and our results was not possible. This example from the three Texan stations and our experience with other stations show that scattering

(which is defined in this context; includes the effects of diffraction, focusing by tectonic structures, and response due to the structure beneath the recording station) along the propagation path influences greatly the characteristics of the observed waves.

We have also explored the possibility of using the amplitudes of Lg coda to determine the slope of the amplitude-yield relation. By following the recommendations of Rautian and Khalturin (1978) and Chouet et al. (1978), we measured the amplitudes of Lg waves at a group velocity of about 1.75 km/sec, i.e. about twice the time interval between the origin time and the onset of Lg, for four of the closest stations: ALQ, BKS, DUG, and TUC. We then chose the amplitude from the event with the lowest yield as a reference point, unity in our case, and plotted the relative amplitudes versus the estimated yields. This method offers one definite advantage. Even for the largest event, the wave trace was visible rather than an unmeasurable blur at the closest station ($\Delta \sim A^{o}$), DUG, thus increasing the number of useful data points at ALQ, DUG, and TUC significantly.

The plots of relative amplitude versus estimated yield like that shown in Figure 1-5 indicate that the results derived from coda are compatible with those derived from measurements of amplitude maxima. Finally, the slopes of log-amplitude versus log-yield plots for the Lg waves are plotted as a function of epicentral distance in Figure 1-6. Similar to our previous findings on the amplitude ratios for Lg waves, no dependence on distance or particle-motion seems to exist.

C. Excitation of Pg and Lg Waves by Explosive Sources

We calculated the relative excitation of Pg and Lg waves by underground nuclear explosions at NTS. The source amplitude for the Lg wave is 3352 $\pm$ 300, roughly three times the source amplitude for the Pg wave, 1406 $\pm$ 241. Since this ratio corresponds quite closely to the theoretical amplitude ratio of S to P waves in a Poisson solid (Aki and Richards, 1980), we believe that the radiation of Pg and Lg waves is directly related to that for P and S waves.

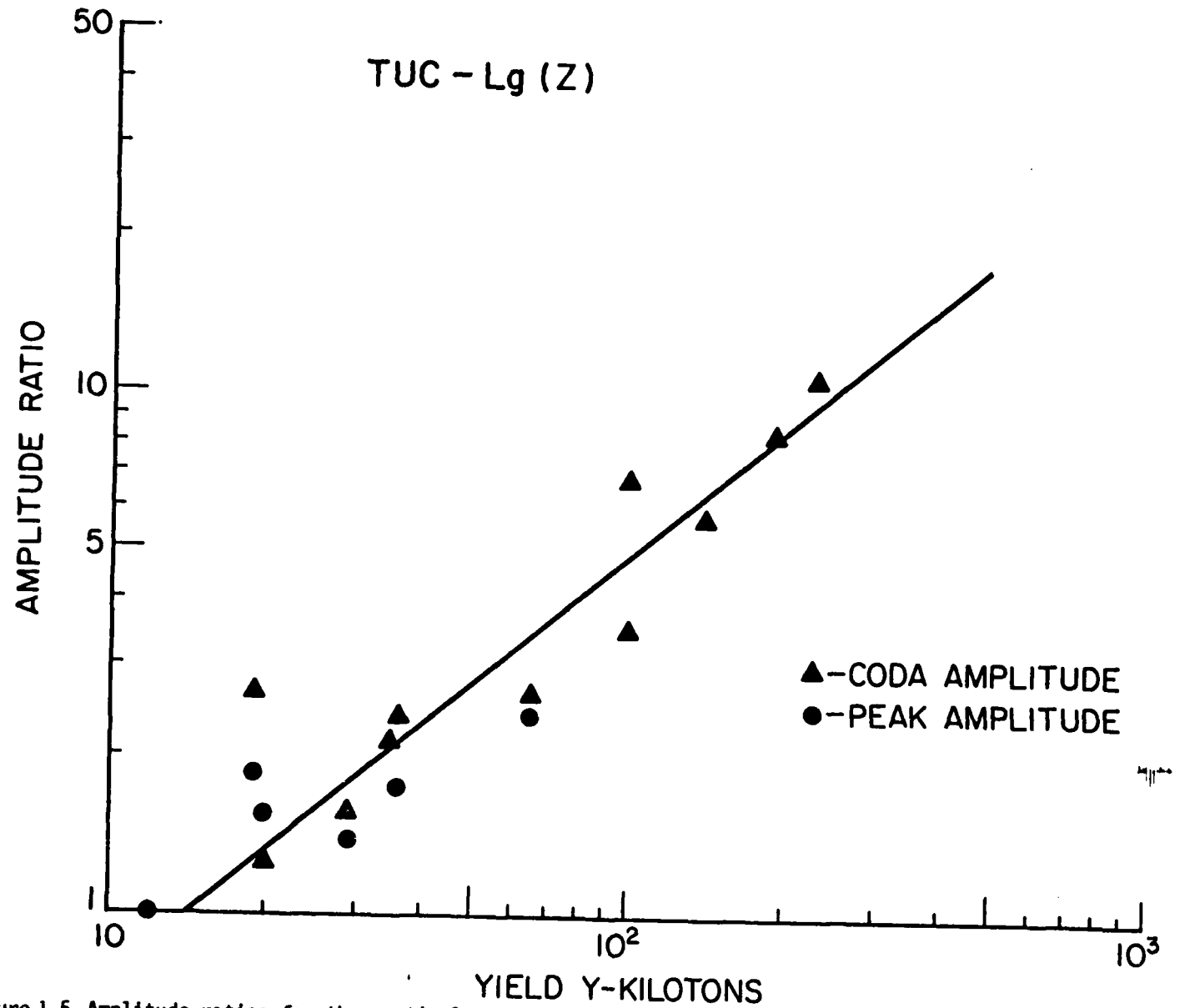

Figure 1-5. Amplitude ratios for the vertical component of Lg waves at TUC as a function of estimated yields. The ratio is taken with respect to the event with the smallest yield. Triangles and circles represent data derived from coda amplitude and amplitude maxima, respectively.

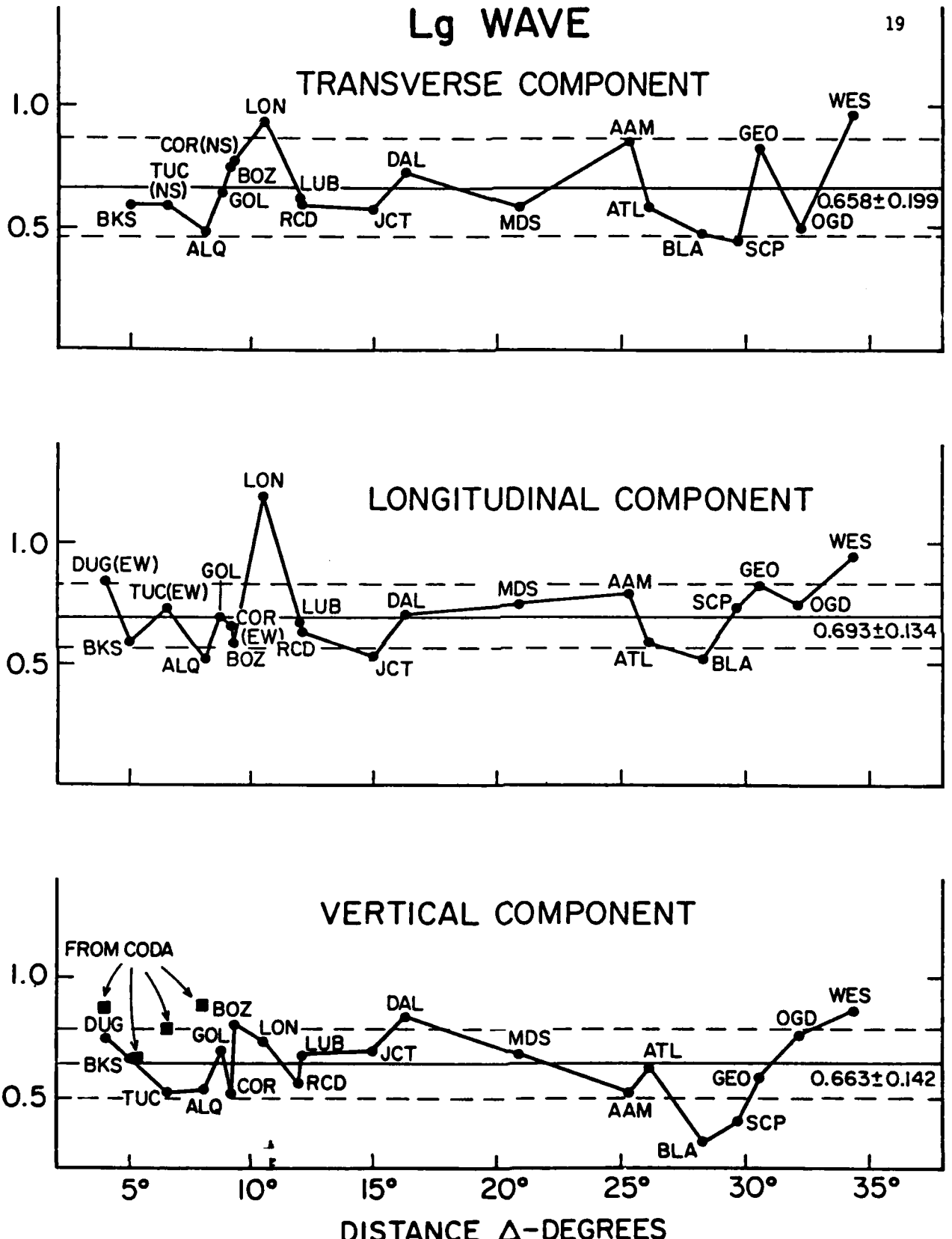

Figure 1-6. The slopes of log-amplitude versus log-yield plots for the Lg wave. The solid and dashed horizontal lines denote mean and one standard deviation, respectively.

Application of Amplitude-Yield Relation to Other Tests

We have applied our amplitude-yield relations to the estimation of the yield of three underground explosions outside of Yucca Flat, NTS : PILEDRIVER at Climax Stock, NTS; GASBUGGY near Dulce, New Mexico; and SALMON near Hattiesburg, Mississippi. The measured amplitudes for these events at each station, after correcting for instrument magnification, were equalized to a distance the same as the epicentral distance of the station to Yucca Flat, NTS. That is, the resultant amplitudes are assumed to have undergone the effects of geometrical spreading and inelastic attenuation from Yucca Flat, NTS, instead of from their respective source locations. The yields estimated by us are listed in Table 1-2.

Conclusions

The principal results of this study are:

1. Contamination of Lg(Z) and Lg(T) by the anisotropic component of the source is not significant for these events as recorded in the U.S. The effects of propagation path have been qualitatively evaluated and discarded as the likely causes for the lack of correlation between the surface wave amplitudes of the long period fundamental mode and those of short period higher modes.
2. Lg(Z) and Lg(T) provide reasonable and independent supplementary estimates of the yield.
3. Amplitude yield relationships of the type derived in this study can be used to estimate the yields of underground explosions in different geographic and geologic environments.
4. The use of Lg(Z) and/or Lg(T) to determine yield is particularly important
   a. for events from test areas like Shagan River where M_S is suspect, and
   b. for events of lower yield on the same continental land mass as the recording station.
5. Since Lg is, in many areas the largest amplitude signal observed on many regional seismograms ($\Delta = 10^{\circ}$-35°), it is particularly useful to provide a supplemental yield determination.

References

Aki, K. and P. G. Richards, 1980, Quantitative Seismology-Theory and Methods, W. H. Freeman and Co., San Francisco, 932 p.

Aki, K. and Y. B. Tsai, 1972, Mechanism of Love-wave excitation by explosive sources, J. Geophys. Res., 77, 1452-1475.

Bache, T. C., 1976, The effect of tectonic stress release on explosion P-wave signatures, Bull. Seism. Soc. Am., 66, 1441-1457.

Burdick, L. J. and D. V. Helmberger, 1979, Time functions appropriate for nuclear explosions, Bull. Seism. Soc. Am., 69, 957-973.

Chen, T. C. and P. W. Pomeroy, 1980, Regional seismic wave propagation, Semi-Annual Technical Report #5, Rondout Associates, Inc., Stone Ridge, New York.

Cheng, C. C. and B. J. Mitchell, 1980, Crustal Q structure in the United States from multi-mode surface waves, Semi-Annual Technical Report #3, Saint Louis University, St. Louis, Missouri.

Chouet, B., K. Aki, and M. Tsujiura, 1978, Regional variation of the scaling law of earthquake source spectra, Bull. Seism. Soc. Am., 68, 49-79.

Nuttli, O. W., 1973, seismic wave attenuation and magnitude relations for eastern North America, J. Geophys. Res., 78, 876.

Rautian, T. G. and V. I. Khalturin, 1978, The use of the coda for determination of the earthquake source mechanism, Bull. Seismc. Soc. Am., 68, 923-948.

Richter, C. F., 1935, An instrumental earthquake scale, Bull. Seism. Soc. Am., 25, 1-32.

Springer, D. L. and R. L. Kinnaman, 1975, Seismic-source summary for U.S. underground nuclear explosions, 1971-1973, Bull. Seism. Soc. Am., 65, 343-349.

Sutton, G. H., W. Mitronovas, and P. W. Pomeroy, 1967, Short-period seismic energy radiation patterns from underground nuclear explosions and small-magnitude earthquakes, Bull. Seism. Soc. Am., 57, 249-267.

Figure Captions

Figure 1-1 Location of the seismograph stations (solid triangles) and underground nuclear explosions (asterisks) used in this study. The tectonic map is modified from that of King (1977). In the insert, solid, half-filled, and open circles represent strong-, intermediate-, and weak- exciters of Love waves (modified from Aki and Tsai, 1972). CR = Coastal Ranges, GV = Great Valley, SN = Sierra Nevada.

Figure 1-2 Amplitude-ratios of transverse-component Lg wave to that of the vertical component as a function of increasing epicentral distance.

Figure 1-3 Log-log plots of Lg wave ground amplitude at RCD in centimicrons (10^{-8} m) vs. announced yield in kilotons. The squares, circles, and triangles represent strong, intermediate, and weak exciters of long-period Love waves respectively.

Figure 1-4 Log-log plots of Lg wave ground amplitude at GOL in centimicrons (10^{-8} m) vs. announced yield in kilotons. The squares, circles, and triangles represent strong, intermediate, and weak exciters of long-period Love waves respectively.

Figure 1-5 Amplitude ratios for the vertical component of Lg waves at TUC as a function of estimated yields. The ratio is taken with respect to the event with the smallest yield. Triangles and circles represent data derived from coda amplitude and amplitude maxima, respectively.

Figure 1-6 The slopes of log-amplitude versus log-yield plots for the Lg wave. The solid and dashed horizontal lines denote mean and one standard deviation, respectively.

SECTION 2

ANALYSES OF SEISMIC DATA FROM THE HARZER NUCLEAR EXPLOSION AS RECORDED AT THE CATSKILL SEISMIC ARRAY (CSA), STONE RIDGE, NEW YORK

Executive Summary

The high quality digital recordings of the HARZER nuclear event at the Catskill Seismic Array, a distance of 32.5^{o}, provide a unique data set for the analyses of propagation characteristics. This distance range, 32.5^{o},is approximately the same as that between the USSR Semipalatinsk test site and the nearest recording stations to the south. The propagation path in the present case is, to a large degree, analogous to some propagation paths from USSR events.

The specific results of this study include:

1. P, Lg and sedimentary Rayleigh waves were well recorded on the array.

2. The impulsive P waves, as recorded on the vertical component instruments of the array, have a broad spectrum with amplitudes of 1 to 5 microns in the frequency range .1 to 1 hertz. Spectral amplitudes in the 1 to 2 hertz range are 2 orders of magnitude smaller. The P wave spectra are essentially identical at all three stations.

3. Cross correlation of the P waves shows very high correlation coefficients i.e. 213 Z and TON Z .9661
213 Z and PEK Z .9248
TON Z and PEK Z .8747
indicating excellent signal coherence across the array (dimensions of the order of 2 kms).

4. Coherence plots of the P waves show high values (.8 to .9) at frequencies less than 1 hertz. At frequencies greater than 1 hertz, the coherence drops rapidly for the station combinations TON Z-PEK Z and 213 Z-PEK Z. The station pair 213 Z-TON Z show relatively high coherence (.4 to .6) at frequencies between 1 and 2 hertz.

5. The signal to noise ratio for the P waves on the vertical component indicates that, in the frequency range .3 to .8 hertz signal to noise ratios are greater than 3. Band pass filtering the P wave would result in major improvements in the signal to noise ratio. Delay and sum array processing would also result in significant signal to noise improvements.

6. The wave spectra for a 40 second sample of Lg show that the highest amplitudes are recorded on the transverse instruments and the lowest amplitudes on the longitudinal instrument. The shape of all Lg spectra is remarkably similar but spectral amplitude differences of as much as a factor of 10 are observed between different components. The amplitude spectra fall off at approximately 18 db/octave from .1 to 10 hertz.

7. High values of the cross correlation functions between similar components are observed on the vertical and transverse Lg data. Lower correlation values are observed on the longitudinal (E-W) pairs consistent with the low signal to noise ratios on these instruments.

8. All of the transverse and vertical component pairs show high coherence for Lg in the frequency range .1 to .3 hertz. No coherent energy is observed at frequencies greater than 1 hertz. With the exception of the station pair 213 Z-TON Z which exhibits a.55 coherence in the frequency band .5 to .7 hertz, no significant coherence is observed on the vertical components at frequencies greater than .3 to .4 hertz.

9. Significant signal to noise ratios in Lg (2 to 4) are found principally in the .3 to .8 hertz frequency range i.e. in approximately the same frequency range as the noise maxima. Therefore, band-pass filtering will not significantly enhance signal to noise ratios in Lg.

10. The sedimentary Rayleigh waves from this event with periods from 12 to 3 seconds are highly unusual in that one would expect the shorter period waves not to exist since their propagation requires continuity in the upper 5 kms of the wave guide. Since they do exist, in spite of radical changes in the upper 5 kms of the wave guide between NTS and the Catskill Seismic Array, a detailed investigation of the propagation characteristics of these waves is in order.

In a later study of HARZER data, we will carry out the following studies:

i. F-k plots of all components of Lg-phase velocity.
ii. Construction of synthetic seismograms for the entire wave train.
iii. Phase and group velocity of the sedimentary Rayleigh waves.
iv. Determination of the seismic yield from P and Lg.
v. Particle motion in Lg where the signal is highly coherent.
vi. Band pass filtering and trace integration for energy distribution studies.
vii. Three dimensional moving window Fourier analyses of the entire wave train.

The improved understanding of the propagation properties, particularly of Lg, is of particular importance in connection with the use of these waves for yield determination.

Introduction

The nuclear explosion HARZER generated seismic waves which were well recorded at the Catskill Seismic Array (CSA) at a distance of $\sim 32.5^{\circ}$ from the Nevada Test Site (NTS). This section deals with the preliminary analyses of the broad band seismic data recorded by the array. The available information on the explosion is given in Table 2-1.

The array, shown diagramatically in Figure 2-1, consists of three (3) elements: 213, PEK, and TON. Coordinates for these locations are given in Table 2-1 together with station elevations and interelement distances. The Catskill Seismic Array is operated under a cooperative research agreement between Rondout Associates Incorporated and the University of Nevada.

At each of the three elements, there are 3-component (2H's-1Z) Teledyne-Geotech Model SL-210 and SL-220 seismometers operating at a natural period of 15 seconds. The velocity output from each seismometer is amplified and filtered to allow recording from long periods up to 12.5 hertz. The analog output is then digitized at 25 samples a second and the digital data from all three instruments is multiplexed onto a 1200 hertz carrier for telephone line transmission. Telephone lines run from the three remote sites to the central recording facility at the corporate headquarters of Rondout Associates, Incorporated at 1 Stilba Lane in Stone Ridge, New York.

At the central recording facility, data from the three remote sites are recorded on digital magnetic tape under the control of an Andromeda Systems LSI-11 computer. Two Digidata magnetic tape drives are used and tapes are changed once a day. Entry of parameters is via a Decwriter IV terminal. Satellite time is provided for the system via a Kinemetrics-True Time satellite time receiver which enters date, hour, minute and second information on the tape as it is derived from a geostationary satellite. Data tapes from the array are nominally saved for a one week period and information on earthquakes of interest is obtained on a weekly basis. Following 1 September 1981, the array data was saved entirely up to the termination of the array operation on 19 November 1981.

The Catskill Seismic Array is unique in several respects:

1. It is the only array with dimensions small enough to study high frequency seismic waves in the eastern and central U.S.
2. It is the only array of broad-band instruments in the eastern and central U.S.

3. It is the only array of three-component instruments in the eastern and central U.S.
4. It is the only fully digital array in the eastern and central U.S.

These unique qualities are providing a vast quantity of data on propagation characteristics of earthquakes within the North American continent.

The distance from the CSA to the NTS is significant in that the closest monitoring stations to the south of the USSR test site at Semipalatinsk lie in the same distance range. Moreover, the NTS-CSA propagation path starts in the western mountainous region and then traverses the high Q areas of the eastern and central United States. The propagation paths between the USSR test site and the southern stations are somewhat analogous since the waves from events at Semipalatinsk traverse broad, low lying relatively high Q areas and then, in general cross mountainous terrain prior to being recorded at the southern stations. Thus, it is particularly important to study a well recorded event like HARZER at CSA to analyze the propagation characteristics in detail. Particular emphasis in these preliminary studies is placed on the spectral content of P and Lg and the coherence of these waves across the array.

TABLE 2-1

HARZER DATA

COORDINATES(1)	37° 18′ 12.2258″ NORTH 116° 19′ 32.1466″ WEST
ELEVATION(1)	6890.9 FT.
MAGNITUDES(2)	m_B = 5.6 M_S = 4.2 M_L = 5.4 (BRK)

(1) INFORMATION PROVIDED BY PUBLIC INFORMATION OFFICE, NEVADA TEST SITE.

(2) MAGNITUDES ARE THOSE REPORTED IN PRELIMINARY DETERMINATION OF EPICENTERS NO. 23 - 81 DATED JULY 1, 1981.

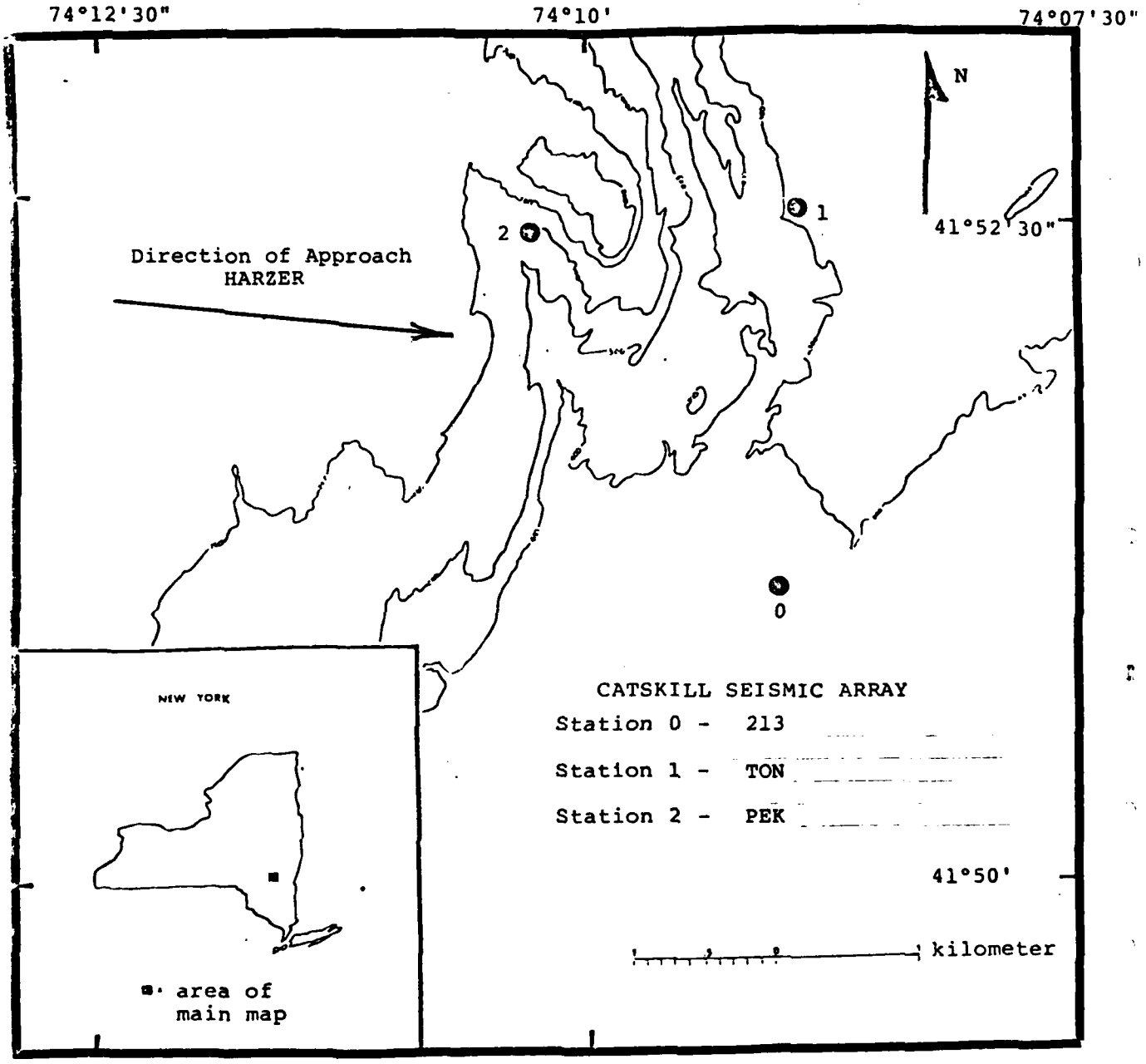

Figure 2-1. Location Map of Catskill Seismic Array.

TABLE 2-2

CATSKILL SEISMIC ARRAY

	STATION 0-213	STATION 1-ION	STATION 2-PEK
COORDINATES	41.8517°N LAT. 74.1500°W LONG.	41.8756°N LAT. 74.1492°W LONG.	41.8742°N LAT. 74.1714°W LONG.
ELEVATION	105.2 METERS	85.3 METERS	176.8 METERS
HARZER DISTANCE	32.5823°	32.5807°	32.5640°
HARZER AZIMUTH	276°	276°	276°
AZIMUTH FROM HARZER	68°	68°	68°

INTERELEMENT DISTANCES

0-1	2.64 KM
0-2	3.04 KM
1-2	1.84 KM

Data

The entire seismic wave train, as recorded on the array, is presented in Figure 2-2. Distances to each of the three component elements are indicated at the left of the figure. Time, in hours and minutes is indicated along the top. The smallest tick marks at the top and bottom are 5 second marks.

1. The P arrival, particularly sharp and impulsive in character, is especially evident on the vertical components and can also be seen on the east-west components which are essentially longitudinal. P is not easily identified on the transverse (N-S) component.

2. No increase in energy levels or identifiable shear energy is apparent around the time that S would normally be expected.

3. Amplitudes on all components begin to increase at a time corresponding to a group velocity slightly greater than 3.5 km/sec and those higher amplitudes--the Lg wave train, continue on the vertical and east-west instruments until they are masked by the arrival of the sedimentary Rayleigh waves at a time corresponding to a group velocity of slightly greater than 3.0 km/sec.

4. The sedimentary Rayleigh waves, with periods lying in the range of 12-4 seconds continue for approximately 2 1/2 minutes and are normally dispersed. On the transverse (N-S) components, the higher amplitudes associated with Lg can be seen to persist to times corresponding to group velocities significantly less than 3.0 km/sec. These trace amplitudes have not been normalized.

5. Comment. In Lg, the highest amplitudes are observed on the transverse (N-S) components while the lowest amplitudes are observed on the longitudinal (E-W) components. These differences will be quantified in our detailed studies of Lg below. Although we have not studied the sedimentary Rayleigh waves in detail for inclusion in this report, it is extremely important to note that, in spite of major changes in structure along the propagation path, these waves, whose particle motion is generally confined to the shallower, and therefore more changeable, layers at the shorter periods persist and propagate out to distances as great as those in this study.

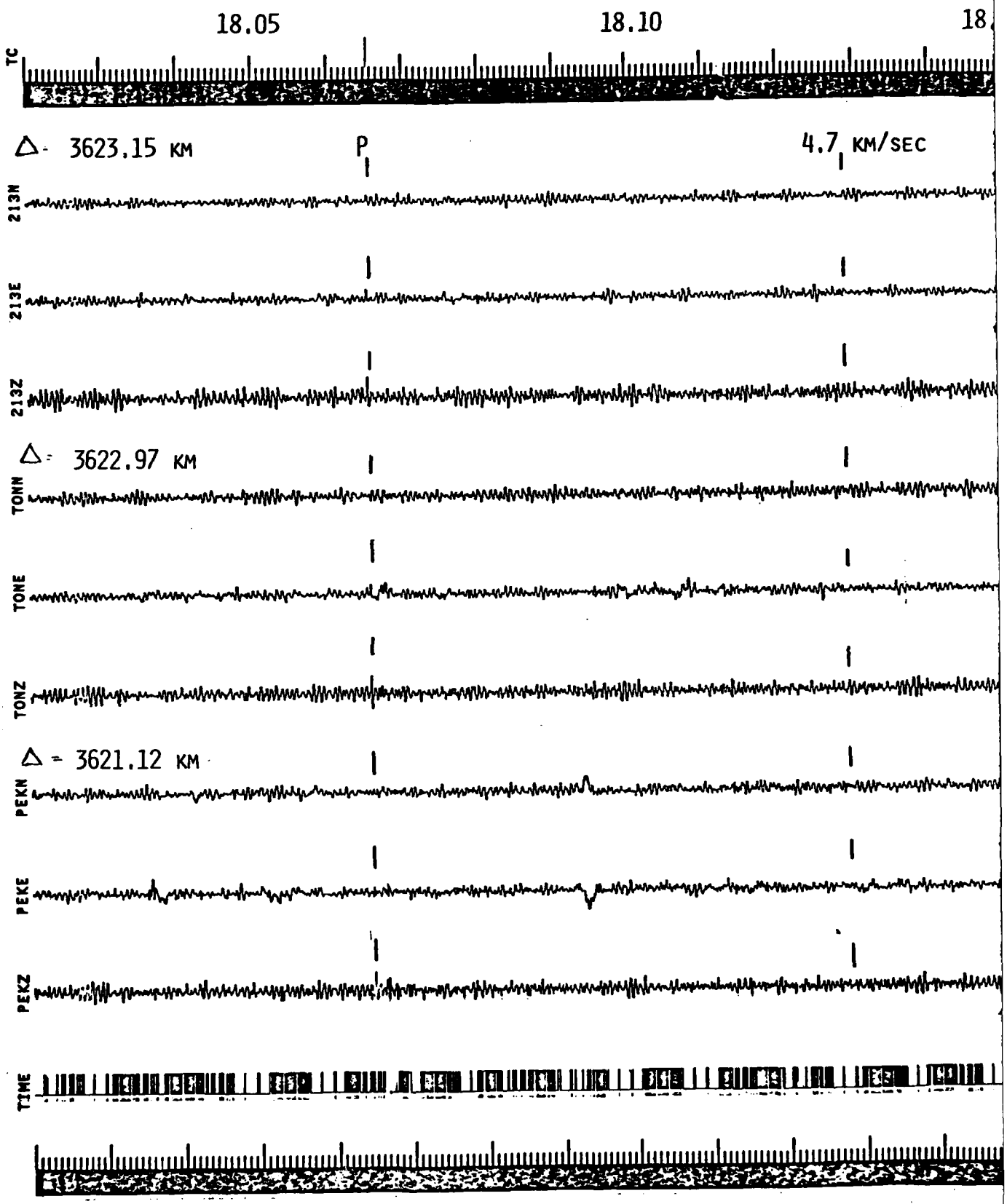

Figure 2-2. HARZER total record -

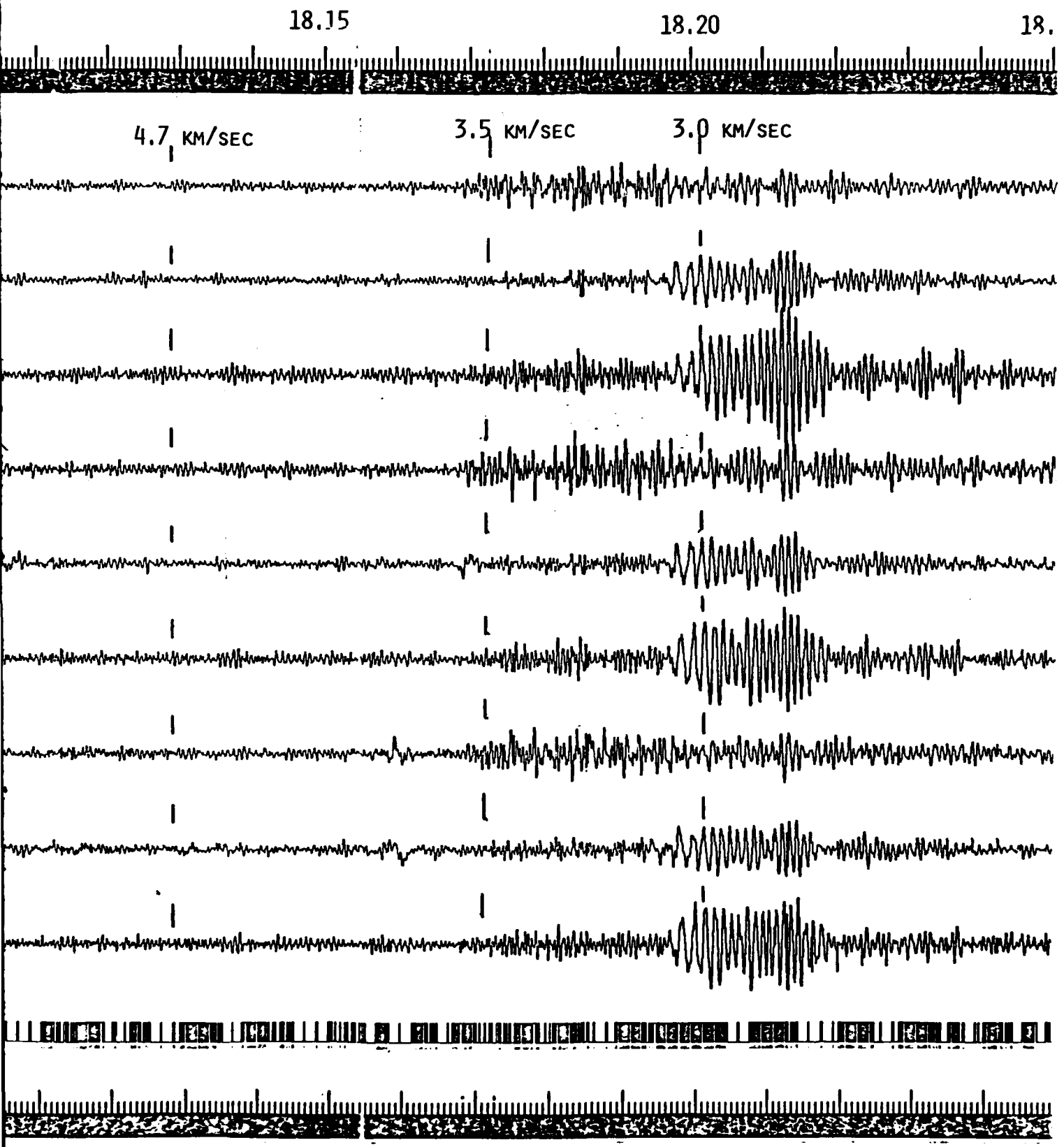

gure 2-2. HARZER total record - all components.

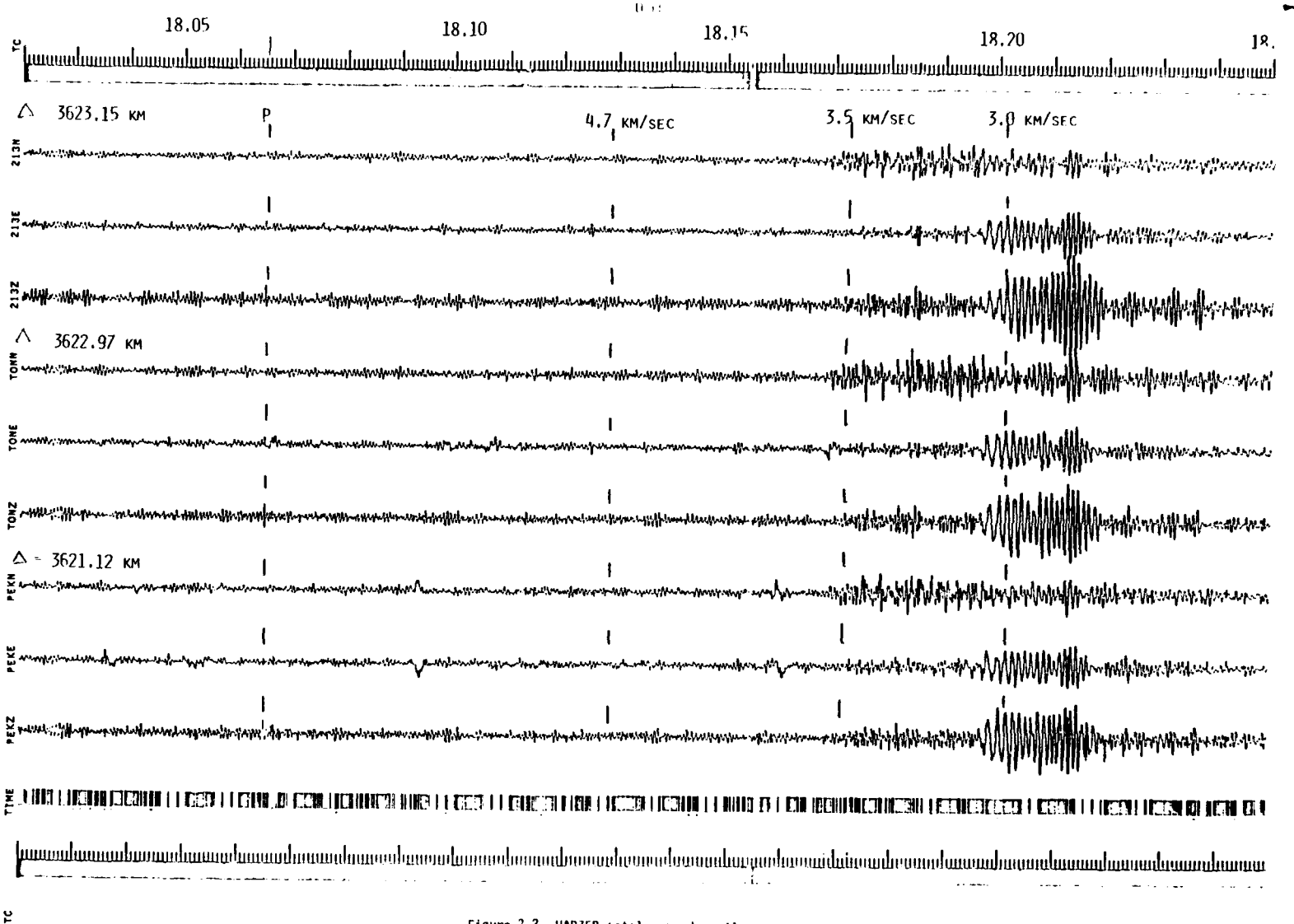

Figure 2-2. HARZER total record - all components.

Analysis and Discussion

I. HARZER P Waves

The P waves from the HARZER event, as recorded on the vertical component instruments of the array are shown on an expanded time scale in Figure 2-3 and on a very expanded time scale in Figure 2-4. Time and amplitude scales are shown on each figure.

A. P Wave Spectra

The vertical component P waves shown in Figures 2-3 and 2-4 were analyzed using an FFT program and then corrected for instrument response. The resultant amplitude spectra are presented in Figures 2-5, 2-6, and 2-7 for the 213Z, PEK Z and TON Z recordings respectively. From these figures, the following conclusions may be drawn.

i. The impulsive P waves have a broad spectrum extending between 1 hertz and .1 hertz (10 seconds) with amplitudes in this frequency range of approximately 1 to 5 μ.

ii. The spectral amplitudes and spectral shapes are essentially identical at all three stations. This can be seen even more clearly in Figure 2-8where all three spectra are superimposed (without instrument correction and thus are velocity spectra for frequencies greater than .1 hertz).

iii. Spectral amplitudes in the 1 to 2 hertz range are roughly 100 times smaller than those in the .1 to 1 hertz range.

iv. Spectral amplitudes at frequencies greater than 2 hertz drop off to a value another factor of 10 smaller than the peak amplitudes. The only exception is 213 Z which shows rising amplitudes in the 7 to 10 hertz region which is the result of transient cultural noise.

v. The rise in spectral amplitudes at frequencies lower than .1 hertz is spurious and results from the lack of accuracy in evaluating the longer period components because of the short duration of the data sample.

vi. In view of the spectral shape, we have not attempted to define a corner frequency or slope in the high frequency end of the spectra.

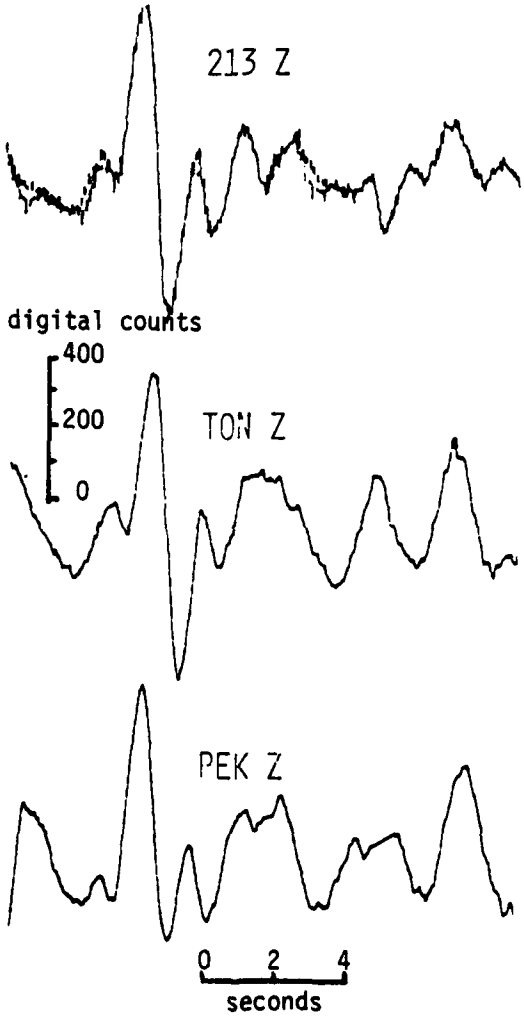

Figure 2-3. HARZER P waves.

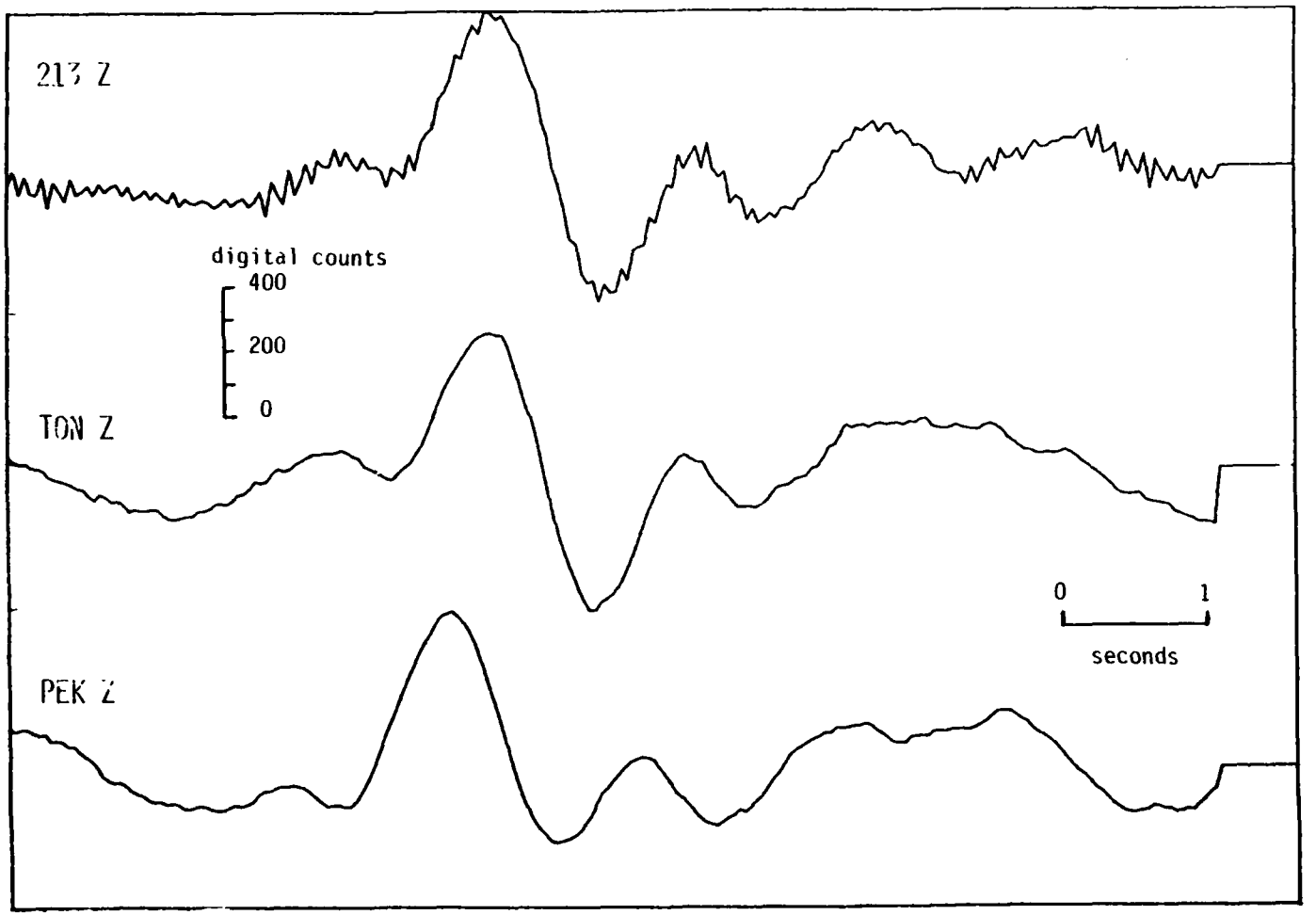

Figure 2-4. HARZER P waves.

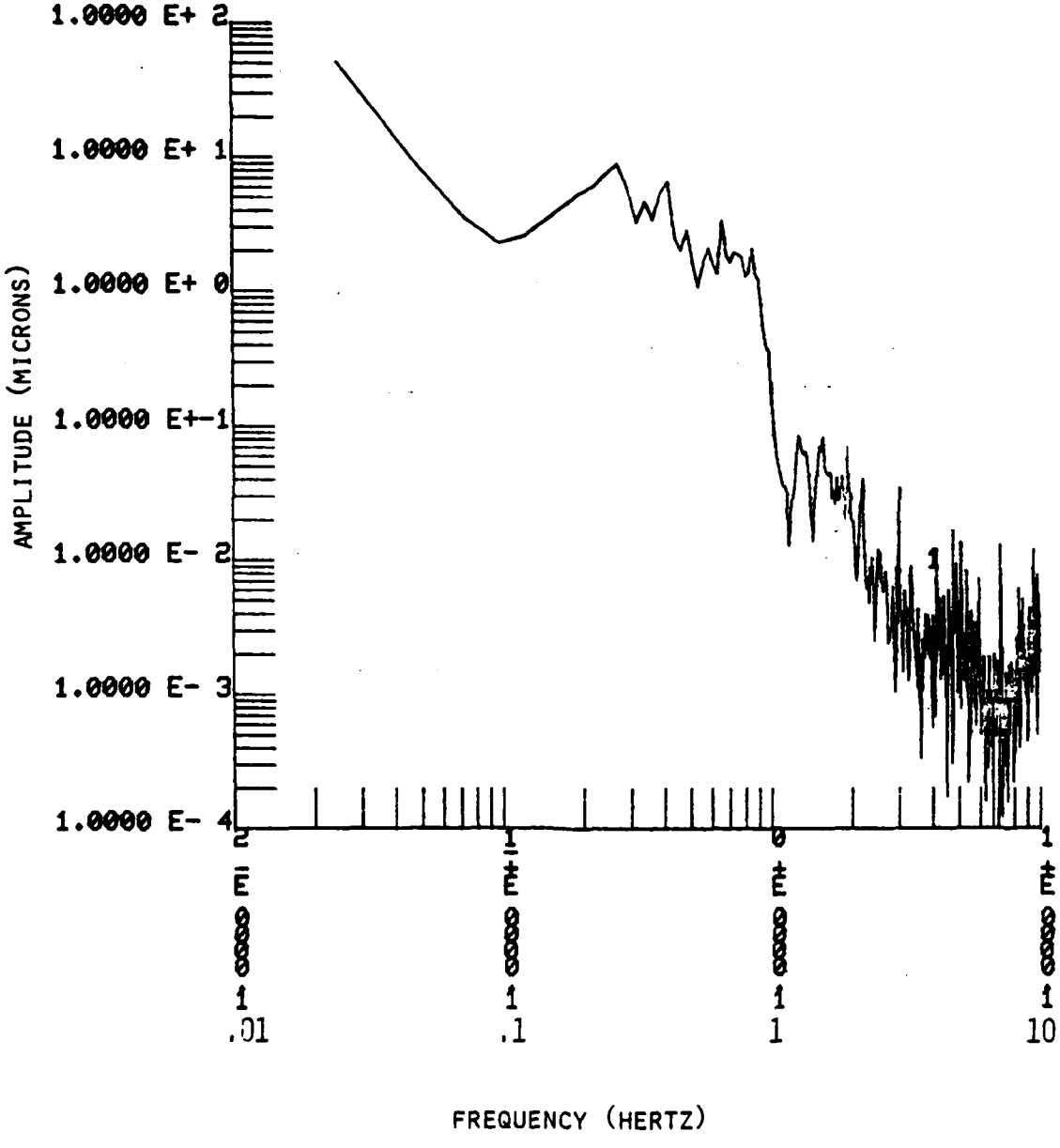

Figure 2-5 HARZER P wave spectrum. 213 Z

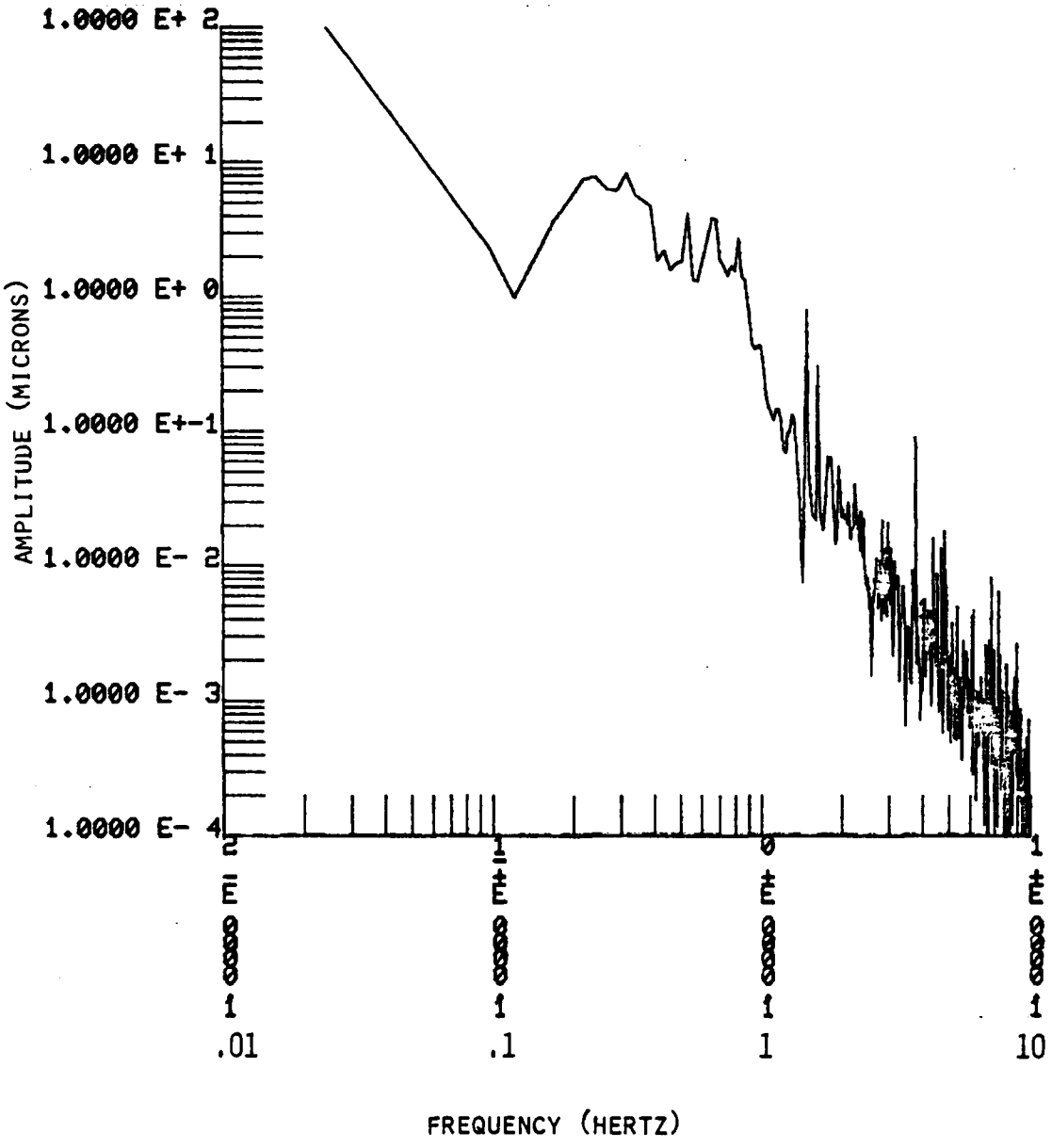

Figure 2-6. HARZER P wave spectrum. TON Z

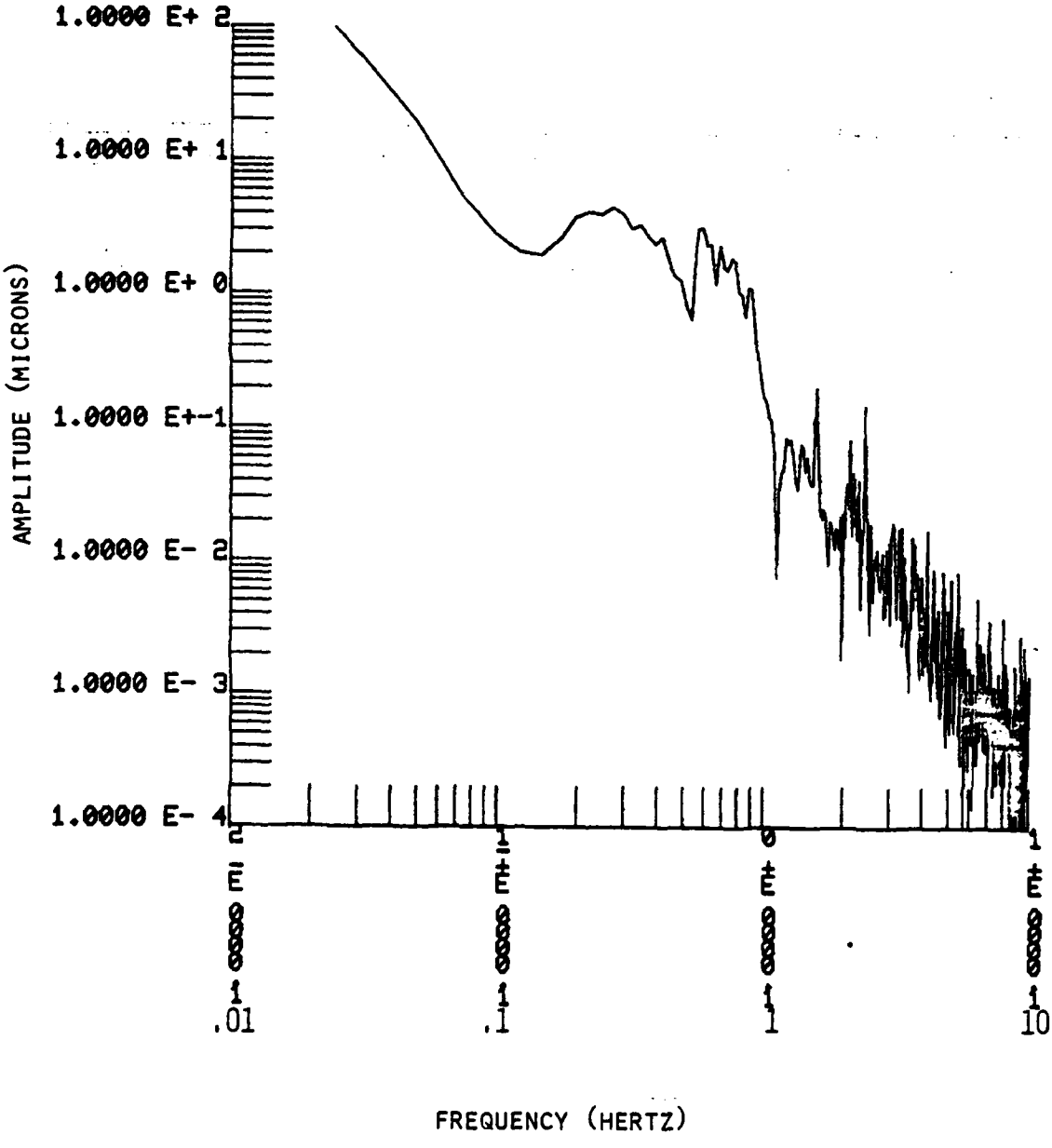

Figure 2-7. HARZER P wave spectrum. PEK Z

B. P Wave Cross Correlation

Using the raw P wave data (i.e. no instrument correction), cross correlation of the data was performed on each two component combination of the P wave time series. The results of the cross correlation are shown in Figures 2-8, 2-9, and 2-10 for the combinations 213 Z and TON Z, 213 Z and PEK Z and TON Z and PEK Z respectively. The lower two traces are the time series used in the cross correlation and the upper trace is the resultant correlation function. The horizontal lag is in samples (25 samples = 1 second).

As we anticipated from a visual analysis of the expanded time series and the results of the spectral analyses, the cross correlation functions show very high maxima indicating almost perfect correlation between the recordings at the individual stations.

The maxima of the correlation functions are:

213 Z and TON Z	.9661
213 Z and PEK Z	.9248
TON Z and PEK Z	.8747

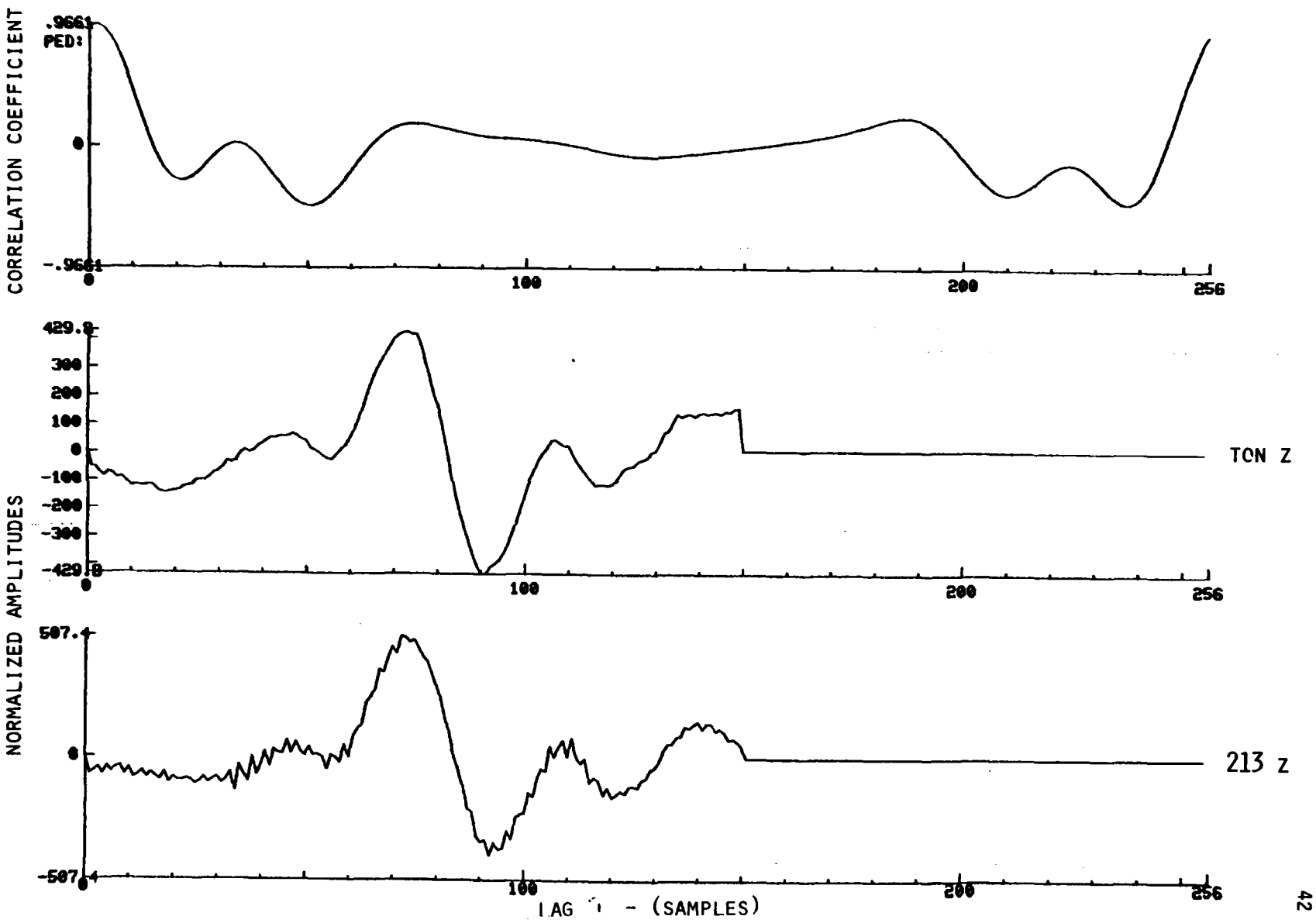

Figure 2-8. HARZER P waves -- cross correlation 213 Z and TON Z.

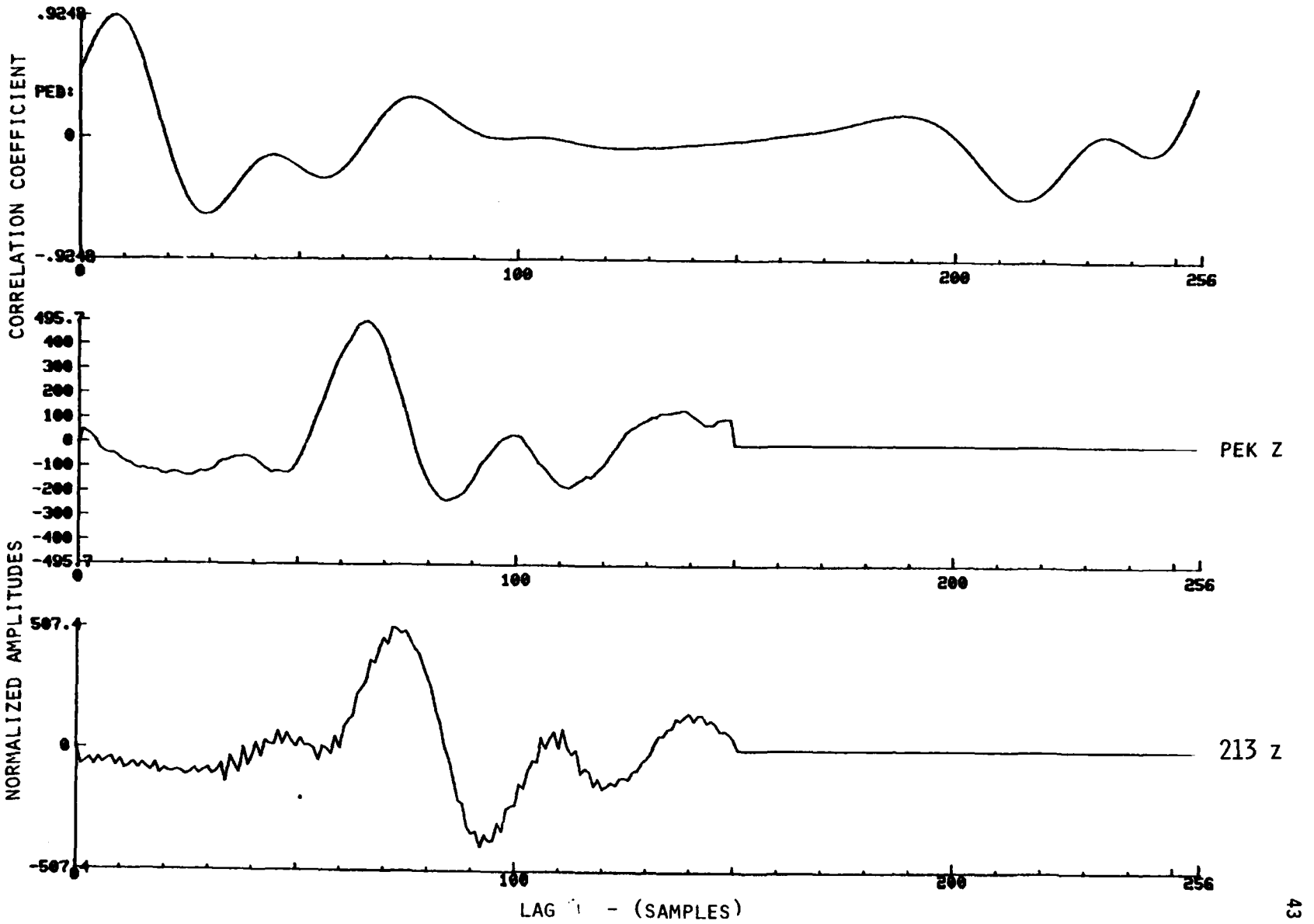

Figure 2-9. HARZER P waves - cross correlation 213 Z and PEK Z

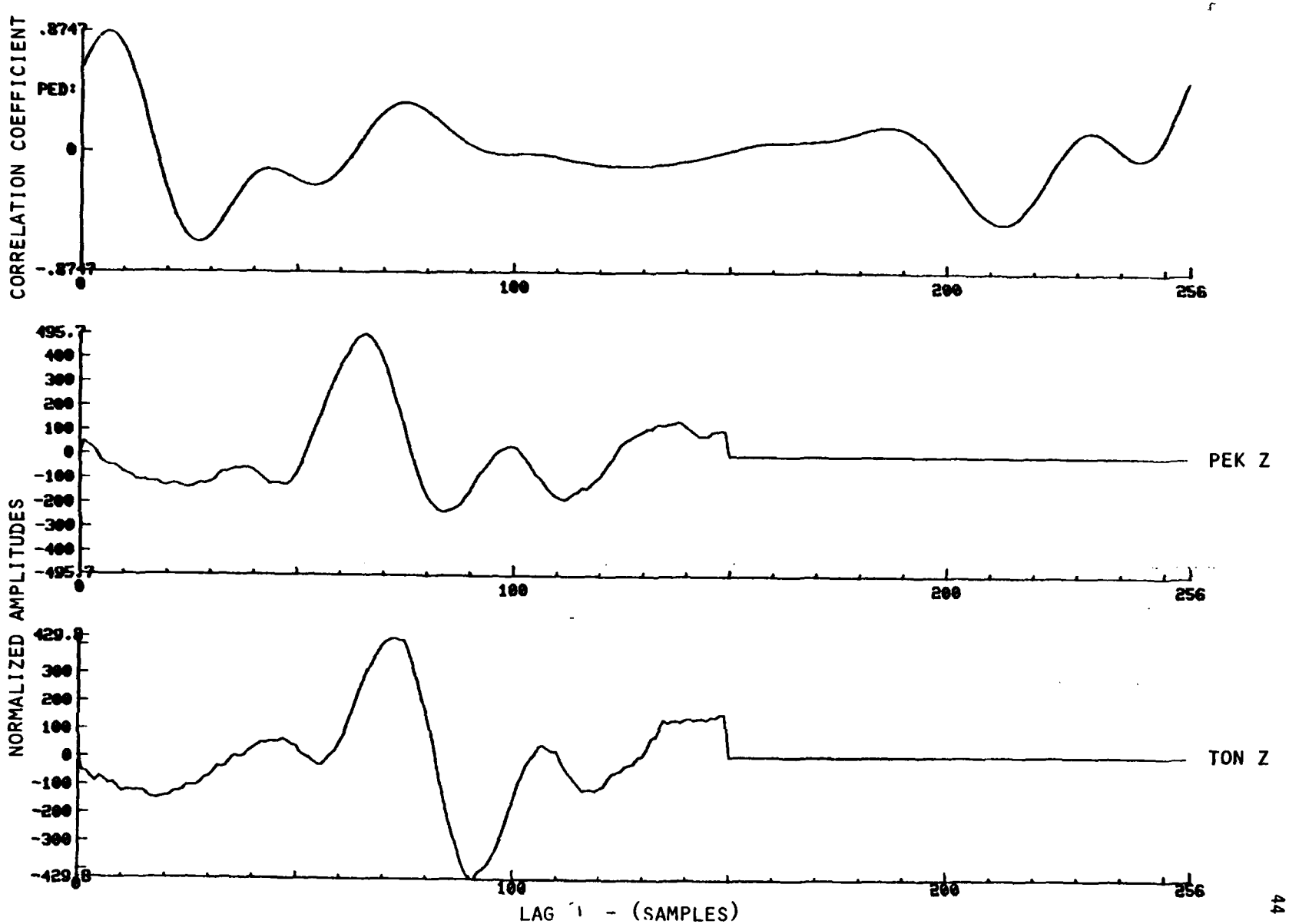

Figure 2-10. HARZER P waves - cross correlation TON Z and PEK Z

C. P Wave Coherence

To investigate the coherence of the P waves across the array, we analyzed the three combinations of vertical component recordings using the 9 second data sample shown in Figure 2-3. Because of the short duration of the data sample, it was not possible to obtain coherence values at frequencies less than approximately .4 hertz but the results are significant and instructive. Coherence data as a function of frequency are shown in Figures 2-11, 2-12, and 2-13 for the combinations 213 Z and TON Z, 213 Z and PEK Z, TON Z and PEK Z,respectively, using the 9 second data sample. The following conclusions can be drawn from these plots:

1. For the 9 second data sample (pure P waves more or less), the coherence at frequencies less than 1 hertz is very high (.8-.9). Based on the spectral character and the cross-correlation, we would expect it to remain high to about .1 hertz.
2. At frequencies greater than 1 hertz, the coherence drops rapidly for the station combinations TON Z and PEK Z and 213 Z and PEK Z.
3. Surprisingly, coherence values between .4 and .6 are observed at frequencies between 1 and 2 hertz for the station pair 213 Z and TON Z and a spike in the coherence in this frequency range is observed for the station pair 213 Z and PEK Z.
4. There are several single frequency spikes observed in these plots at frequencies greater than 2 hertz. These spikes are not significant as we will see below.

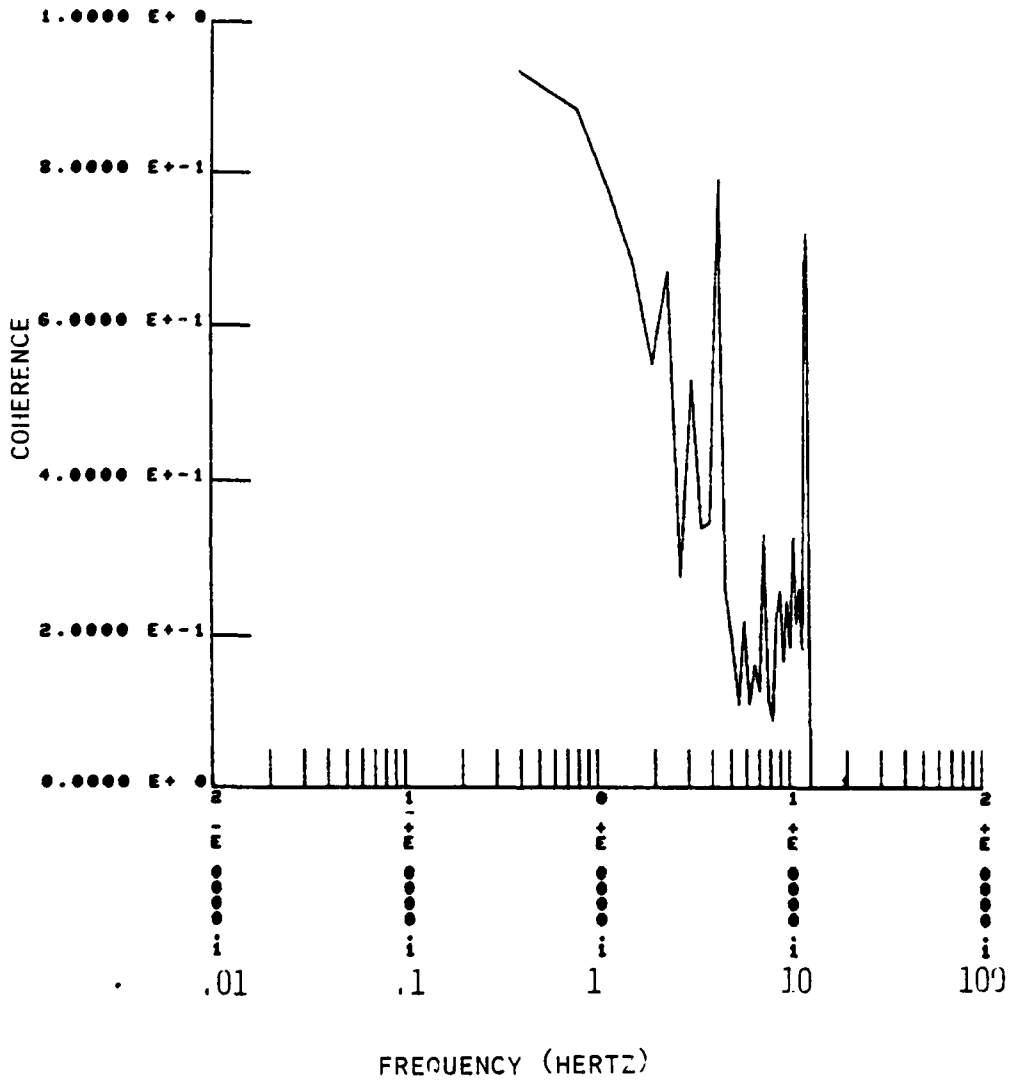

Figure 2-11. HARZER P wave coherence vs. frequency. 213 Z and TON Z. 9 seconds of data.

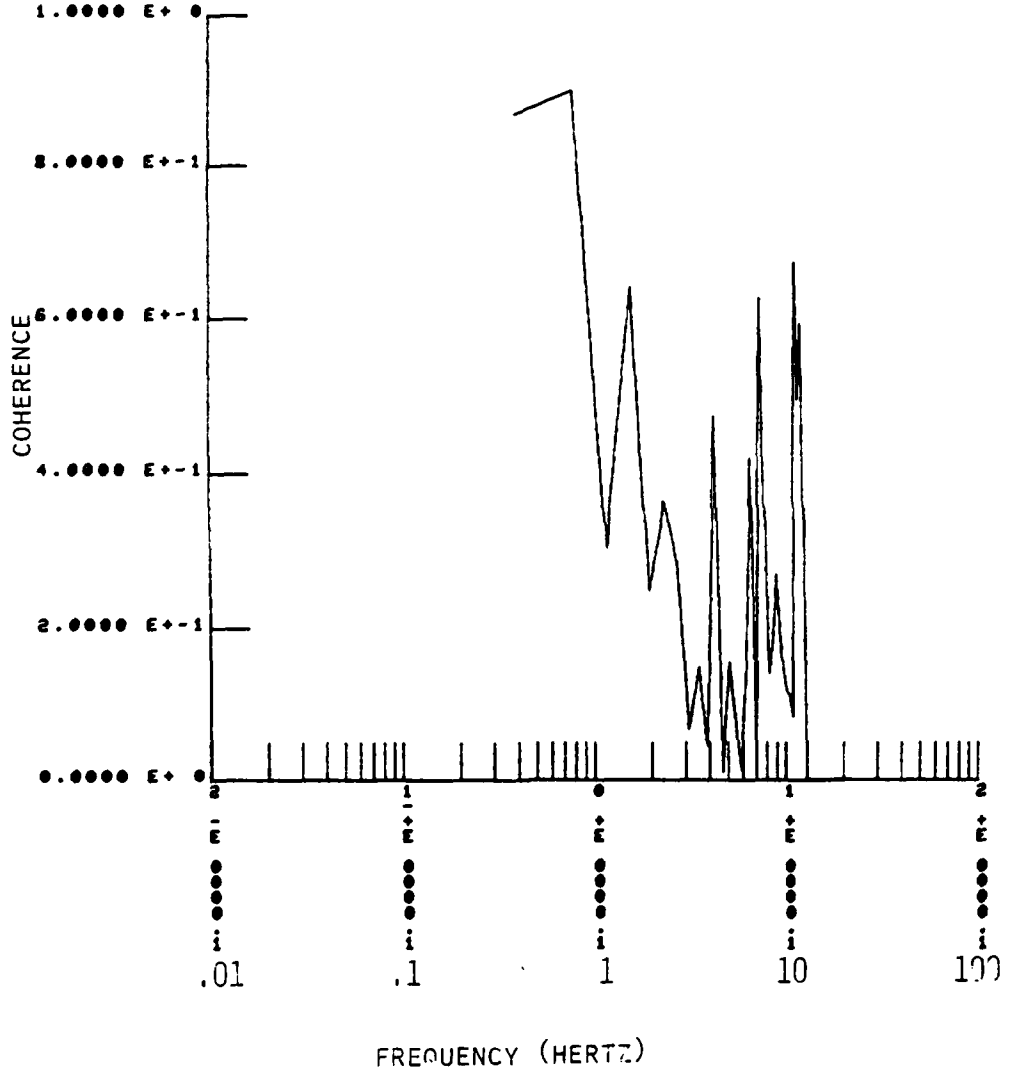

Figure 2-12 HARZER P wave coherence vs. frequency. 213 Z and PEK Z. 9 seconds of data.

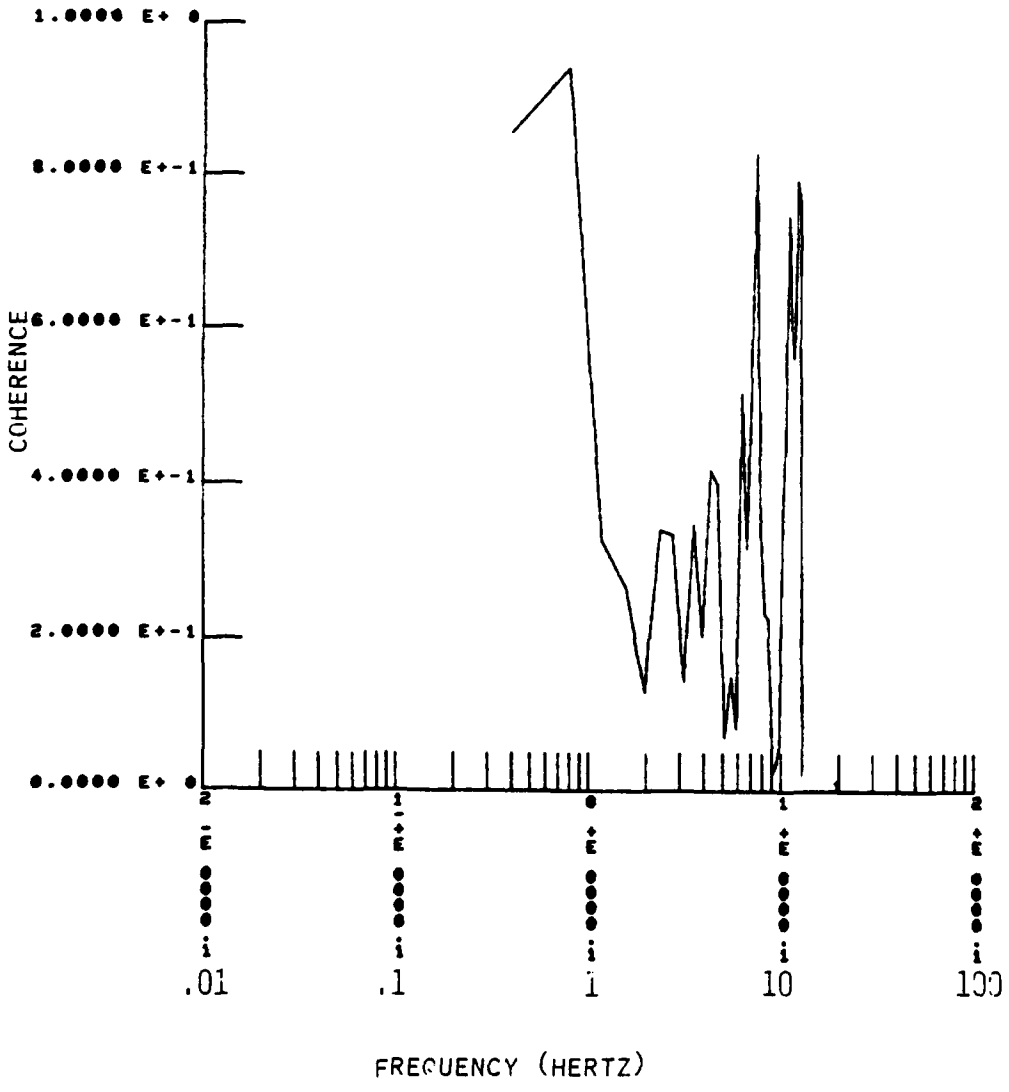

Figure 2-13 HARZER P wave coherence vs. frequency. TON Z and PEK Z. 9 seconds of data.

D. P Wave Signal to Noise Ratios

Signal to noise ratios have been computed for each of the vertical component P waves recorded on the array. The results of these analyses are presented in Figures 2-14, 2-15, and 2-16 for the 213 Z, TON Z, and PEK Z records, respectively The ratios were determined by dividing, frequency by frequency, the amplitude spectra of the P waves as recorded at the station (Figures 2-5, 2-6, and 2-7) by the noise spectra for the 40 second window immediately preceding the P wave on that instrument. These noise spectra are presented in Rondout Associates, Incorporated Technical Report CSA-RAI-81-03.

In evaluating these signal to noise ratios, the original spectra must be kept carefully in mind. For all three plots of the signal to noise ratio, values for frequencies greater than 1 hertz, fall, on the average, in the range of 1 to 2 with extremely wide scatter. The wide scatter is the result of division of a small number by a smaller number, and, in general has no meaning. The scatter could be significantly diminished by taking a moving window average over a number of frequencies. This would however, distort the information at frequencies less than 1 hertz and; for that reason, is not carried out here. The average values of signal to noise 1 to 2 at frequencies greater than 1 hertz are the result of the rapid drop-off of the noise toward higher frequencies. Thus, although the signal levels are sharply lower above 1 hertz, the noise levels are even lower.

The most important result is that the signal to noise ratio in the frequency band .3 to .8 hertz, is greater than 3 on all components.

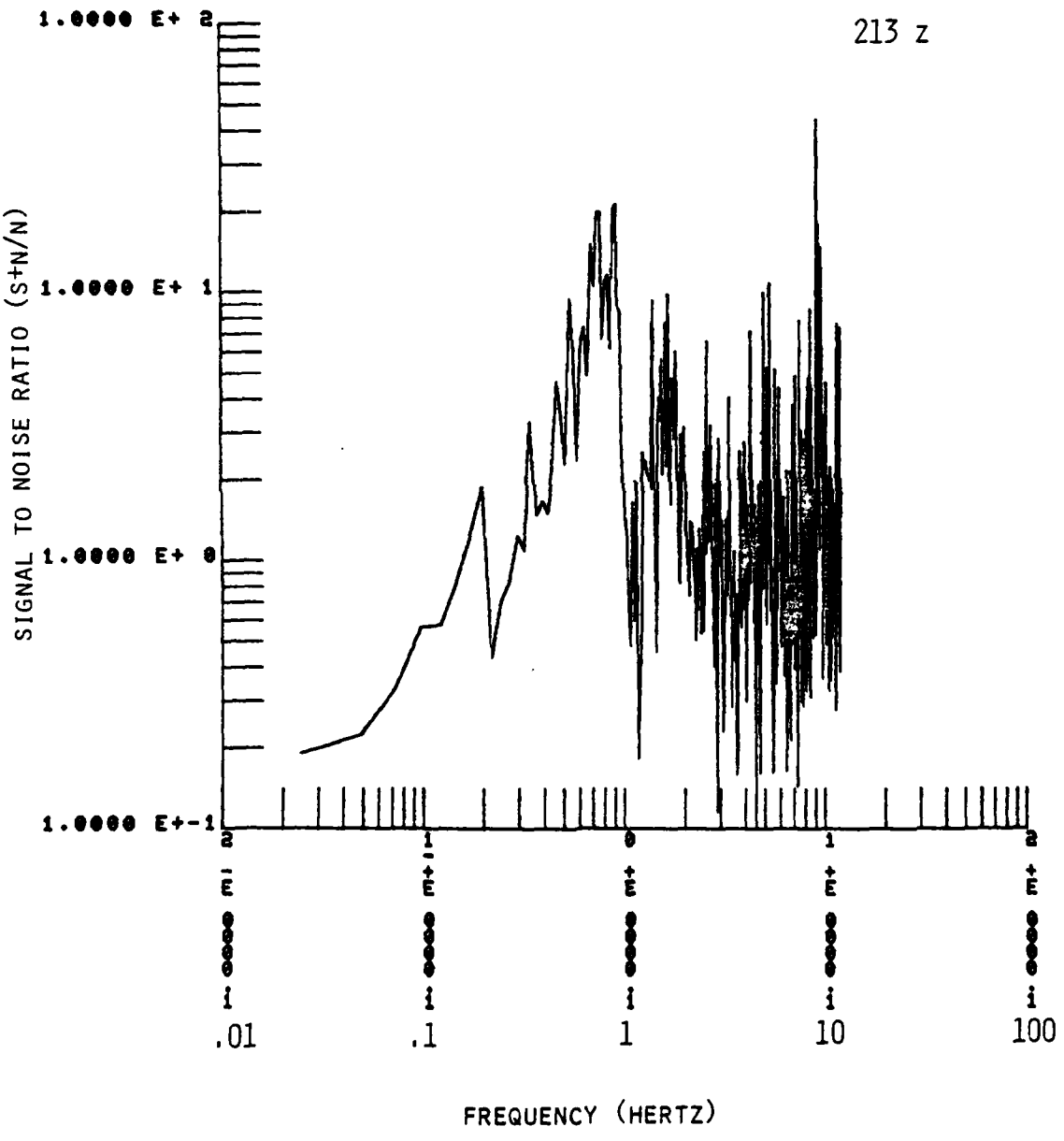

Figure 2-14 HARZER P wave signal to noise ratio. 213 Z

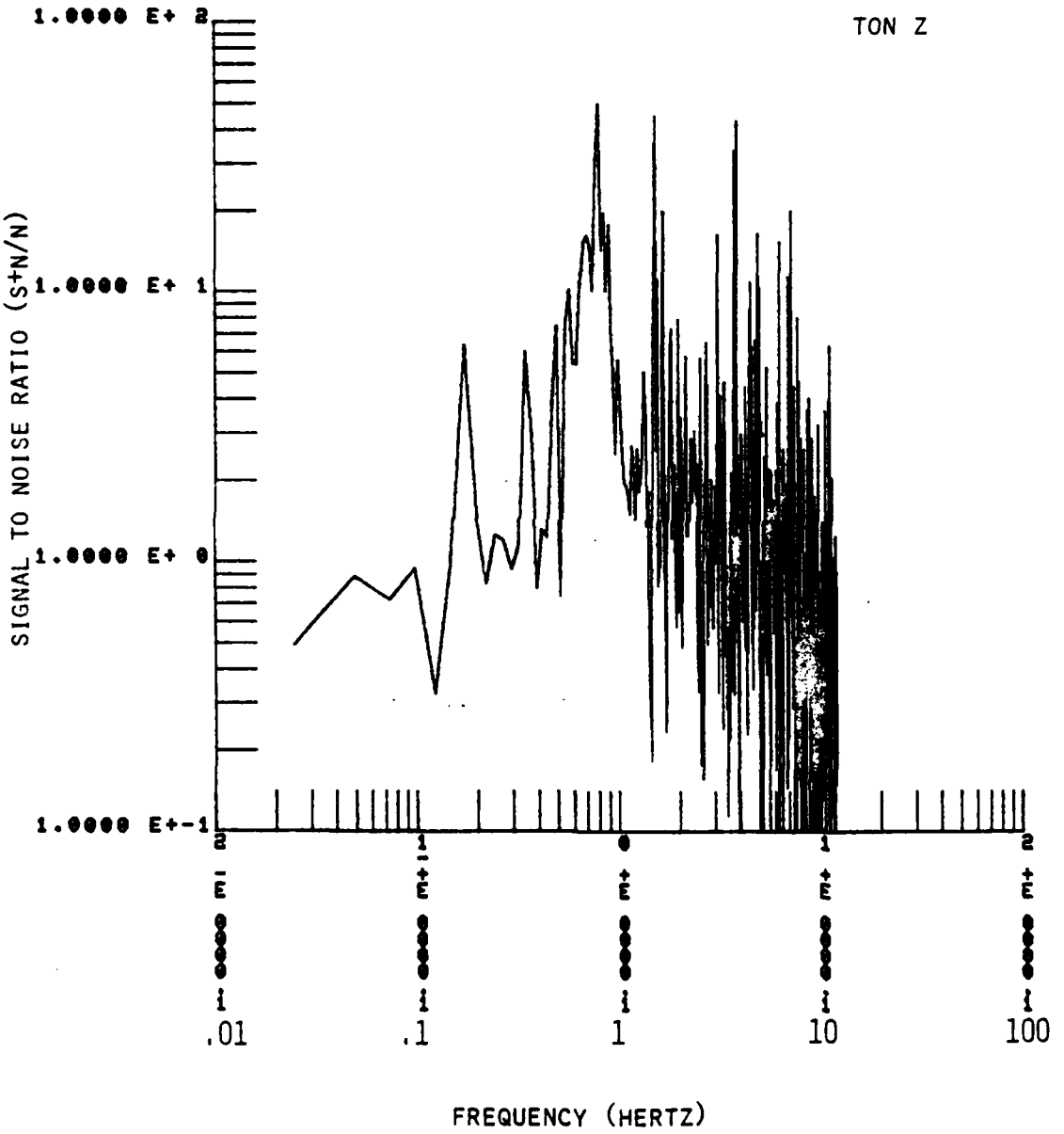

Figure 2-15. HARZER P wave signal to noise ratio. TON Z

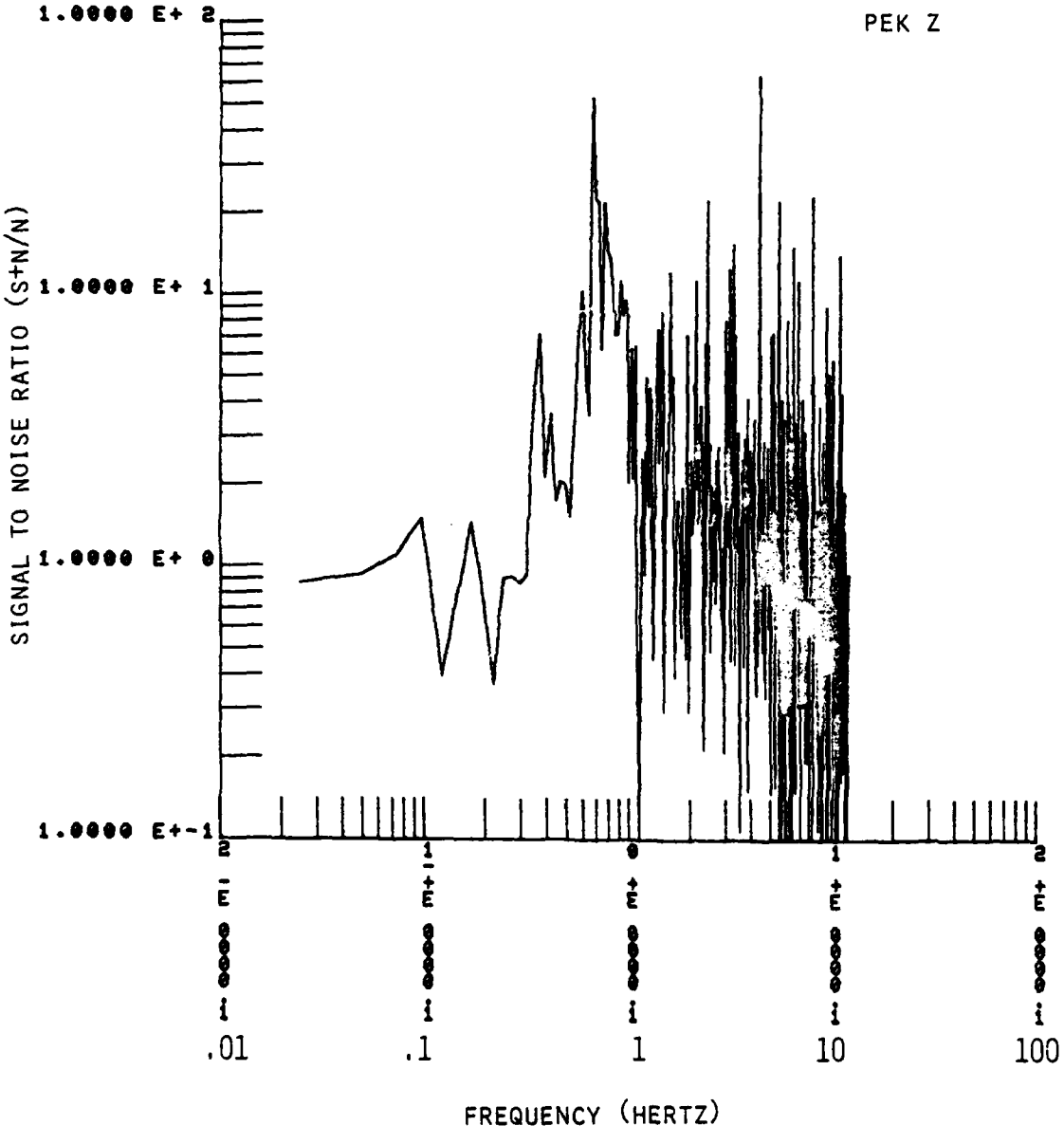

Figure 2-16. HARZER P wave signal to noise ratio. PEK Z

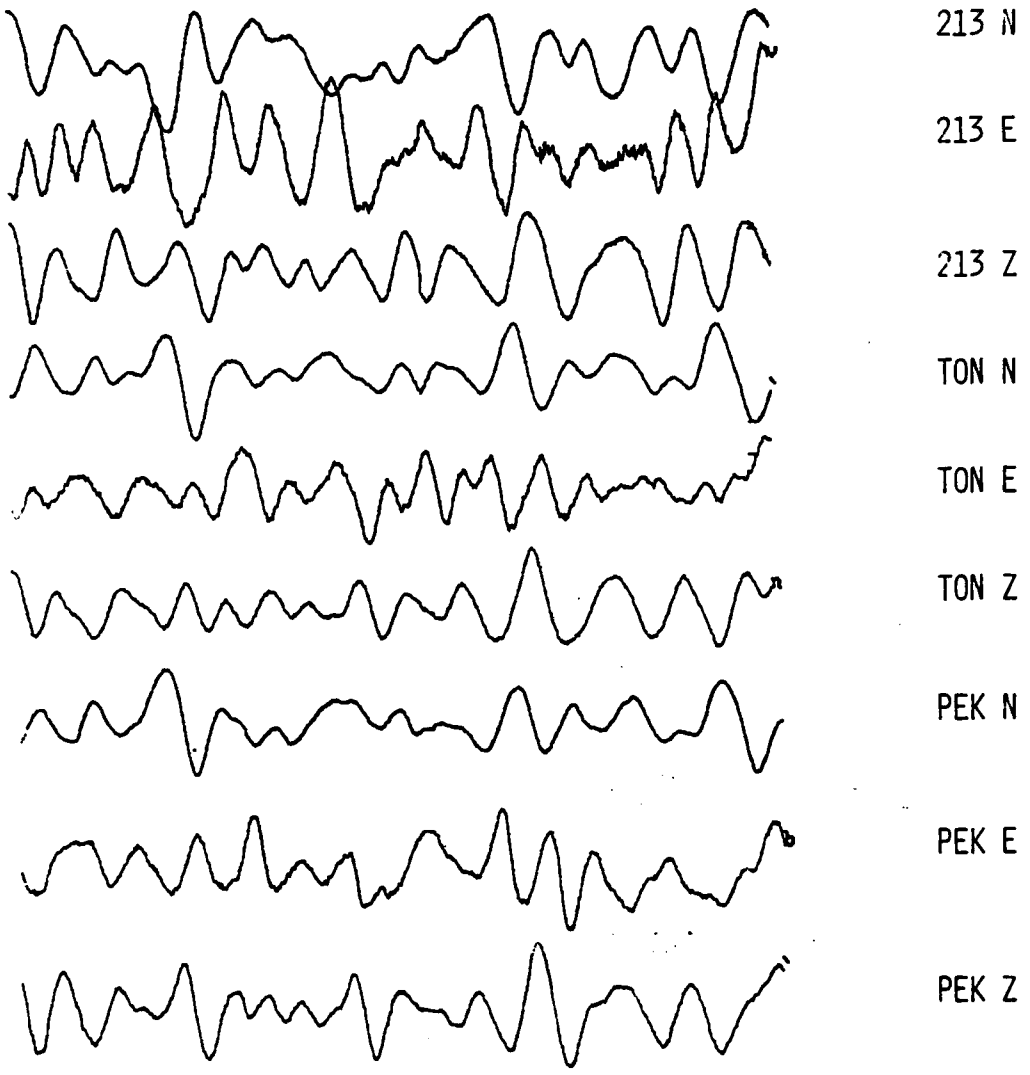

Figure 2-17. HARZER Lg waves.

II. HARZER Lg Waves

The entire Lg wave train can be seen in Figure 2-2. In the first part of this study of the Lg waves, we have analyzed a 40 second segment of Lg shown in Figure 2-17. In the portion of this study dealing with the coherence of Lg across the array, we have utilized a 120 second sample of the data which consitutes essentially the entire Lg wave train. That data sample is shown in Figure 2-24.

A. Lg Wave Spectra

The Lg wave displacement spectra for three vertical components of the array are presented in Figures 2-18 to 2-20. Important features of these plots and those of the other components are:

1. Lg amplitudes are highest on the transverse (N-S) component and lowest on the longitudinal (E-W) component as observed visually.
2. The shape of all of the Lg spectra are remarkably similar although spectral amplitude differences as great as a factor of 10 can be observed between components.
3. The amplitude spectra fall off at approximately 18 db/octave across the entire frequency band .1 to 10 hertz.
4. Significant variations in the drop off occur only in the 2 to 9 second period range ($\sim$.1 to .5 hertz). This confirms the visual observation that Lg, for this event at this distance range, appears to have the same frequency content as the predominant background noise. Lg is thus a relatively narrow band signal and frequency filtering alone will not allow significant enhancement of the signal to noise ratio.

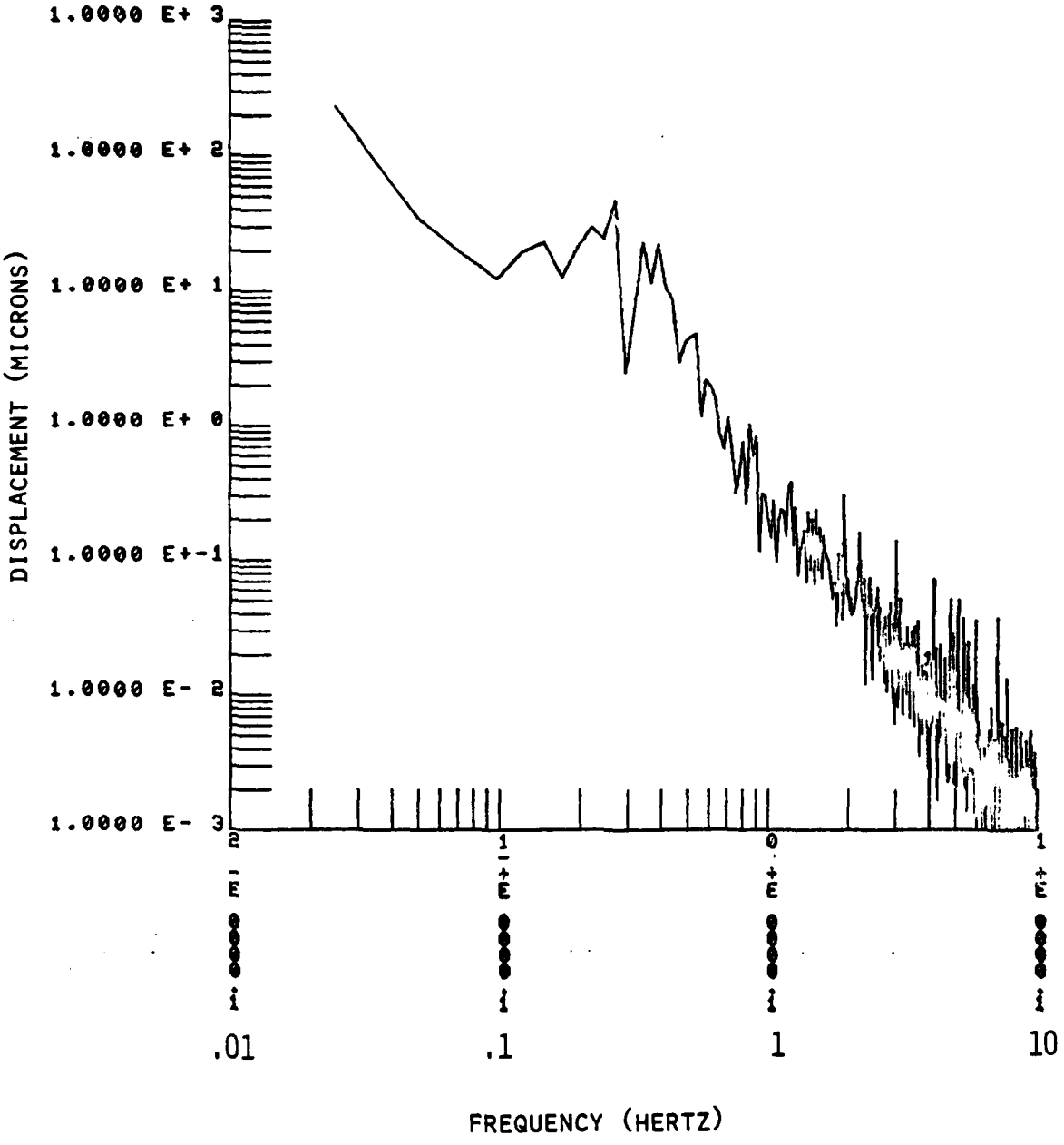

Figure2-18.HARZER Lg wave spectrum. 213 Z

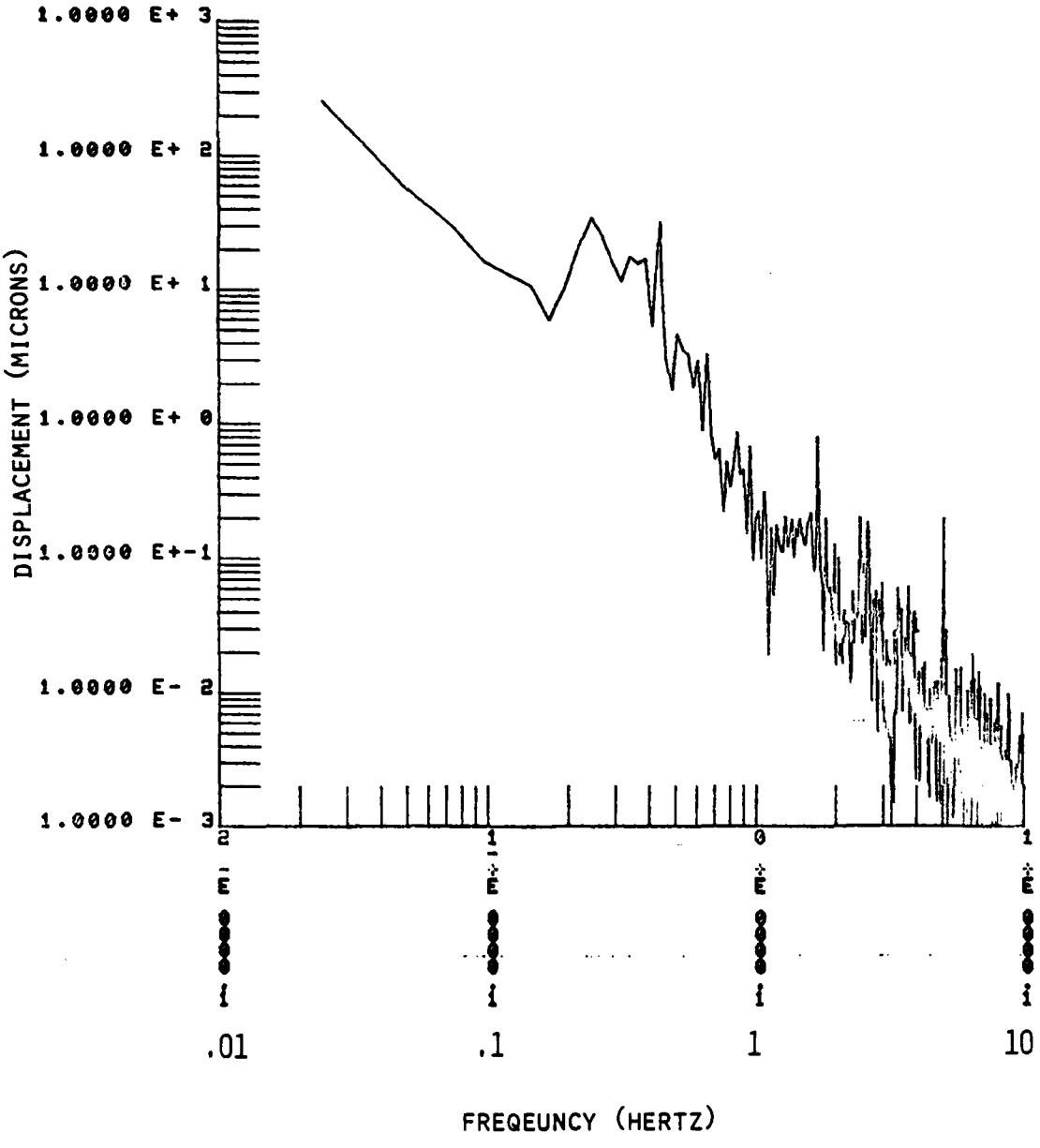

Figure 2-19. HARZER Lg wave spectrum. TON Z

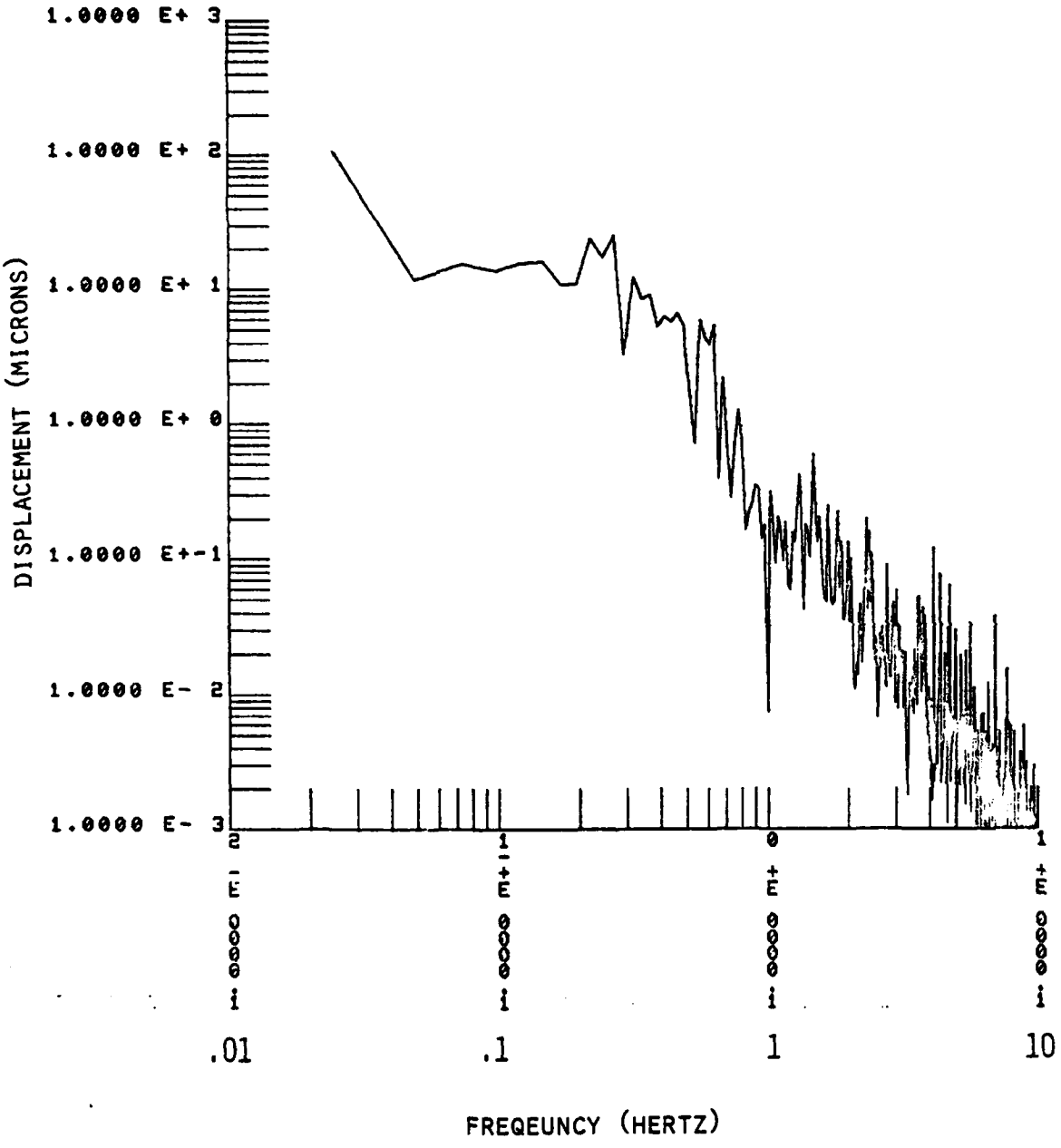

Figure 2-20. HARZER Lg wave spectrum. PEK Z

B. Lg Wave Cross Correlation

Using the 40 second sample of Lg depicted in Figure 2-17, cross correlation between all station pairs were carried out. The results of the cross correlations of the verticals are presented in Figures 2-21 to 2-23. In these figures, as for the P waves discussed earlier, the bottom two traces are the time series as recorded at the two stations and the top trace is the cross correlation in samples (25 samples equals 1 second). The results of the cross correlation are tabulated in Table 2-3. There are several important aspects of this data. These include the following:

1. Relatively high correlation is observed between the vertical pairs (.71 to .83).
2. Low correlation values are observed for the station pairs 213 E and PEK E and 213 E and TON E. These low correlation values are probably the result of the low signal to noise ratios on the east-west instruments which results in approximately equal mixtures of signal and noise at each station. A higher correlation ($\sim$.66) is observed for the station pair TON E and PEK E.
3. High correlation values between all north-south station pairs are observed ($\sim$.76 to .86). The astute reader will realize at this point that the polarity of 213 N is reversed resulting in the minus value of the cross correlation.
4. The measured lags could be utilized to determine an 'average' phase velocity for this segment of Lg across the array. However, in a later study, we plan to do frequency-wave number analysis of this data and thus we defer phase velocity studies until that time.

TABLE 2-3

CROSS CORRELATION

Lg - 40 SECONDS OF DATA

213 Z AND TON Z	=	.8332
213 Z AND PEK Z	=	.7556
TON Z AND PEK Z	=	.7169
213 E AND PEK E	=	.4178
213 E AND TON E	=	.4838
TON E AND PEK E	=	.6576
213 N AND PEK N	=	-.8185
213 N AND TON N	=	-.7642
TON N AND PEK N	=	.8616

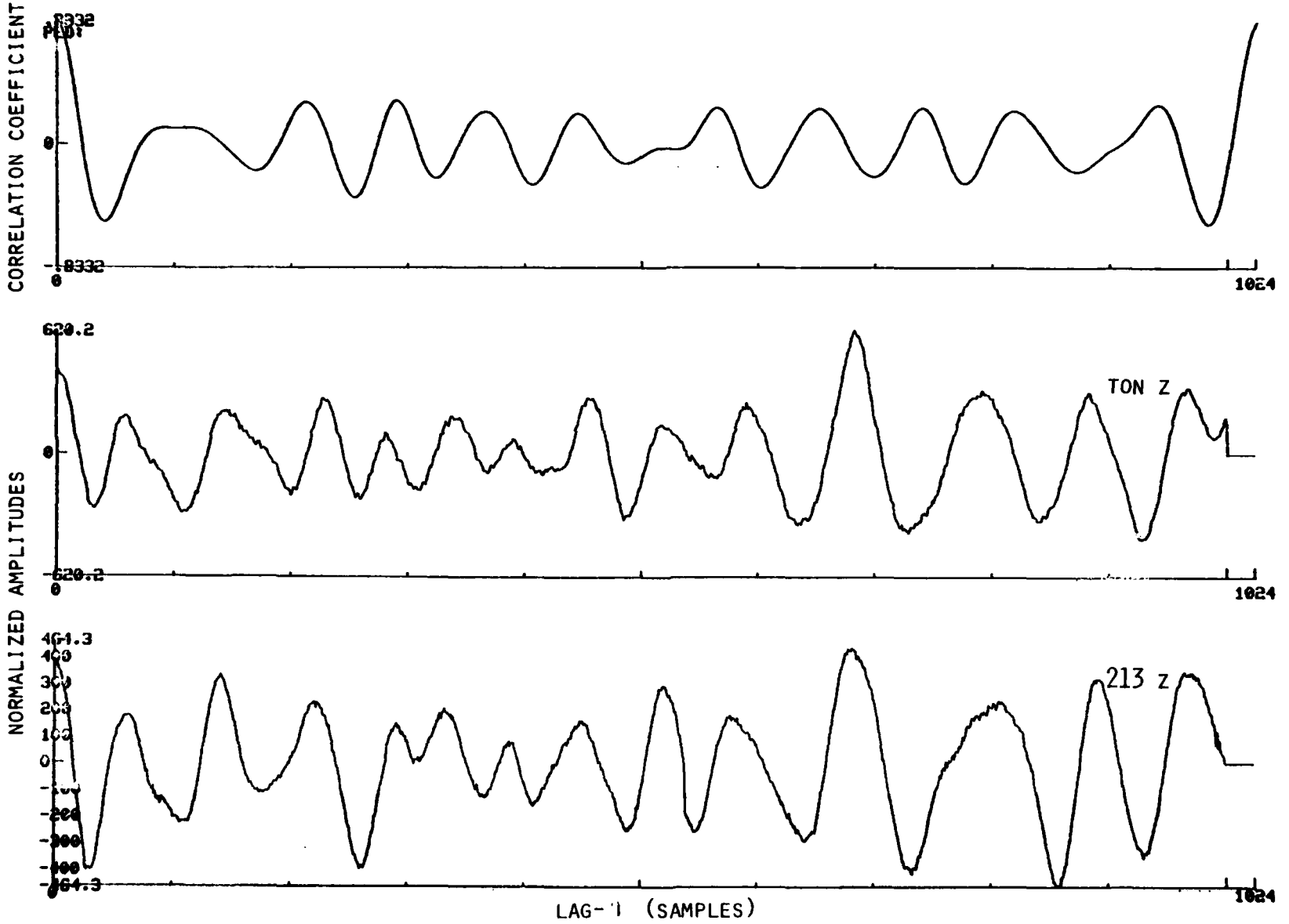

Figure 2-21 HARZER Lg waves - cross correlation 213 Z and TON Z.

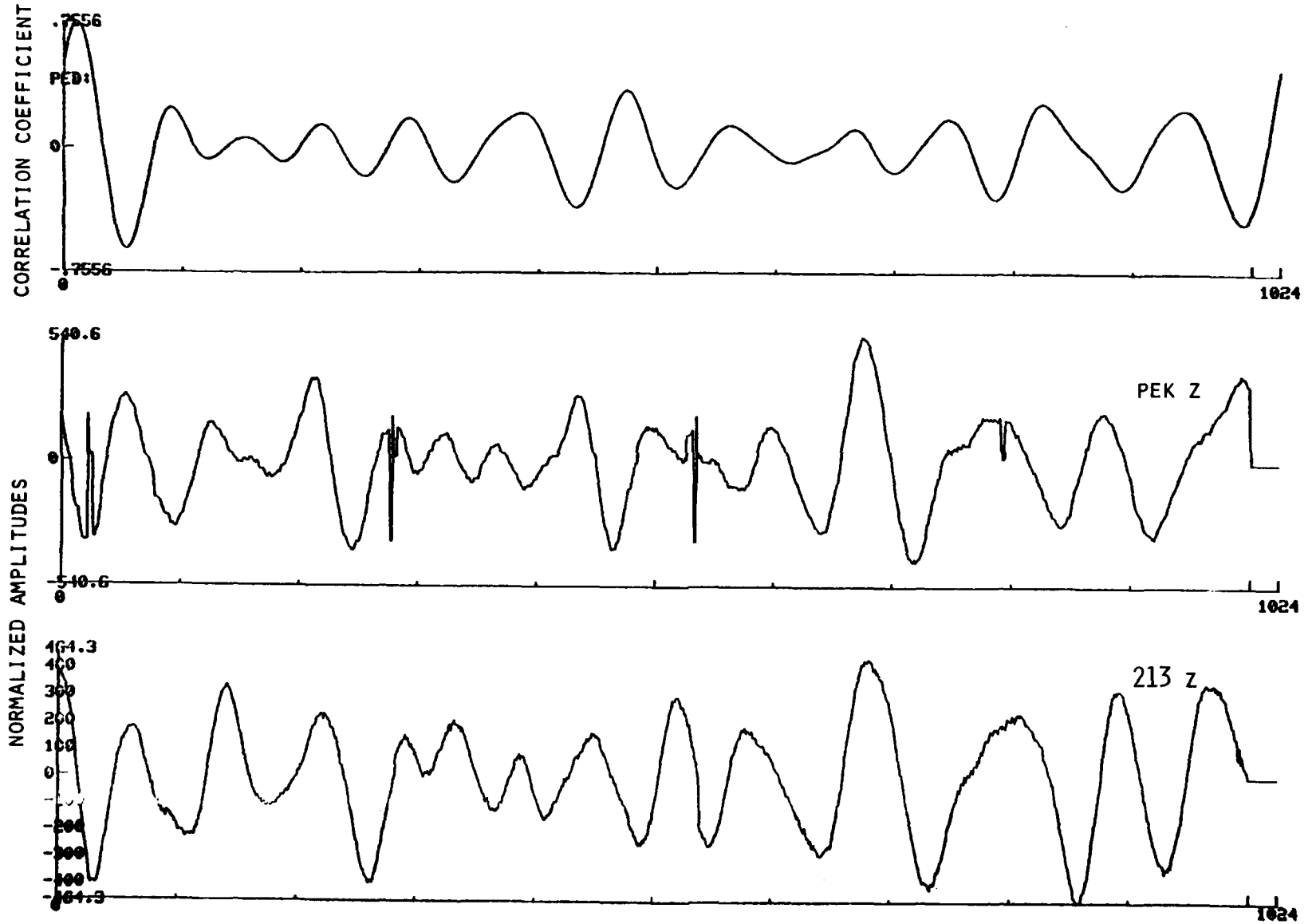

Figure 2-22HARZER Lg waves - cross correlation 213 Z and PEK Z.

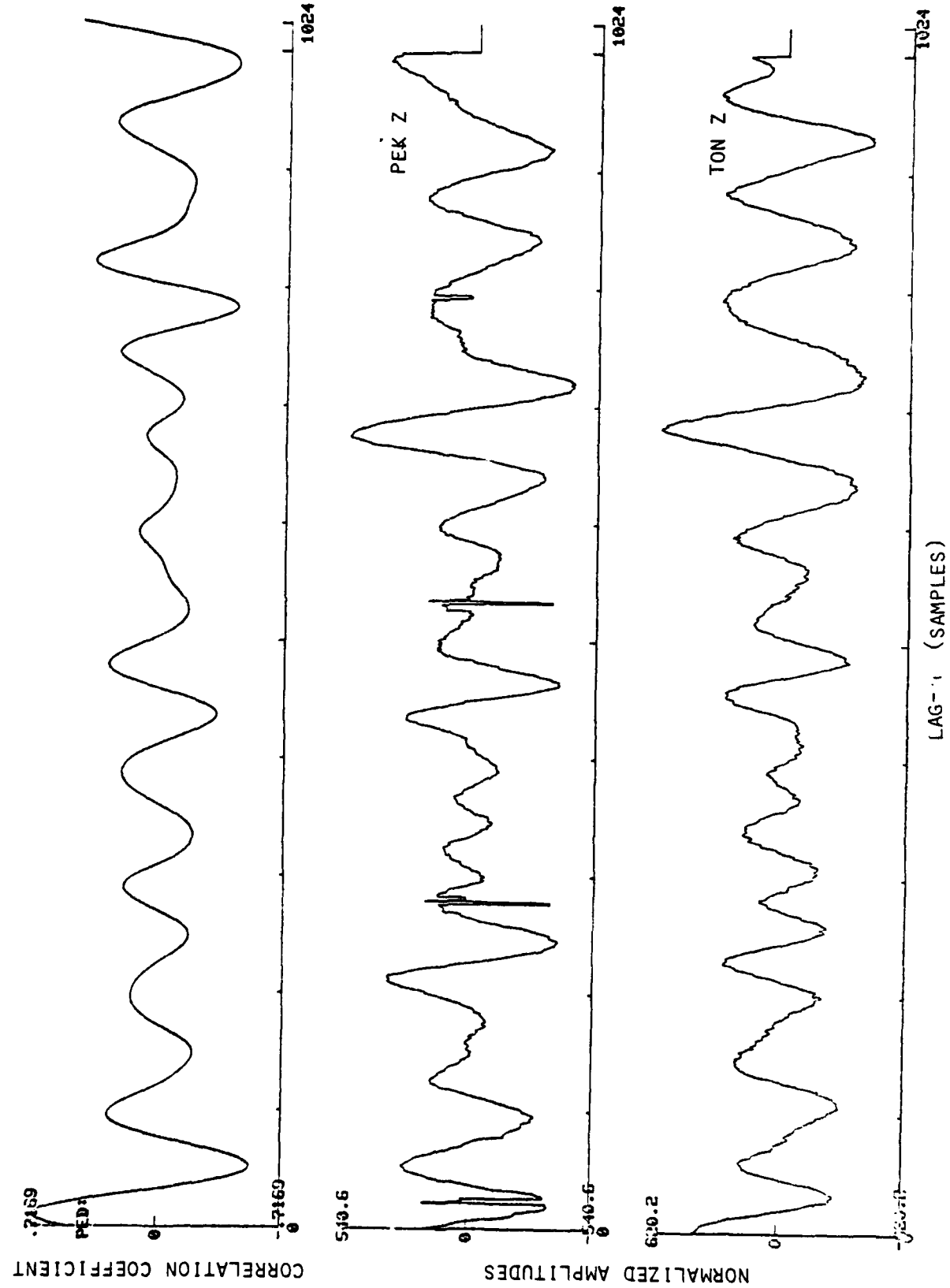

Figure 2-23 HARZER Lg waves - cross correlation TON Z and PEK Z.

C. Lg Wave Coherence

The data samples used here are 120 seconds long and are depicted for the vertical components in Figure 2-24. The results of the coherence analyses for the vertical components are presented in Figures 2-25 to 2-27. From the analyses of all nine components, the following conclusions can be drawn.

1. The coherence of Lg on all three of the north-south station pairs has a maximum value of approximately .8 in the frequency range .1 to .3 hertz. Coherence values fall off rapidly (as did the amplitude spectra) toward higher frequencies.

2. No coherent energy is observed at frequencies greater than 1 hertz.

3. The 213 E and TON E station pair exhibits a maximum coherence of about .75 at a frequency of approximately .2 hertz although the cross correlation of this pair was only .48. The TON E - PEK E combination exhibits a maximum coherence of about .55 at 5 seconds with no significant coherence at frequencies greater than .5 hertz. This combination had the relatively high (for the longitudinal or east-west component) value of .66 in the cross correlation section. The 213 E - PEK E combination has a maximum of approximately .55 at .1 hertz but that is a single data point and thus open to doubt. Otherwise, that station pair exhibits no significant coherence. This combination also showed a very low value (.4) in the cross correlation section.

4. All of the vertical combinations exhibit high coherence (.7-.8) in the frequency band .1 to .3 hertz. All of the vertical coherences drop precipitously at frequencies higher than .3 hertz. With the exception of the station pair 213 Z and TON Z which exhibits a sharp, relatively high ($\sim$.55) peak in the frequency band .5 to .7 hertz, no significant coherence is observed at frequencies greater than .3 to .4 hertz.

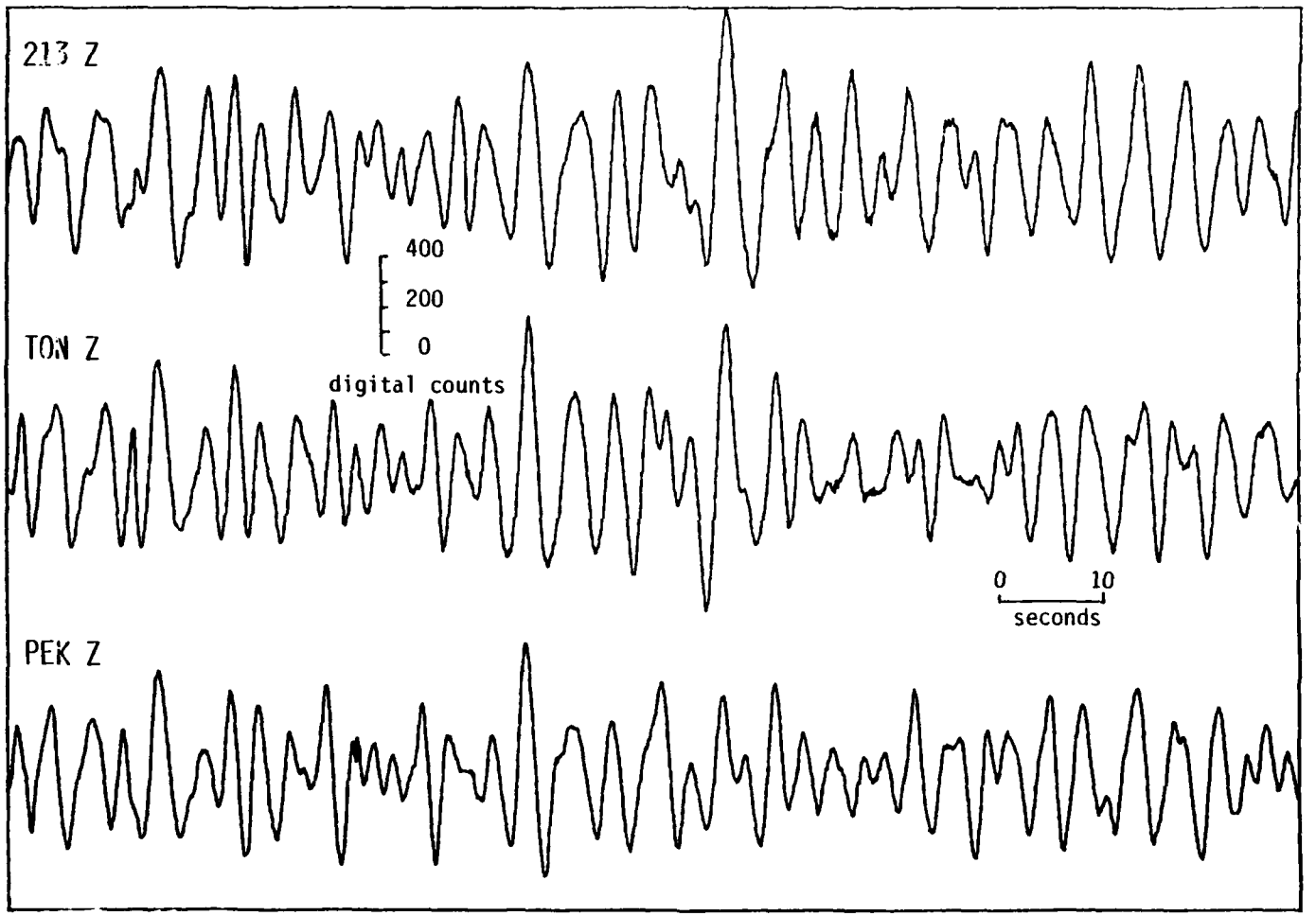

Figure 2-24.HARZER Lg waves. 120 seconds of data. 213 Z, TON Z and PEK Z.

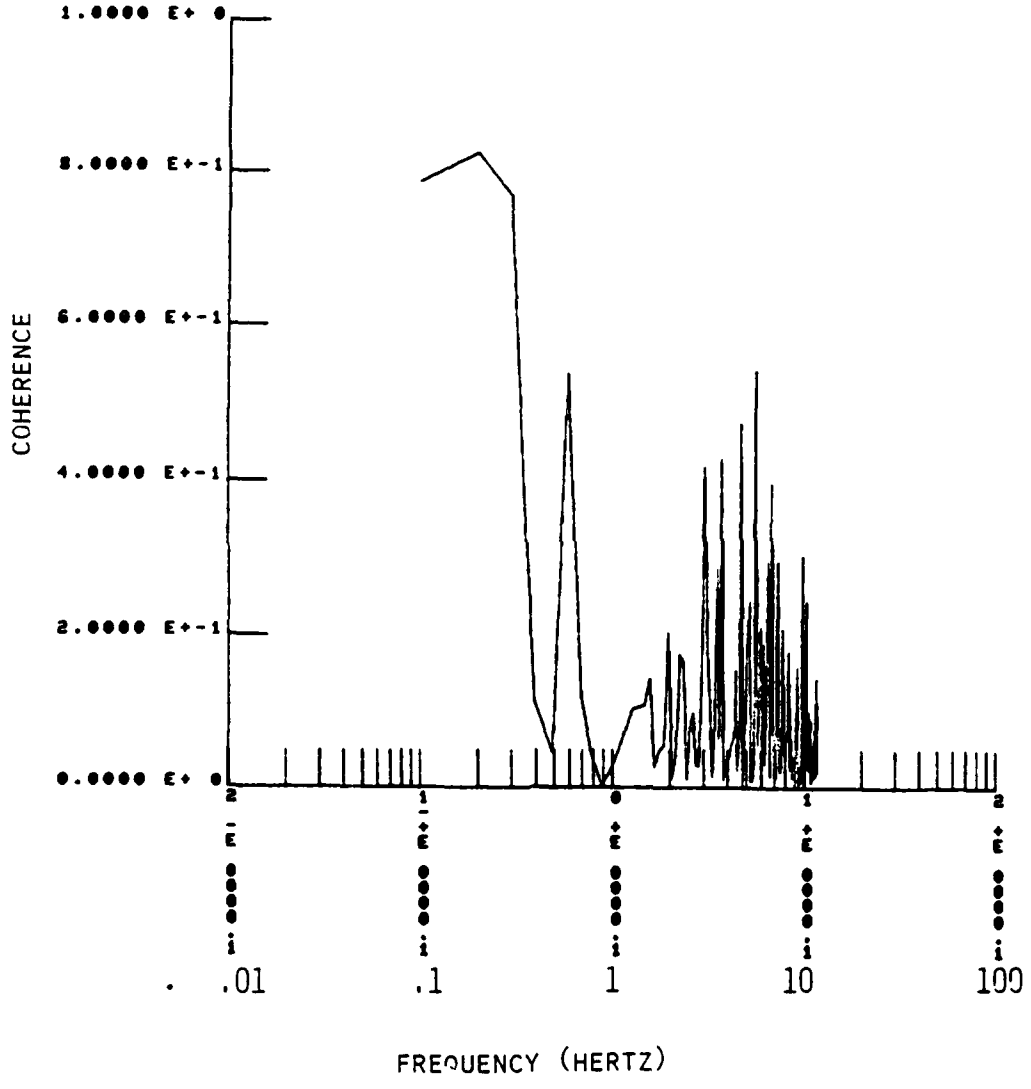

Figure 2-25 HARZER Lg wave coherence vs. frequency. 213 Z and TON Z. 120 seconds of data.

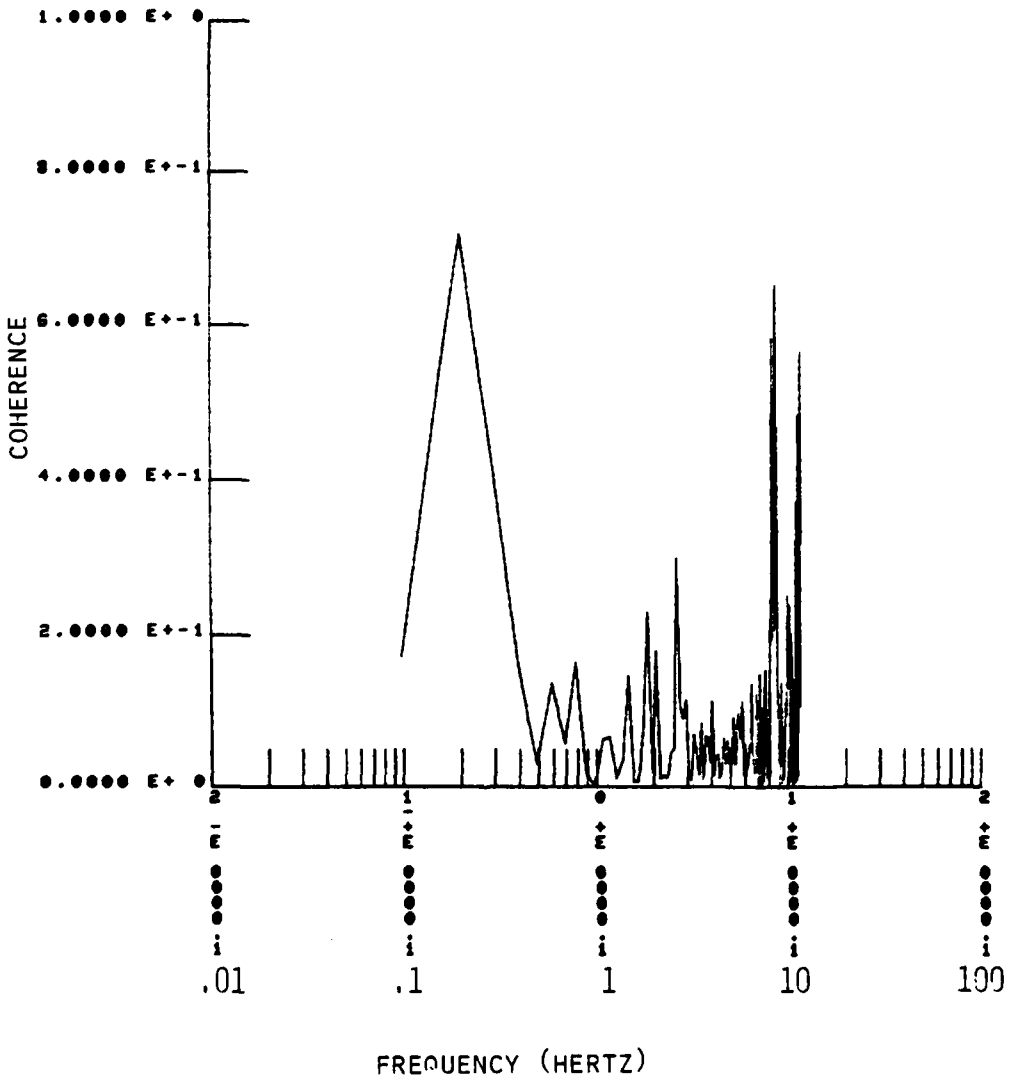

Figure 2-26 HARZER Lg wave coherence vs. frequency. 213 Z and PEK Z. 120 seconds of data.

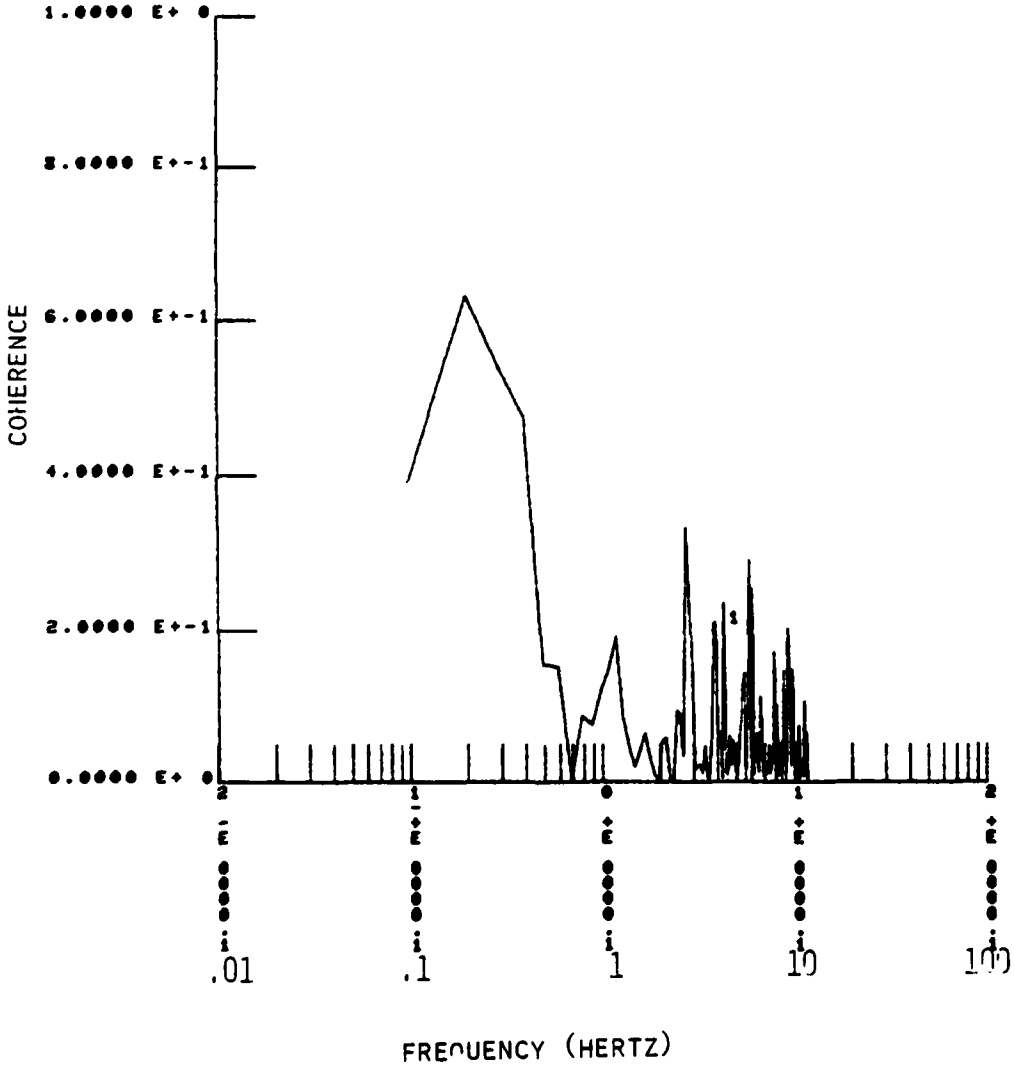

Figure 2-27. HARZER Lg wave coherence vs. frequency. TON Z and PEK Z. 120 seconds of data.

SECTION 3
NOISE CHARACTERISTICS AT THE CATSKILL SEISMIC ARRAY

Executive Summary

The Catskill Seismic Array provides a unique data source for the study of broad band (10 seconds to 10 hertz) seismic noise characteristics in the eastern and central United States since: a. it is the only broad band array with dimension small enough to study high frequency seismic waves and

b. it is the only fully digital array with three component instruments at each element in the area.

The purposes of this preliminary study are to investigate the amplitude, frequency content, cross correlation and coherence properties of the noise across the array. To carry out this first study, three (3) 40 second samples of the seismic noise immediately prior to the HARZER nuclear event were analyzed. The principal results of the study are:

1. Noise Spectra

a. Maximum amplitudes occur in the in the 4 to 9 second period range. The range of amplitudes in this period band is .2 to 6 microns per root hertz.

b. The overall shapes of the noise spectra are remarkably similar from component to component at the same element and at different elements although there are significant variations in amplitude between components. Moreover, the drop-off in amplitudes at frequencies greater than .4 hertz is remarkably uniform at approximately 18 db/octave.

2. Cross Correlation of the Seismic Noise

Twenty-seven cross correlations of the seismic noise were carried out for the three 40 second seismic noise samples.

a. Cross correlation values vary significantly (e.g. .7138 to .8597 on the 213 Z-TON Z combination) from sample to sample.

b. Correlation values of the vertical component noise are generally higher than those obtained from horizontal components. This may be explained by the surface wave composition of the noise.

c. The east-west combinations tend to demonstrate the lowest cross correlation values.

d. For noise data sample 2, the correlation values among the north-south components is significantly higher than that obtained for Sections 1 and 3.

3. Noise Coherence

The three noise samples used in the studies above were combined into 120 second samples and coherence values as a function of frequency were obtained. These studies show:

a. Peak coherence is observed in the 4 to 9 second period range.

b. The peak coherences between the vertical components of seismic noise across the array lie in the range .8 to 1.0 while, for the horizontal components, peak values tend to be lower (.6 to .8).

c. No significant coherence is observed in the noise at frequencies greater than 2 hertz.

d. On certain components, the coherence peak is significantly broader than on other components.

e. At frequencies around 1 hertz, the 213 E-TON E combination shows a secondary peak of coherence with value $\sim$.6 and a coherence minimum at .7 hertz. This same type of phenomena is demonstrated on some but not all of the other combinations. Careful use of the characterization of the noise could allow array tuning that could significantly enhance signal to noise ratios.

4. Future Work

This study represents an important first step in a systematic, detailed study of noise characteristics for the data recorded on the Catskill Seismic Array. The analysis techniques utilized in this study, as well as f-k plots, moving time window Fourier analyses and particle motion studies, will be applied to the following data sets:

a. samples every 2 hours over a 72 hour time period
b. samples every 24 hours over a 30 day time period
c. samples every 7 days over a 6 month period

The purpose of these studies will be to completely delineate the broad band characteristics of the microseismic noise over as long a time period as possible consistent with operational constraints. This complete broad band characterization of the noise will be compared with 1. that recorded by the RSTN system to be installed in the upstate New York region in the fall of 1981 and 2. with that of the SRO system to be installed in northeastern Pennsylvania by Pennsylvania State University.

Introduction

This paper deals with the characteristics of the seismic noise recorded on the Catskill Seismic Array immediately prior to the underground nuclear explosion HARZER detonated at the Nevada Test Site on June 6, 1981 at approximately 1800 UT. The purpose of this study was two-fold:

1. To investigate the amplitude and frequency content of the noise as well as correlation and coherence across the array.
2. To provide the data for signal to noise studies of the HARZER event discussed in Section 2.

The Catskill Seismic Array is unique in several respects:

1. It is the only array with dimensions small enough to study high frequency seismic waves in the eastern and central U.S.
2. It is the only array of broad-band instruments in the eastern and central U.S.
3. It is the only array of three-component instruments in the eastern and central U.S.
4. It is the only fully digital array in the eastern and central U.S.

Data

The entire record for the HARZER event is reproduced in Figure 2-2. Data for the noise study were taken from this record immediately prior to the P wave arrival. For most of this study, three 40 second samples of the noise have been utilized as shown in Table 3-1.

Table 3-1

Date	Time	Designation	Section Length
June 6, 1981	18:04:25 to 18:05:05Z	Section 1	40 seconds
June 6, 1981	18:05:05 to 18:05:45Z	Section 2	40 seconds
June 6, 1981	18:05:45 to 18:06:25Z	Section 3	40 seconds

In addition, for the studies of noise coherence as a function of frequency, the three 40 second samples have been combined into one 120 second sample.

Discussion of Noise Characteristics

The 40 second sample of noise utilized is presented on an expanded time scale in Figure 3-28.

A. Spectra

The fully corrected spectra for section of noise utilized as recorded at three of the nine elements of the array are presented in Figures 3-29 to 3-31. In these figures, the ground amplitude in microns per root hertz are plotted as a function of frequency. There are several notable points about these spectra and others for all elements and two additional 40 second samples.

1. Maximum amplitudes, as expected, occur in the 4 to 9 second period range. The range of amplitudes is approximately .2 to 6 microns per root hertz in this band of frequencies although most values are in the range of 1 to 2 microns per root hertz.

2. The drop-off in the level of the noise is remarkable uniform at frequencies greater than approximately .4 hertz. The drop-off is approximately 18 db/octave.

3. The overall shapes of the noise spectra are remarkably similar from component to component at the same element and at different elements.

4. The spectral values for periods greater than 10 seconds are poorly defined because of record length employed and should be disregarded.

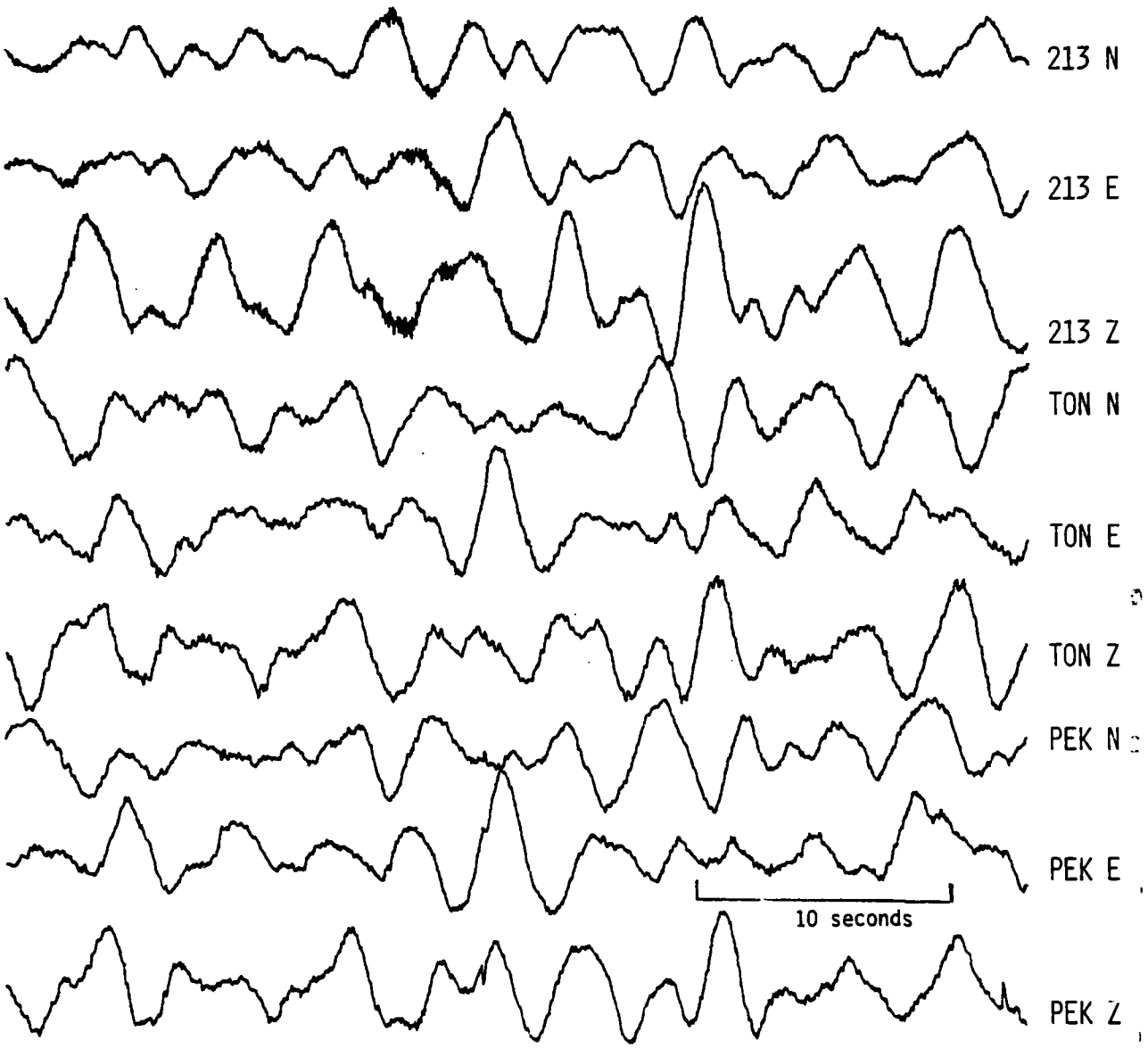

Figure 3-28. HARZER noise - all components - 40 seconds of data.

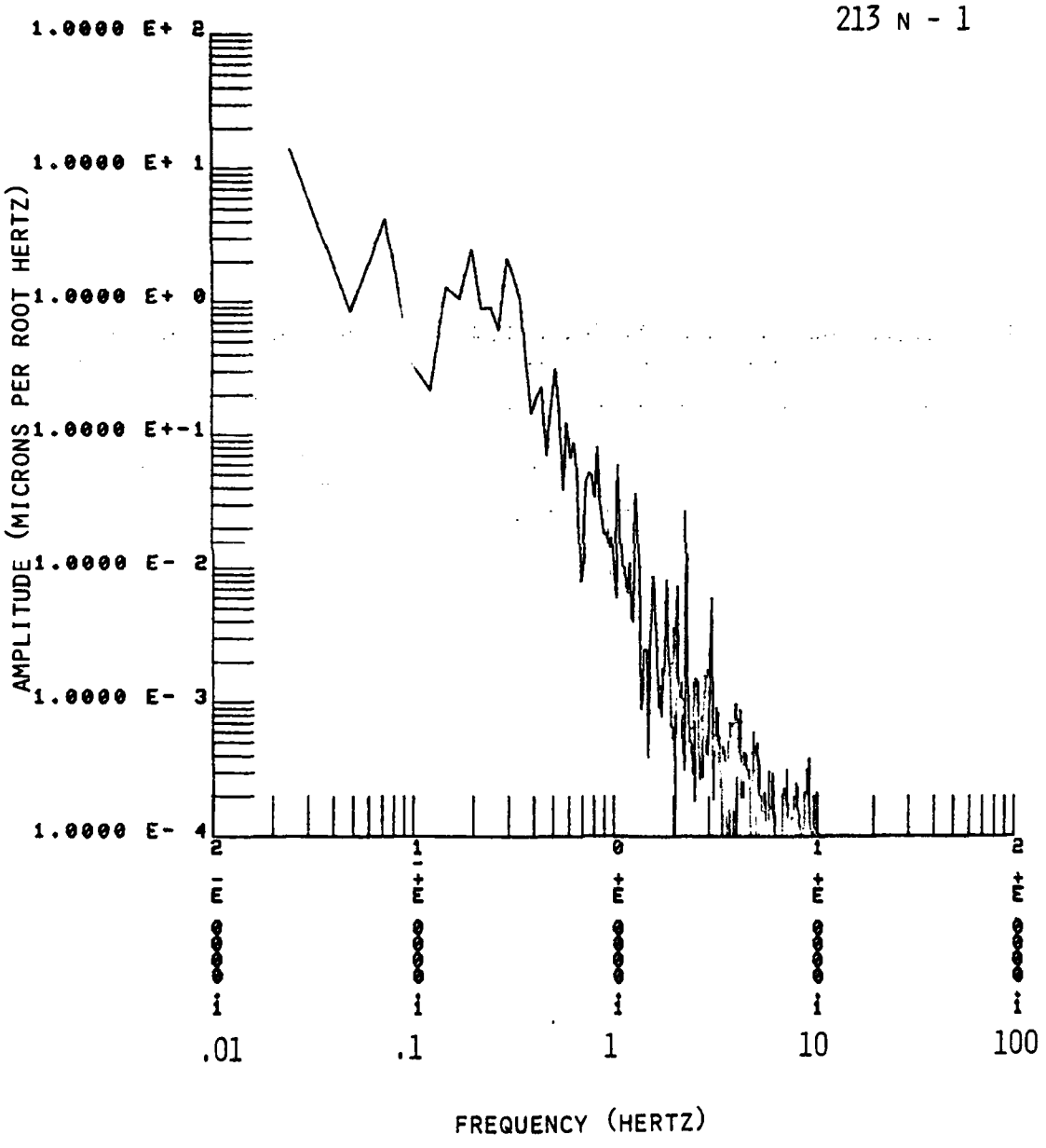

Figure 3-29 HARZER noise spectrum 213 N

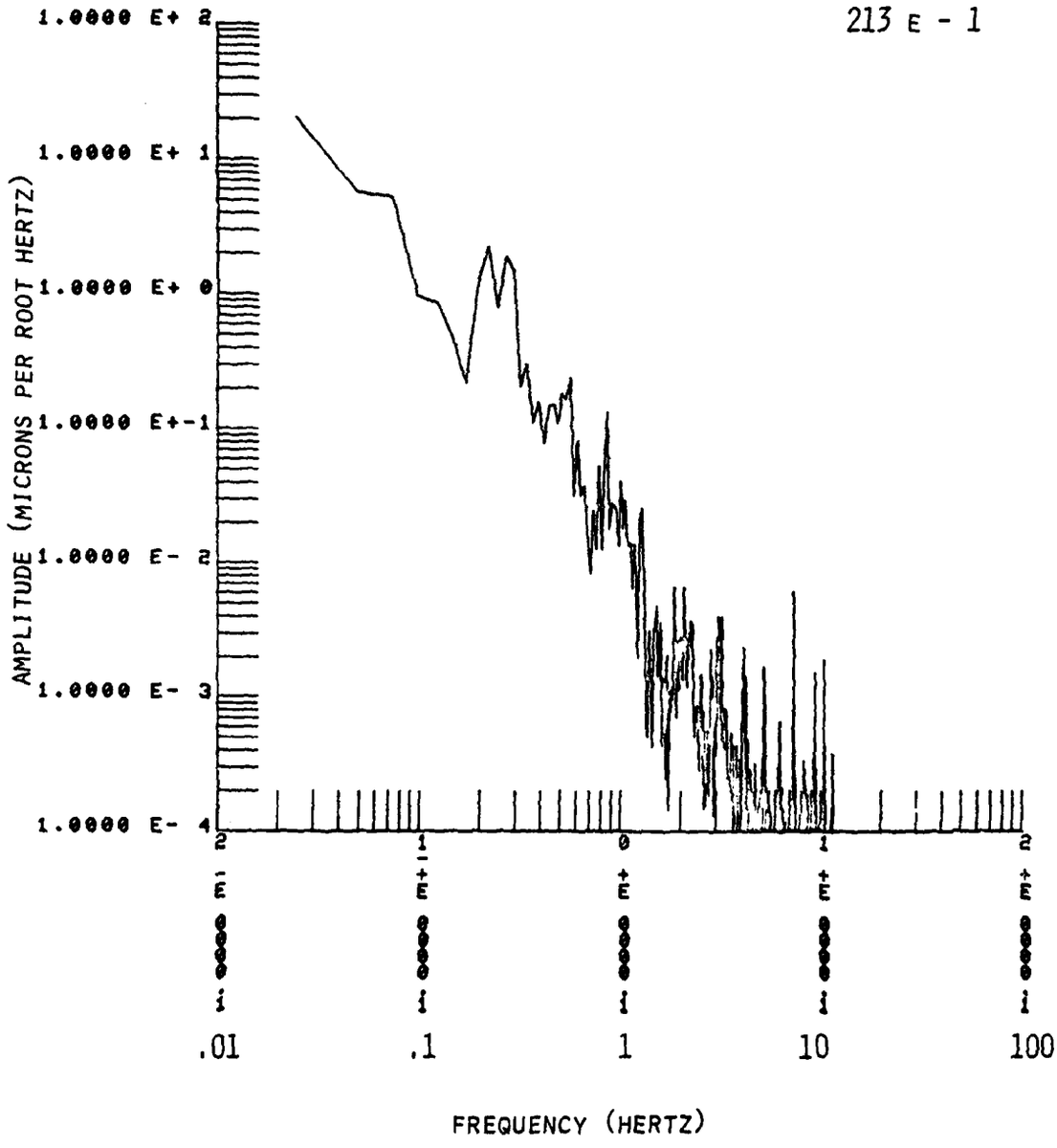

Figure 3-30. HARZER noise spectrum. 213 E

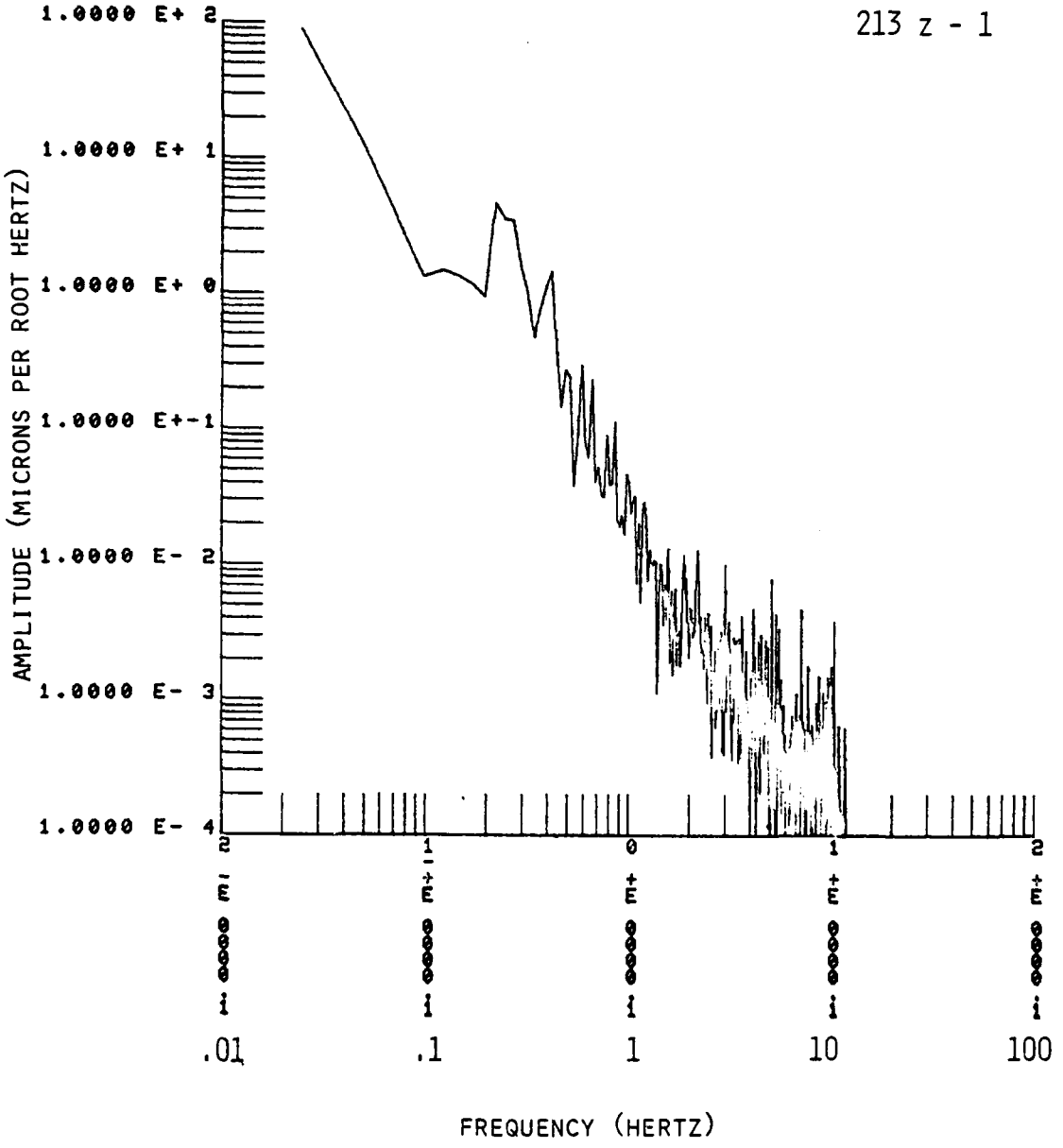

Figure 3-31.HARZER noise spectrum. 213 Z

B. Cross-Correlation

For the 40 second noise sample presented in Figure 3-28,cross-correlations with the corresponding components at the other elements of the array have been carried out. For this section of noise this results in nine-cross correlation functions. The maximum values of the cross correlations for this and two other noise sections are presented in Table 3-2. The cross correlation functions themselves are presented in Figures 3-32 to 3-40.

The following points should be noted regarding these analyses:

1. Correlation values for the vertical component noise samples are generally higher than those for the horizontal correlations. If we consider the noise to be made up principally of surface wave motion generated by ocean wave action, the mixture of Love and Rayleigh wave energy on the horizontal components and the lack of Love wave motion on the vertical may explain the higher correlations observed among the vertical components.

2. From section to section, the cross correlation values between the same instruments show significant variations (e.g. 213 Z and TON Z varies from .7138 in section 1 to .8597 in section 3). This indicates the necessity for multiple sampling to obtain an 'average' number for the cross correlation that is representative.

3. Correlation values for section 2 of the noise among all the N-S components is significantly higher than the values obtained for sections 1 and 3. For the combination TON N-PEK N, the values are closer to those obtained for the vertical components.

4. The E-W components, in general, appear to have smaller correlation values than the N-S or vertical component instruments. Further study is required using the array capabilities to elucidate this point.

5. The astute reader will realize that the negative values shown in Table IIIfor the combinations 213 N-TON N and 213 N-PEK N are the result of a polarity reversed on 213 N. The negative signs should be disregarded here.

Several combinations of different components (e.g. 213 Z and PEK N) were analyzed to determine the sensitivity of this method. In general, extremely low values of the cross correlation function were obtained and/or the cross correlation function itself was oscillatory in character with no meaningful maximum.

TABLE 3-2

NOISE - CROSS CORRELATION

	SECTIONS		
	1	2	3
213 Z - TON Z	.7138	.7536	.8597
213 Z - PEK Z	.7141	.7093	.8497
TON Z - PEK Z	.8728	.9343	.9532
213 E - TON E	.6597	.7172	.6514
213 E - PEK E	.5485	.4857	.6010
TON E - PEK E	.7988	.6812	.6460
213 N - TON N	-.6876	-.8115	-.6680
213 N - PEK N	-.6902	-.7192	-.5329
TON N - PEK N	.7784	.8250	.8118

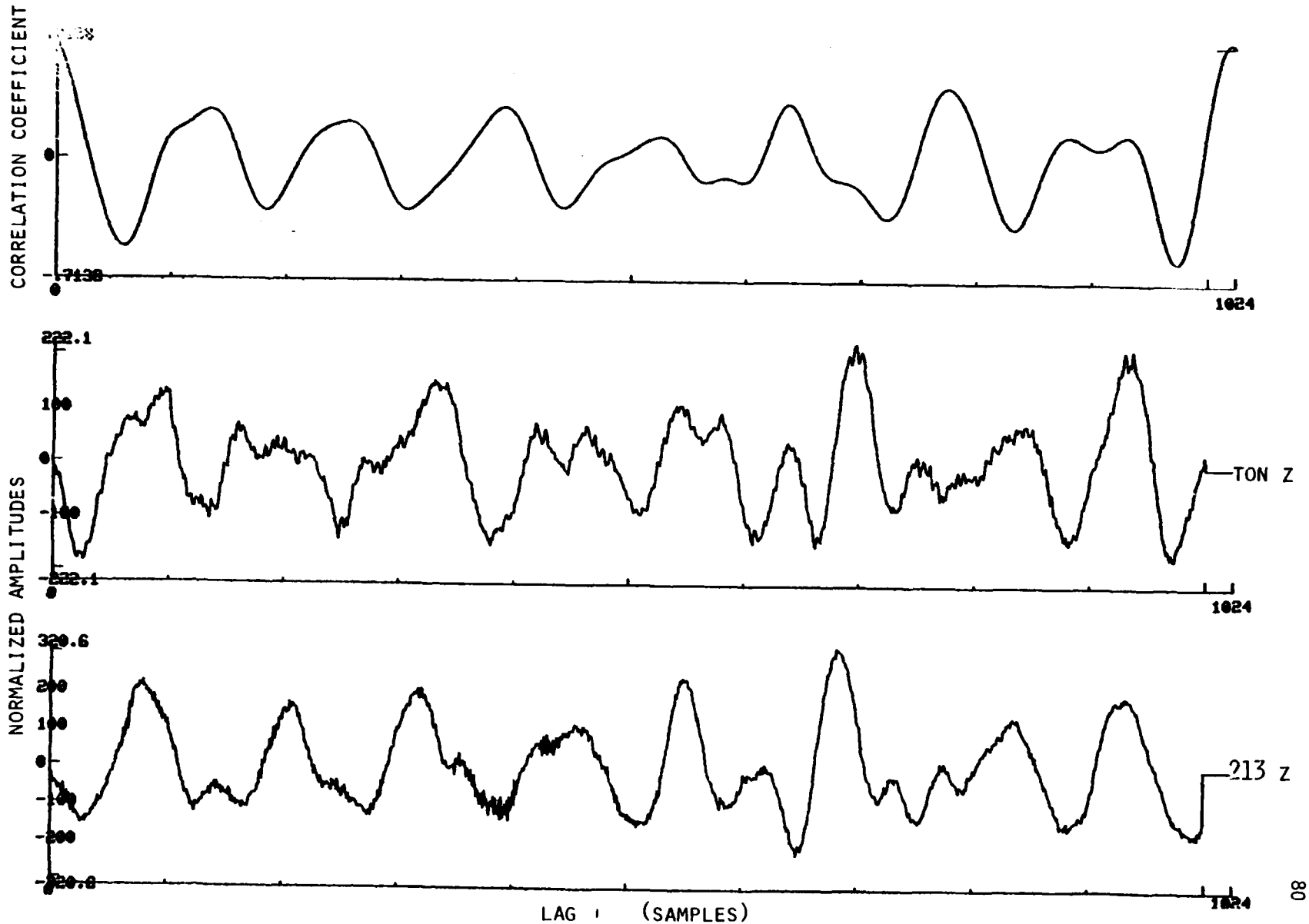

Figure 3-32. HARZER noise - cross correlation - 213 Z and TON Z

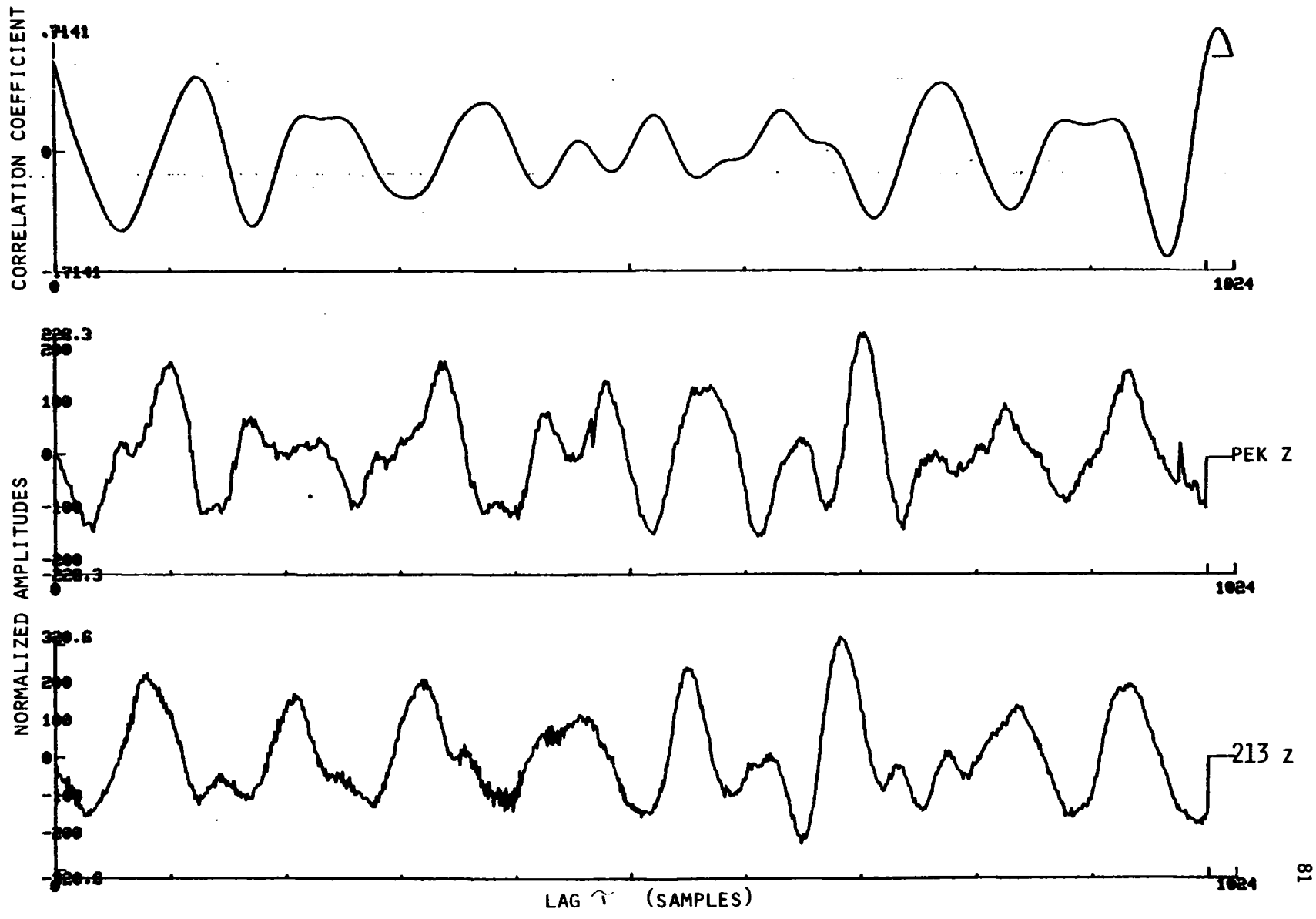

Figure 3-33. HARZER noise - cross correlation - 213 Z and PEK Z

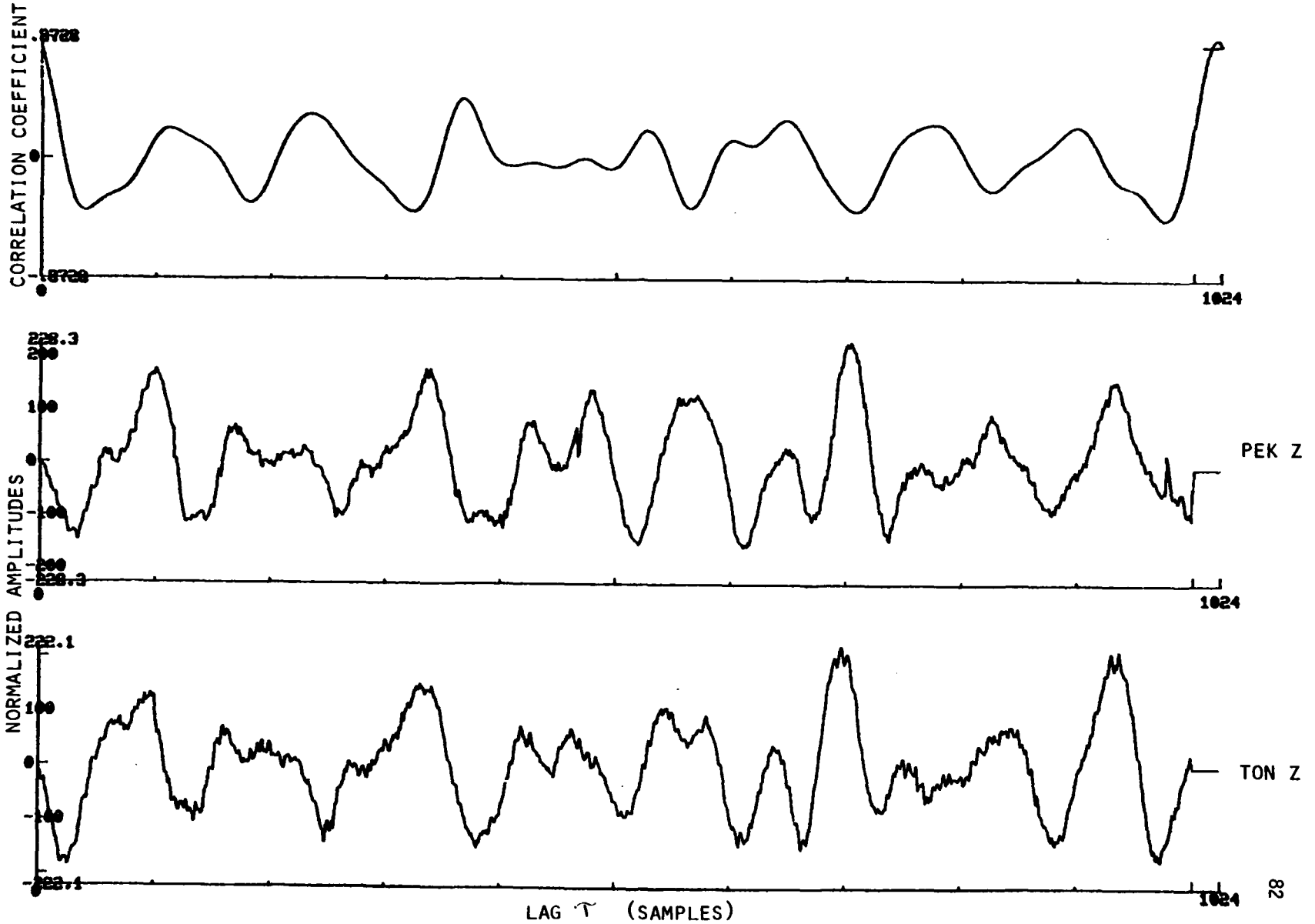

Figure 3-34. HARZER noise - cross correlation - TON Z and PEK Z

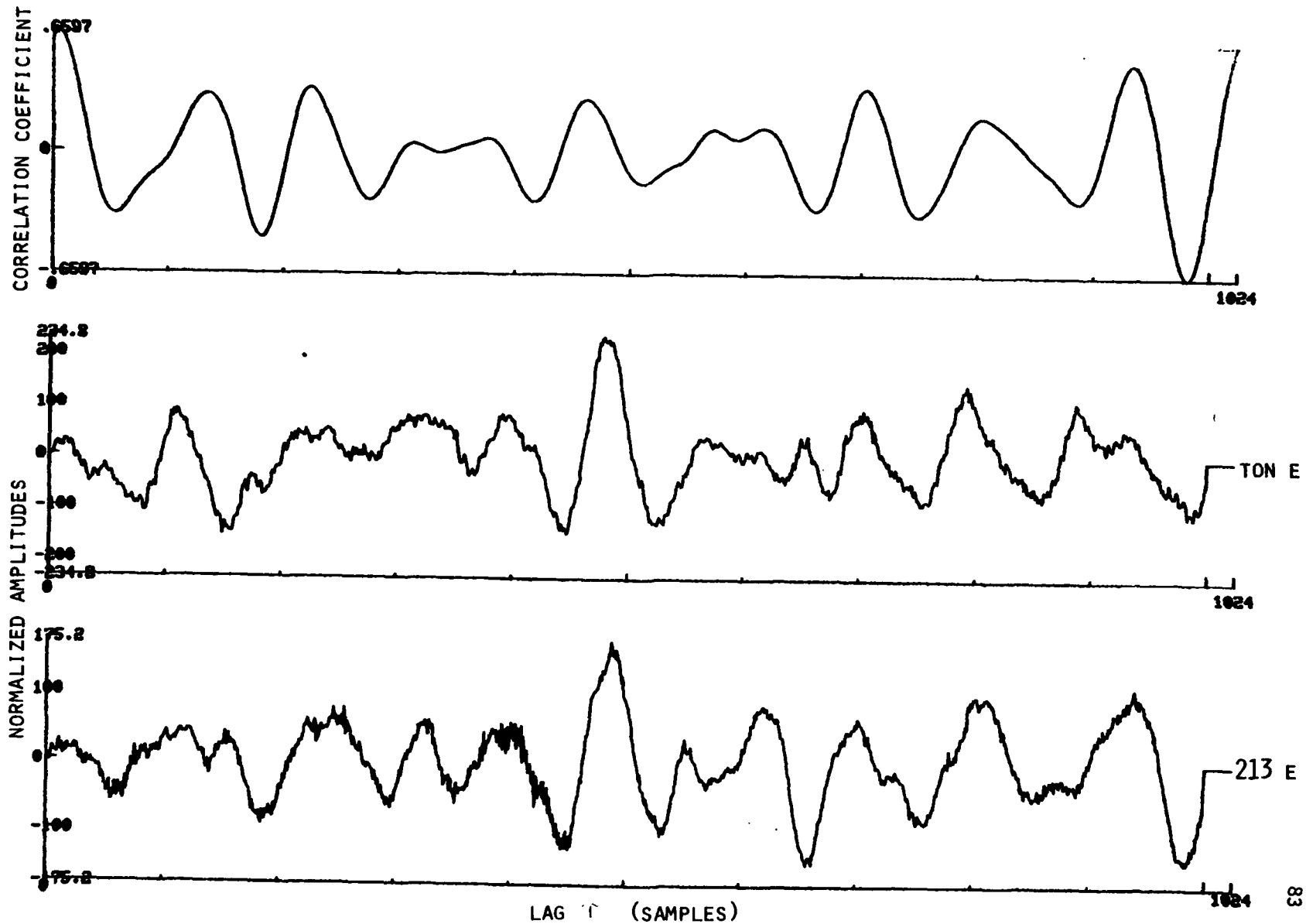

Figure 3-35. HARZER noise - cross correlation - 213 E and TON E

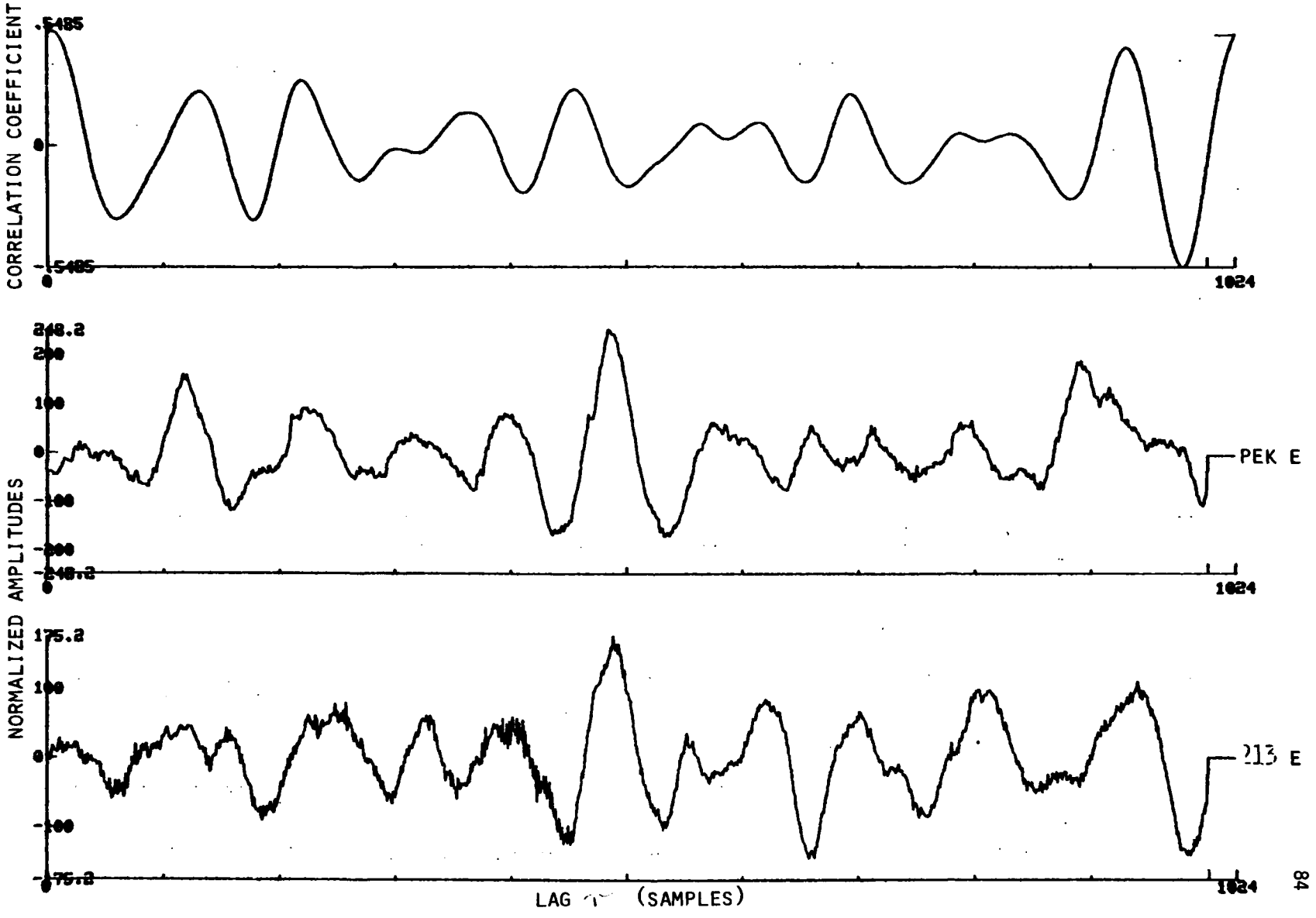

Figure 3-36. HARZER noise - cross correlation - 213 E and PEK E

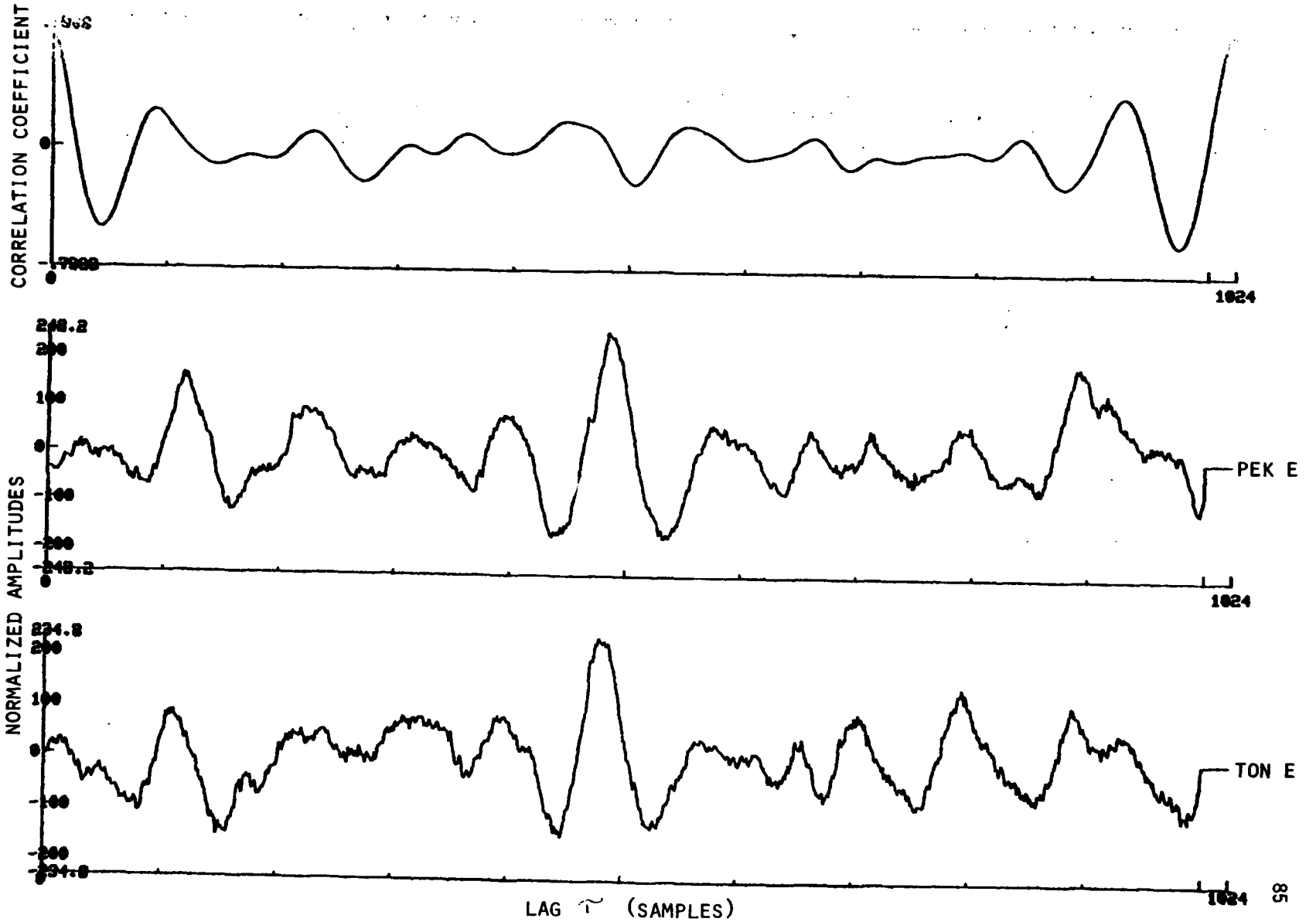

Figure 3-37. HARZER noise - cross correlation - TON E and PEK E

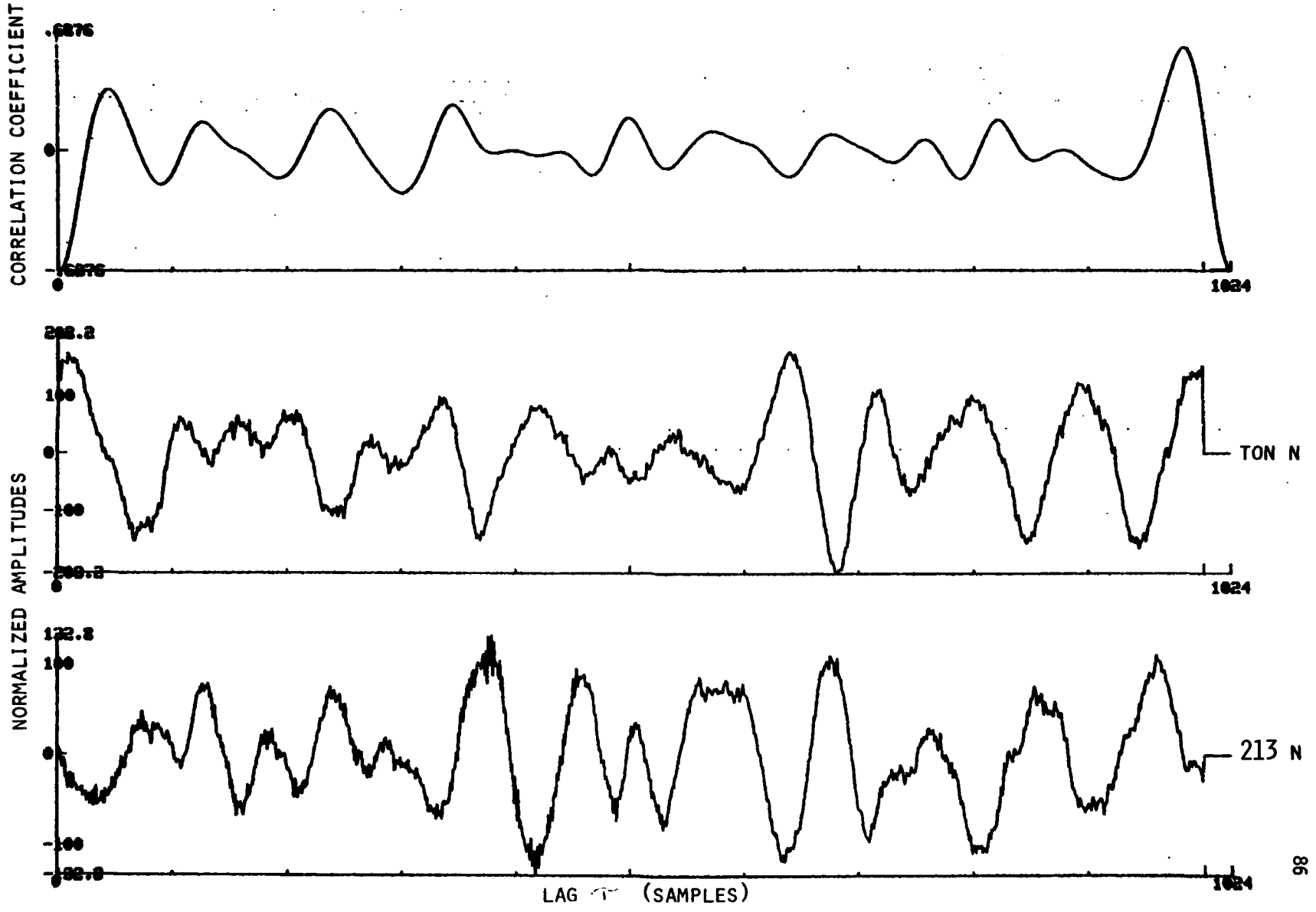

Figure 3-38. HARZER noise - cross correlation - 213 N and TON N

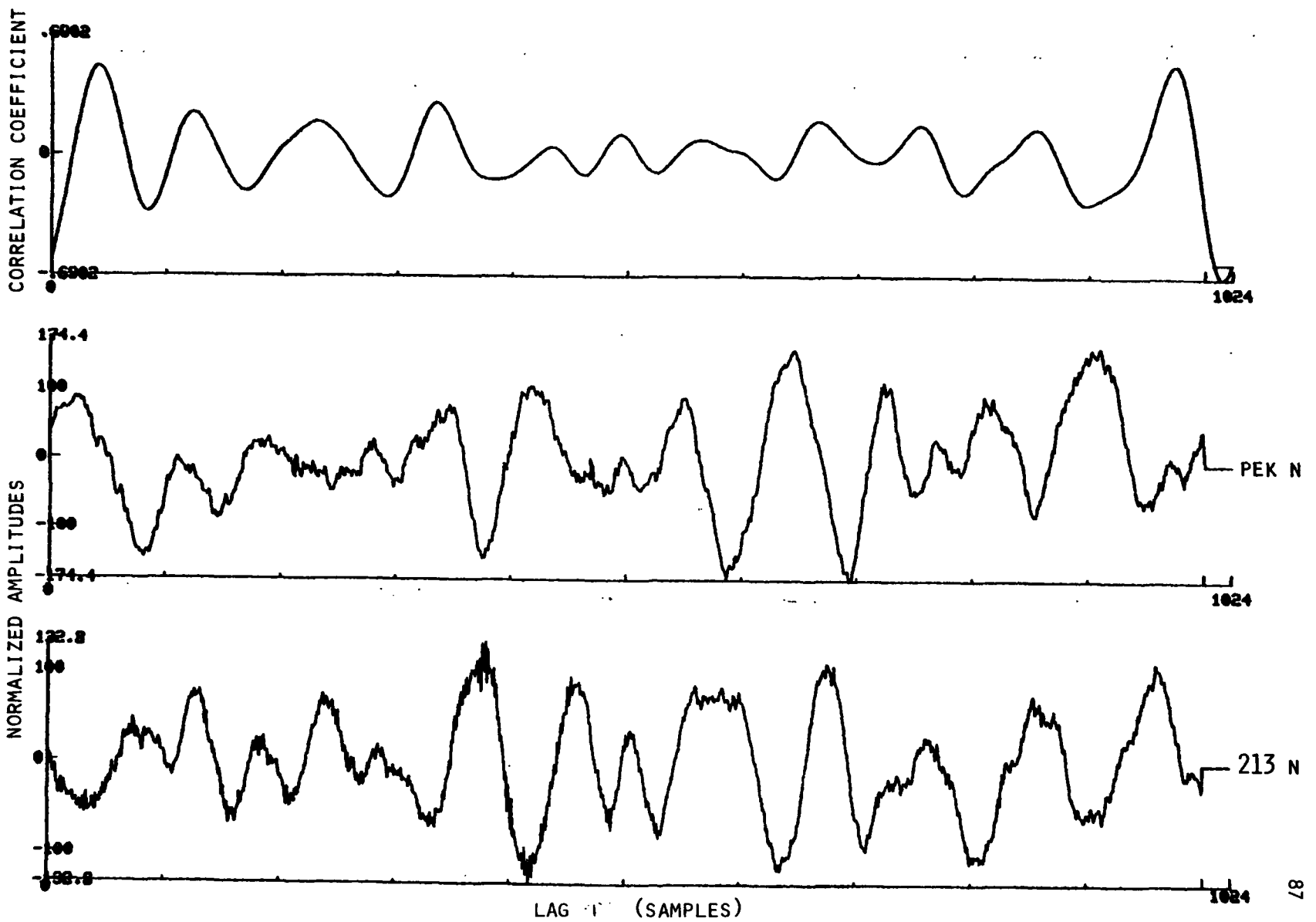

Figure 3-39. HARZER noise - cross correlation - 213 N and PEK N

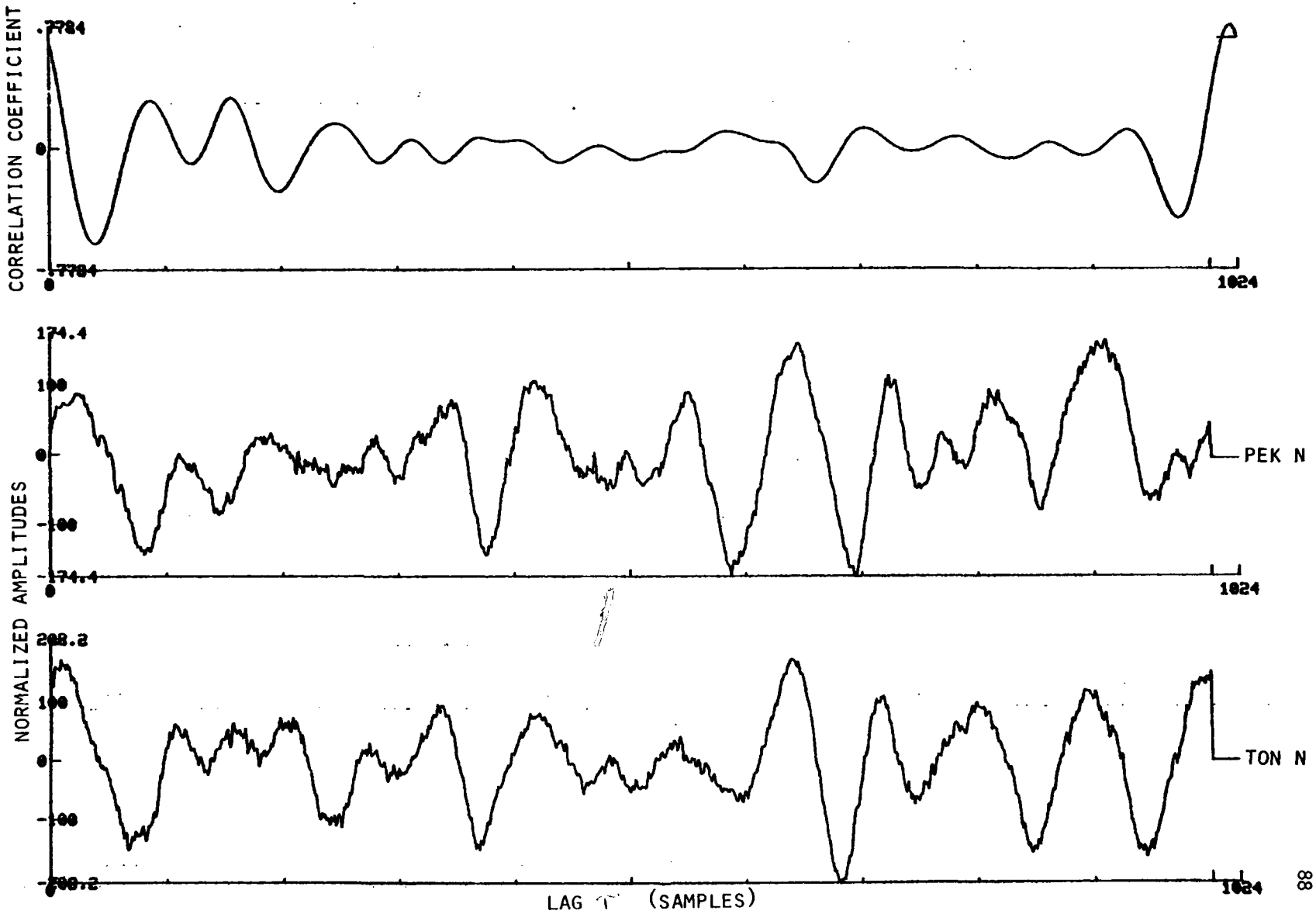

Figure 3-40. HARZER noise - cross correlation - TON N and PEK N

C. Noise Coherence

In this portion of the study, three individual 40 second noise samples have been combined into a single data sample 120 seconds long. The resultant noise samples are reproduced in Figure 3-41 for the vertical component. In this figure, the time scale in seconds and the amplitude scale in digital counts are shown. The coherence between similar components was then calculated as a function of frequency resulting in nine graphs of which the three vertical correlations are presented in Figures 3-42 to 3-44. In these figures, the coherence from 0 to 1.0 is plotted as a function of frequency. Important characteristics of these analyses are the following:

1. Peak coherence is observed in the 4 to 9 second period range on all components.
2. In the three vertical combinations, peak coherences in the 4 to 9 second range lie between .8 and 1.0. In the horizontal combinations in this period range, the maximum coherence values tend to be lower ($\sim$.6 to .8) with the notable exception of the TON N-PEK N combination which shows values between .8 and 1.0. It was this combination that showed high cross correlation values for the individual 40 second noise samples (Table 3-2).
3. No significant coherence is observed at frequencies greater than 2 hertz.
4. On certain components, the width of the coherence peak is significantly broader than on other components.
5. Secondary coherence peaks are observed on several of these combinations between 1 hertz and the maximum peak.

The shifting of the secondary peaks is being investigated further at the present time.

In order to evaluate the sensitivity of these analyses, several combinations such as 213 Z and TON E were analyzed. In general, no coherence greater than .2 was observed on these combinations except in the very high frequency range where a single high point occasionally was observed.

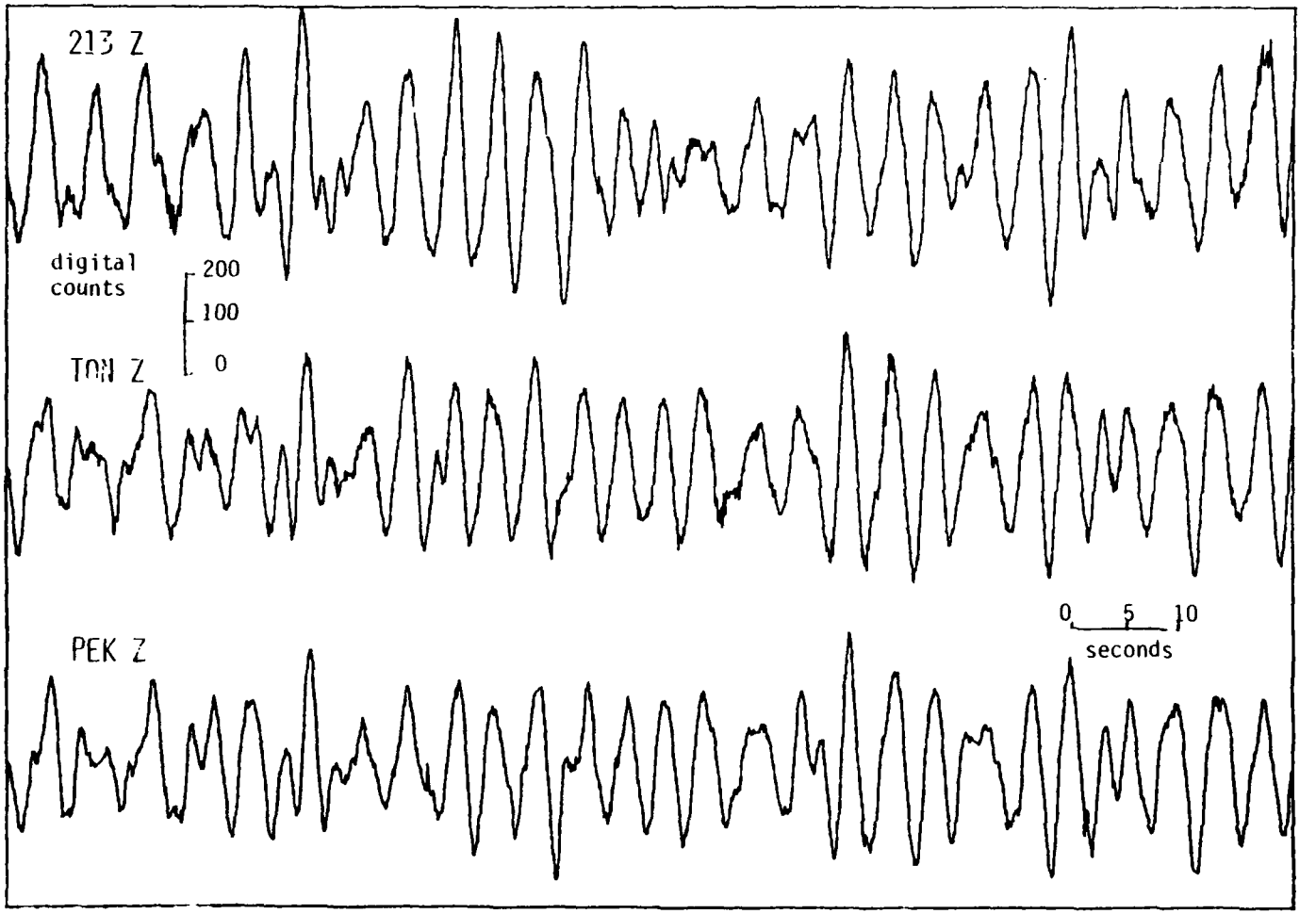

Figure 3-41. HARZER noise - 213 Z, TON Z and PEK Z - 120 seconds of data.

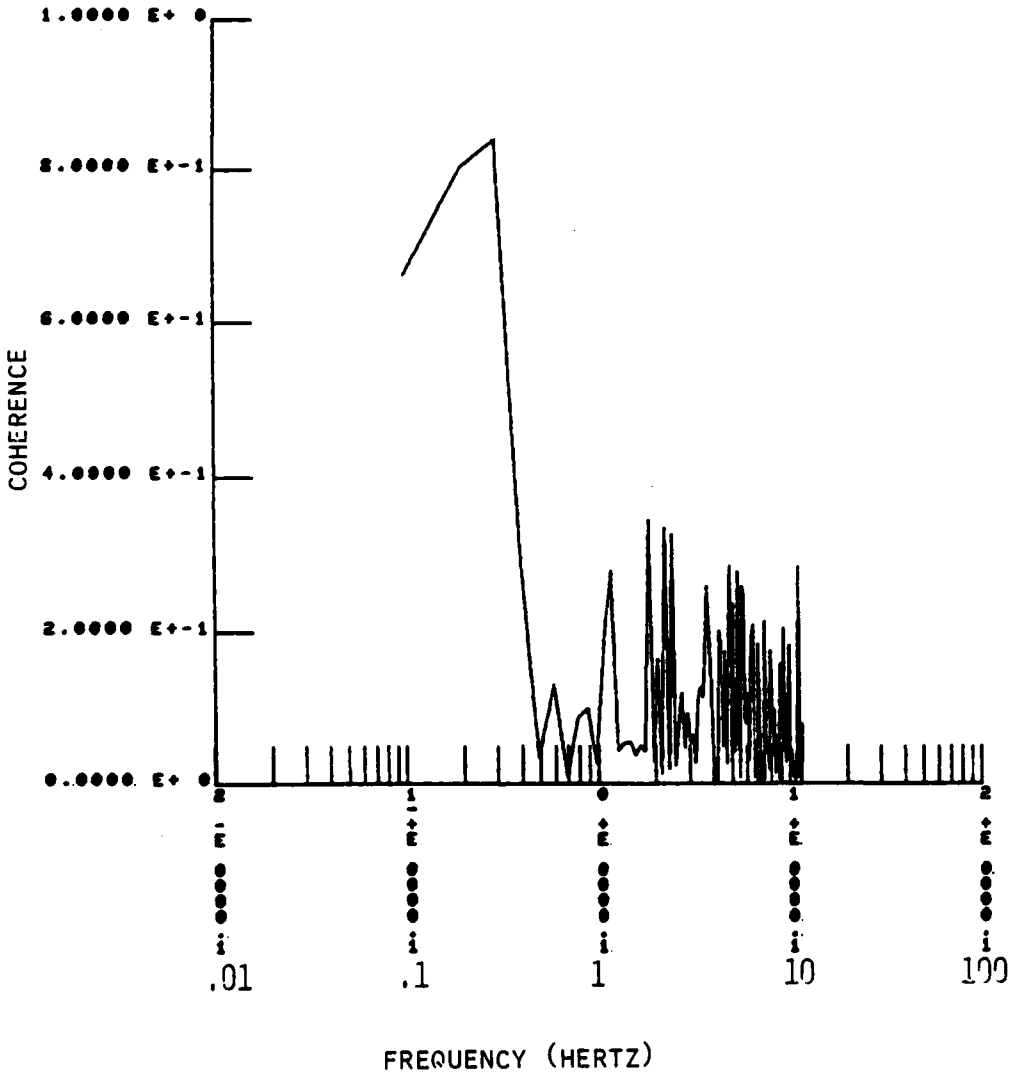

Figure 3-42 HARZER noise coherence vs. frequency. 213 Z and TON Z. 120 seconds of data.

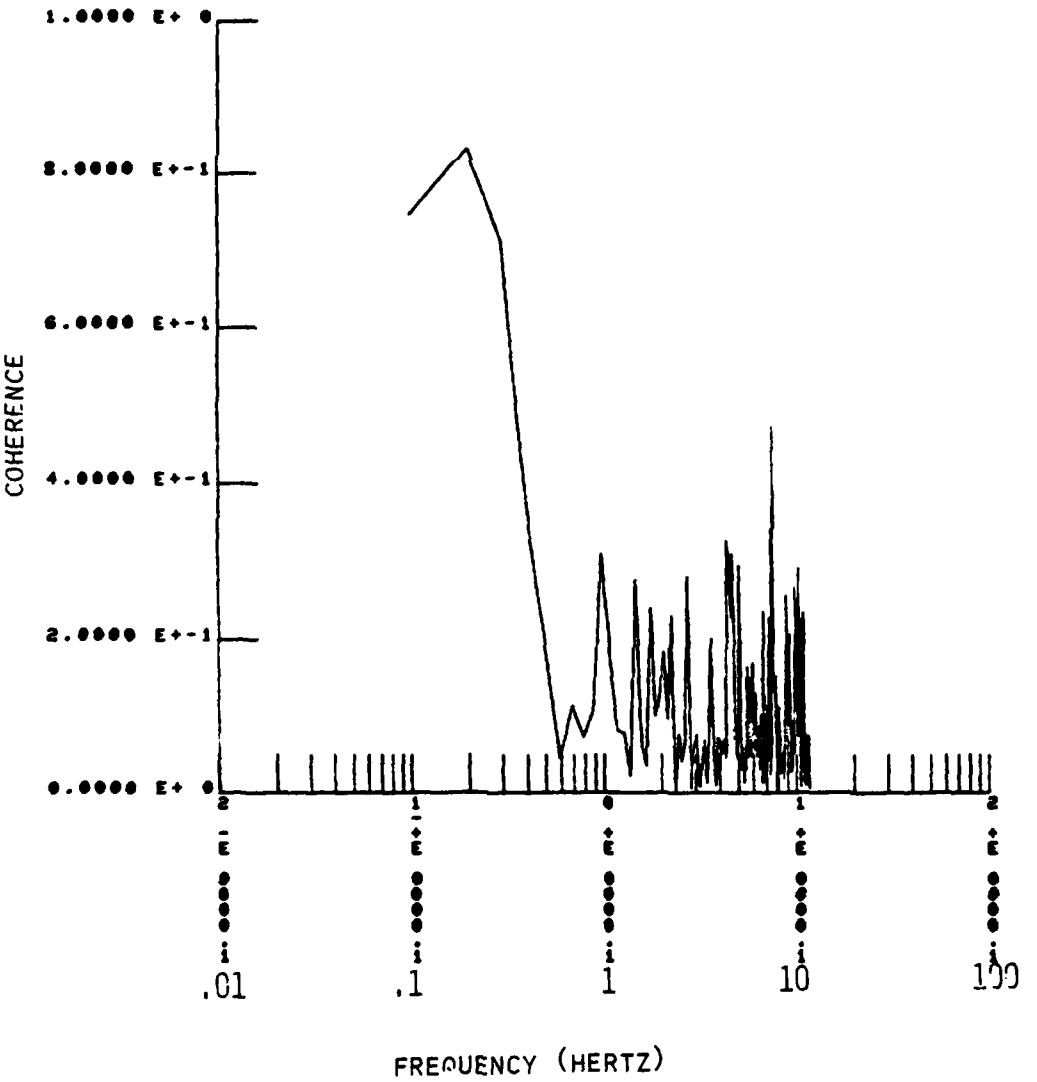

Figure 3-43. HARZER noise coherence vs. frequency. 213 Z and PEK Z, 120 seconds of data.

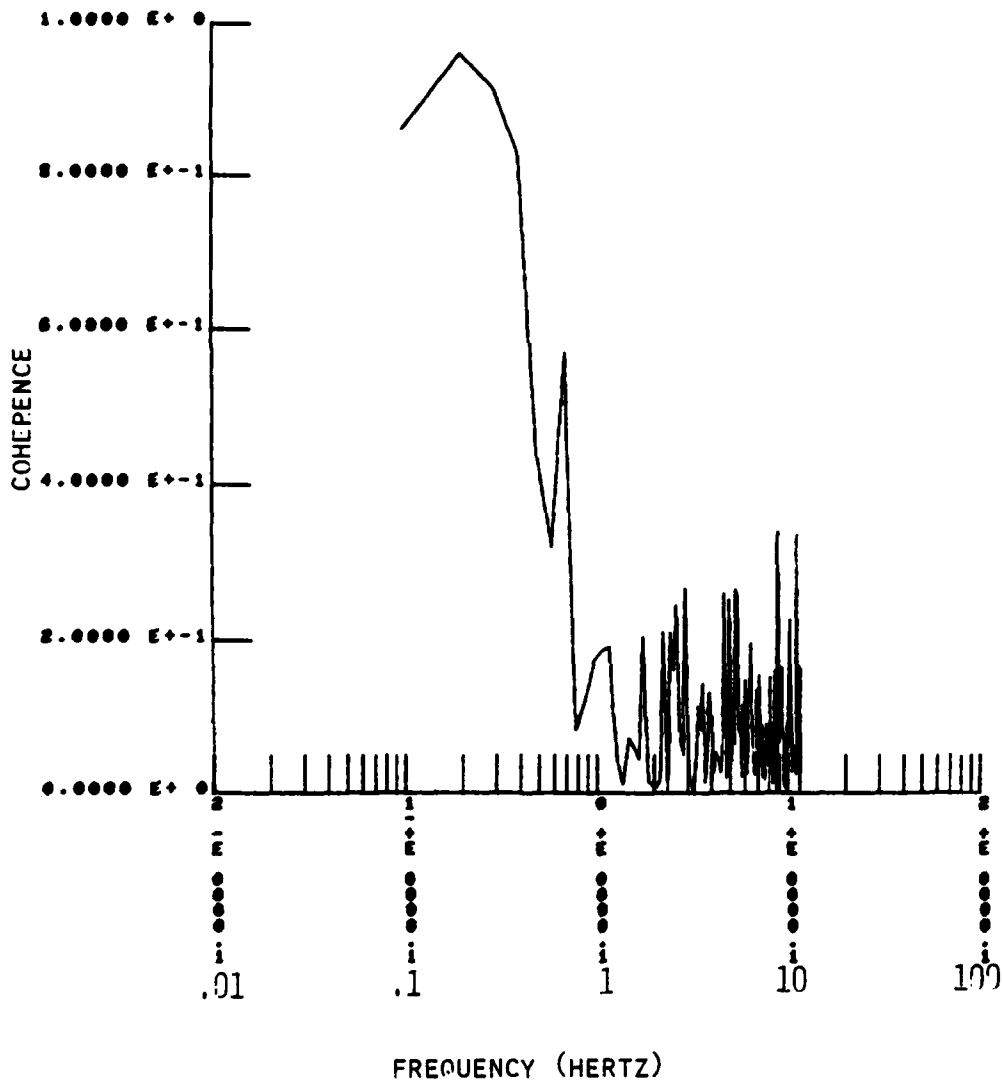

Figure 3-44 HARZER noise coherence vs. frequency. TON Z and PEK Z. 120 seconds of data.

Future Work

Although the immediate purpose of this study was to provide noise data for signal to noise studies on HARZER, it constitutes an important first step in a systematic detailed study of noise characteristics for the data recorded on the Catskill Seismic Array.

The immediate follow-up to this study will involve the following:

1. F-k plots of all components of the noise.
2. Three-dimensional moving time window Fourier analyses of the noise data.
3. Particle motion studies.

The above analyses techniques, as well as those utilized in this study, will be used on the following noise data sets.

1. Samples every two hours over a 72 hour time period.
2. Samples every 24 hours over a 30 day time period.
3. Samples every 7 days over a 6 month time period.

The purpose of these studies will be to completely delineate the broad band characteristics of the microseismic noise over as long a time period as possible consistent with operational constraints. This complete broad band characterization of the noise will be compared with 1. that recorded by the RSTN system to be installed in the upstate New York region in the fall 1981 and 2. with that of the SRO system to be installed in northeastern Pennsylvania by Pennsylvania State University.

SECTION 4
CALIBRATION AND RESPONSE OF THE CATSKILL SEISMIC ARRAY

Calibration Experiment Plan

Calibration of the CSA can be initiated at the central recording facility. Actuation of separate switches for each remote site places a one (1) milliampere step function of current in the seismometer's calibration coil. The resultant motion of the seismometer is digitized, transmitted, and recorded for future analysis. As mentioned earlier, the array was established in November and December, 1980.

At the time, natural periods were carefully set to 15 seconds and critical damping was used. In the time, between the initial set-up and July 14, 1981, small changes in these parameters were noted particularly as slightly different amplitudes on the visible monitors.

On the 14th of July, 1981, a set of calibration pulses were transmitted from the central recording facility to the remote stations. The resultant digital signals were recorded on magnetic tape for later analysis. Then, at each of the remote sites, the natural periods were reset to 15 seconds and damping resistances checked. After allowing the instruments to settle down, a second set of calibration pulses were transmitted to the remote sites and the resultant signals recorded on magnetic tape. Thus, analyses of the first set of calibration pulses yield response curves applicable before the instrumental changes on 14 July 1981 while the second set yield curves applicable after 14 July 1981.

Calibration Pulses

Normalized calibration pulses before the instrument changes of 14 July 1981 are presented in Figure 4-45 The Tongore N-S instrument is clearly much shorter in period than the others and, as a result, clearly underdamped. This difference is also obvious in the calibration curves. Differences in the overshoot ratio (e.g. Peak E vs. Peak Z) are also apparent indicating differences in damping which affect the shape of the response curve near the natural period of the seismometer. Following the instrumental changes on the 14 July 1981, calibration pulses like those shown in Figure 4-46 were obtained. Although small differences in the overshoot ratio are apparent, the general shape of the pulses is much more consistent.

All response curves for the array for the period prior to 14 July 1981 are presented in Figures 4-47 and 4-48 and all for the period following 14 July 1981

CALIBRATION PULSES
PRIOR TO
14 JULY 1981 CALIBRATION
NORMALIZED

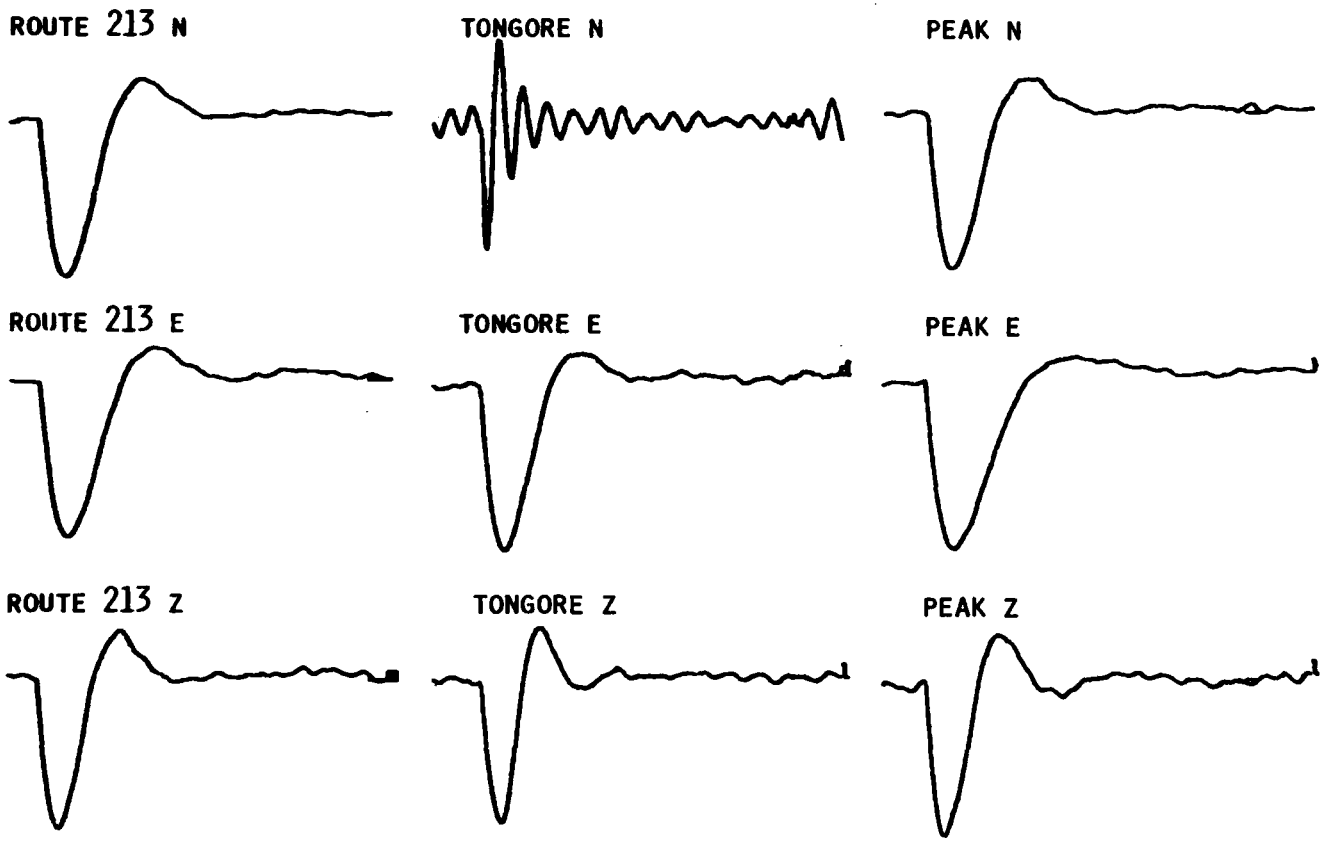

Figure 4-45. Calibration pulses (normalized) - prior to 14 July 1981.

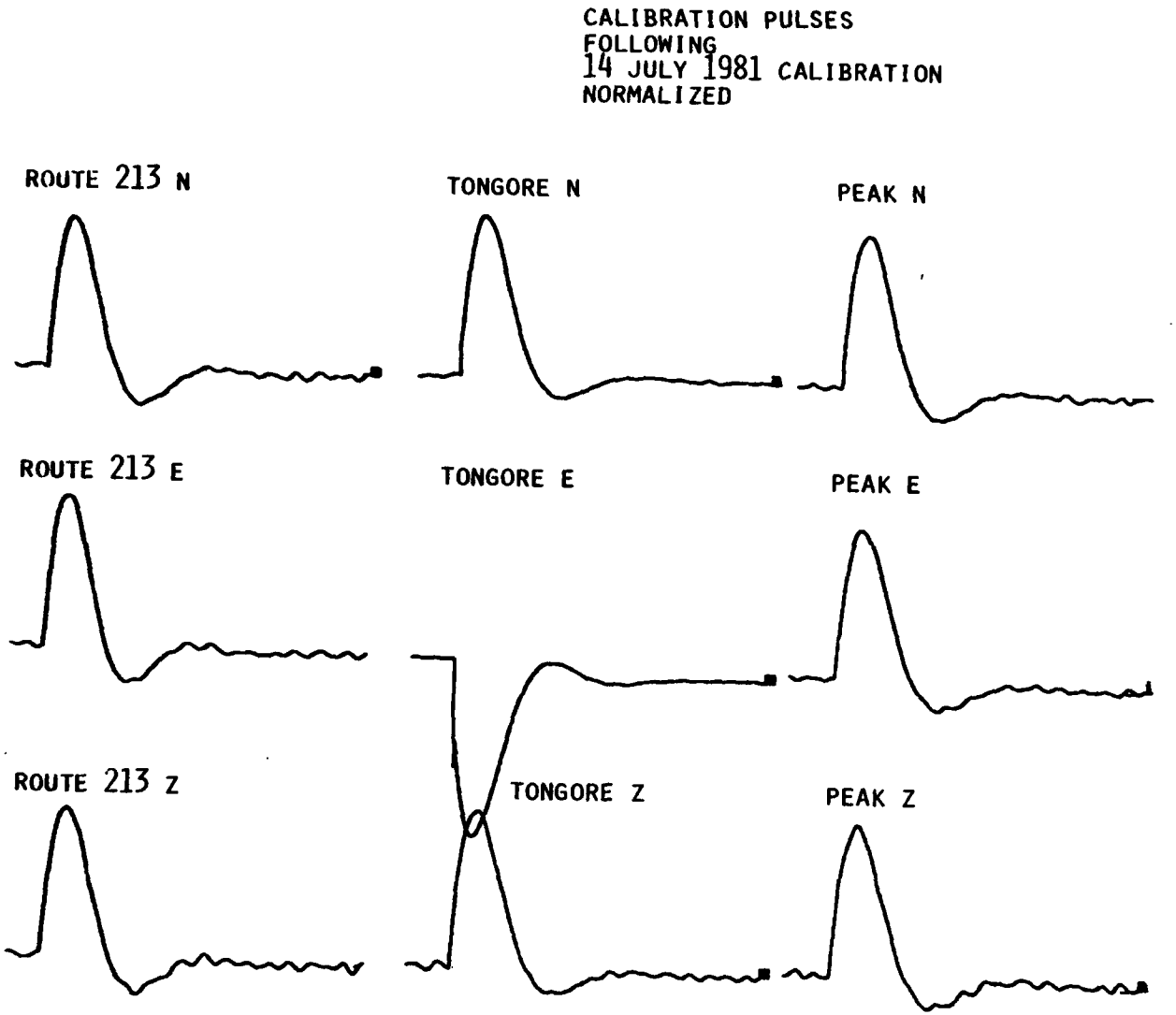

Figure 4-46. Calibration pulses (normalized) - after 14 July 1981.

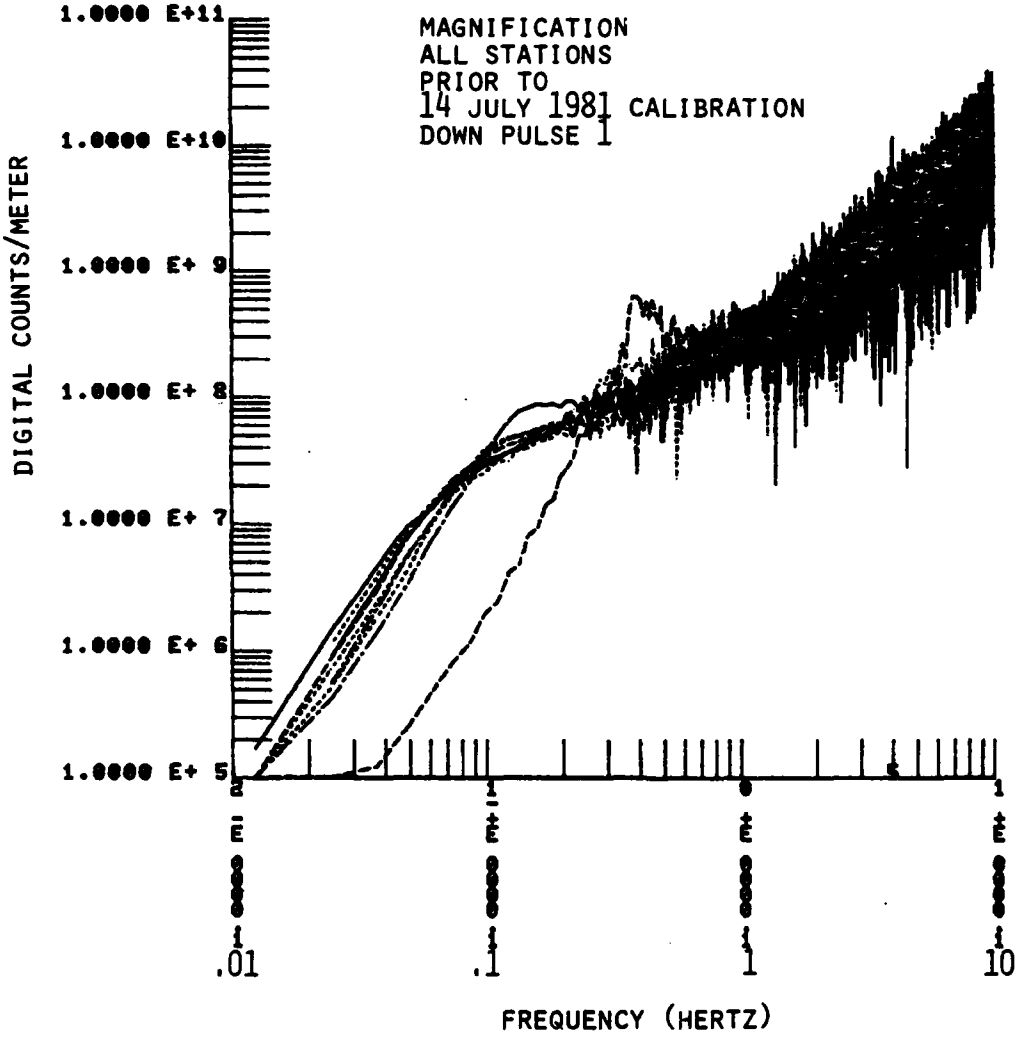

Figure 4-47 Magnification curve - all components - prior to 14 July 1981. Calibration Pulse 1

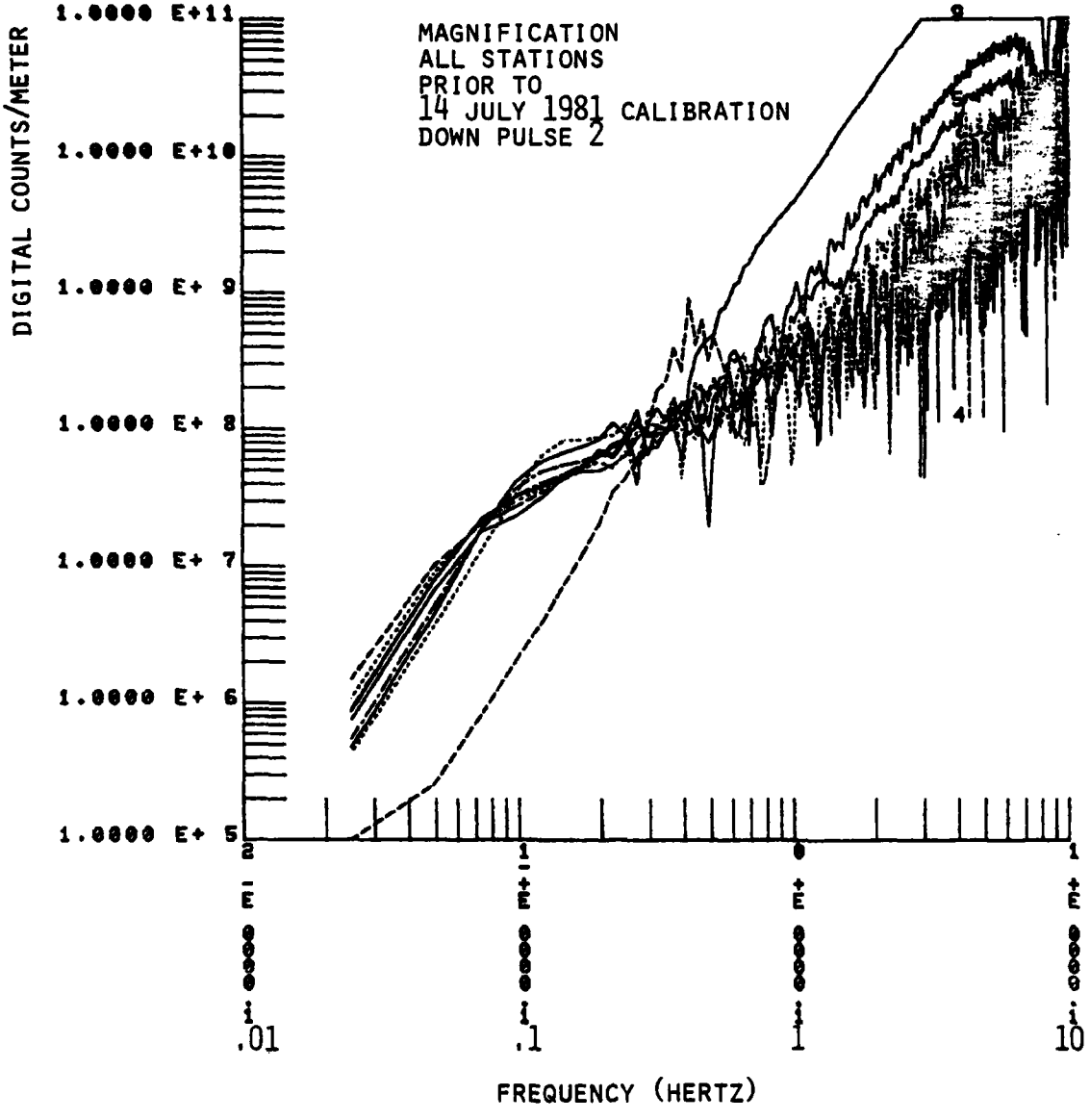

Figure 4-48. Magnification curve - all components - prior to 14 July 1981. Calibration Pulse 2

are presented in Figures 4-49 and 4-50. For each component at the 213 station, response curves derived from two pulses are superimposed in Figures 4-51, 4-52, and 4-53.

All of the response curves were obtained by a Fourier analysis of the calibration pulse followed by a correction of ω^3 ($\omega = 2\pi f$) $-\omega$ for converting the step function of acceleration to an impulse of acceleration and ω^2 to convert to displacement from acceleration. This type of calibration does not give the best results in the high frequency portion of the spectrum. Magnification curves are plotted as digital counts/meter versus frequency from .01 hertz to 10 hertz. To use these in terms of microns, one would simply reduce the exponents on the left hand side by six (6).

The response curves themselves are self-evident. For example, the Tongore N-S component is clearly shorter period. Overall, however, the agreement between all the components is quite good. Two of the magnification curves obtained following the 14 July 1981 instrument adjustments have somewhat higher overall level. This is related to the magnet strengths, coil positions and other factors. It is easily accommodated in subsequent analyses when correcting for instrument response.

It should be noted that, in the frequency range .1 to 1 hertz and above, the instrumental response rises, as predicted, as 6 db/octave i.e. the response is proportional to ground velocity. Thus, uncorrected spectra in this frequency are, by definition, velocity spectra.

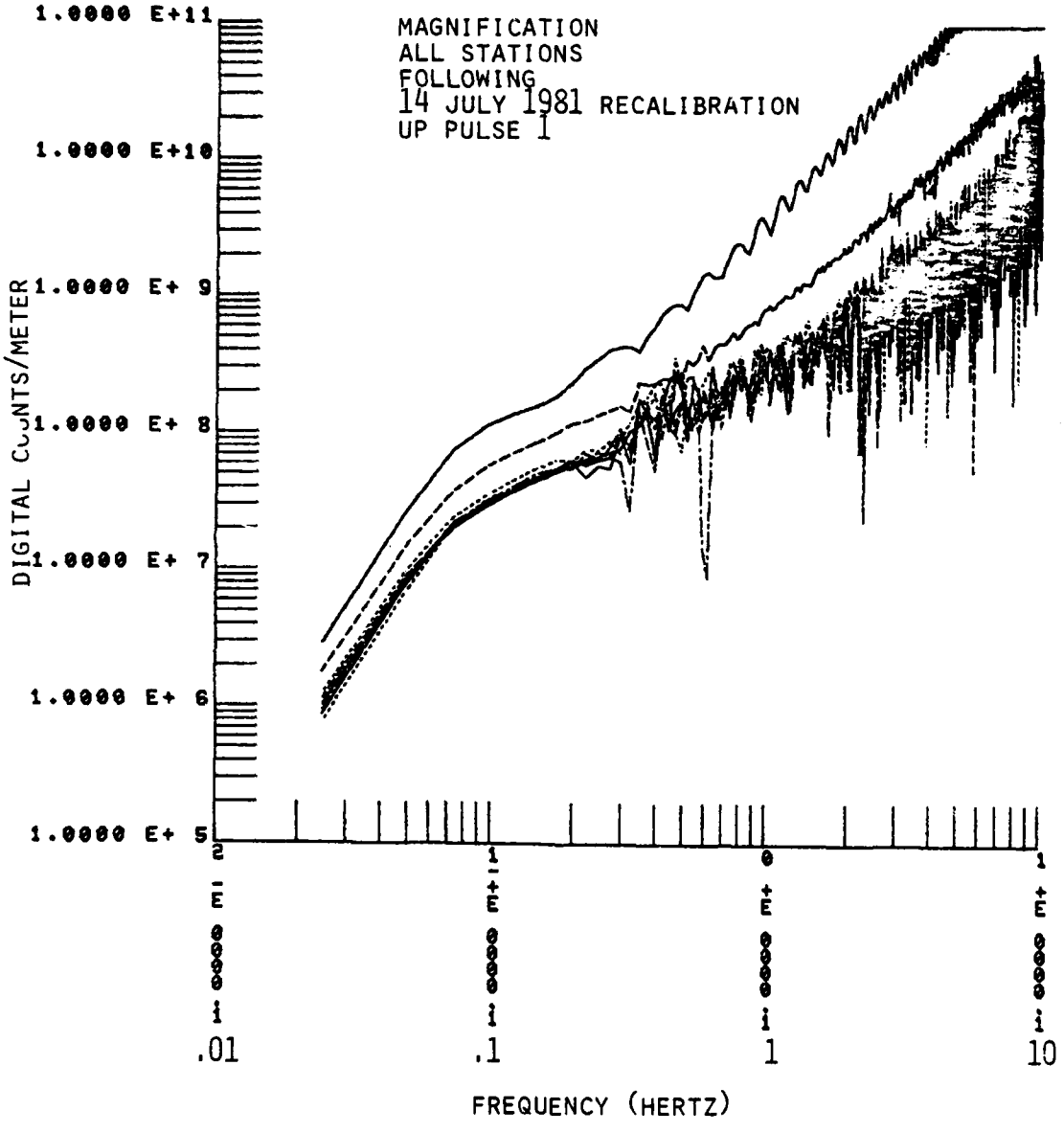

Figure 4-49 Magnification curve - all components - after 14 July 1981. Calibration Pulse 1

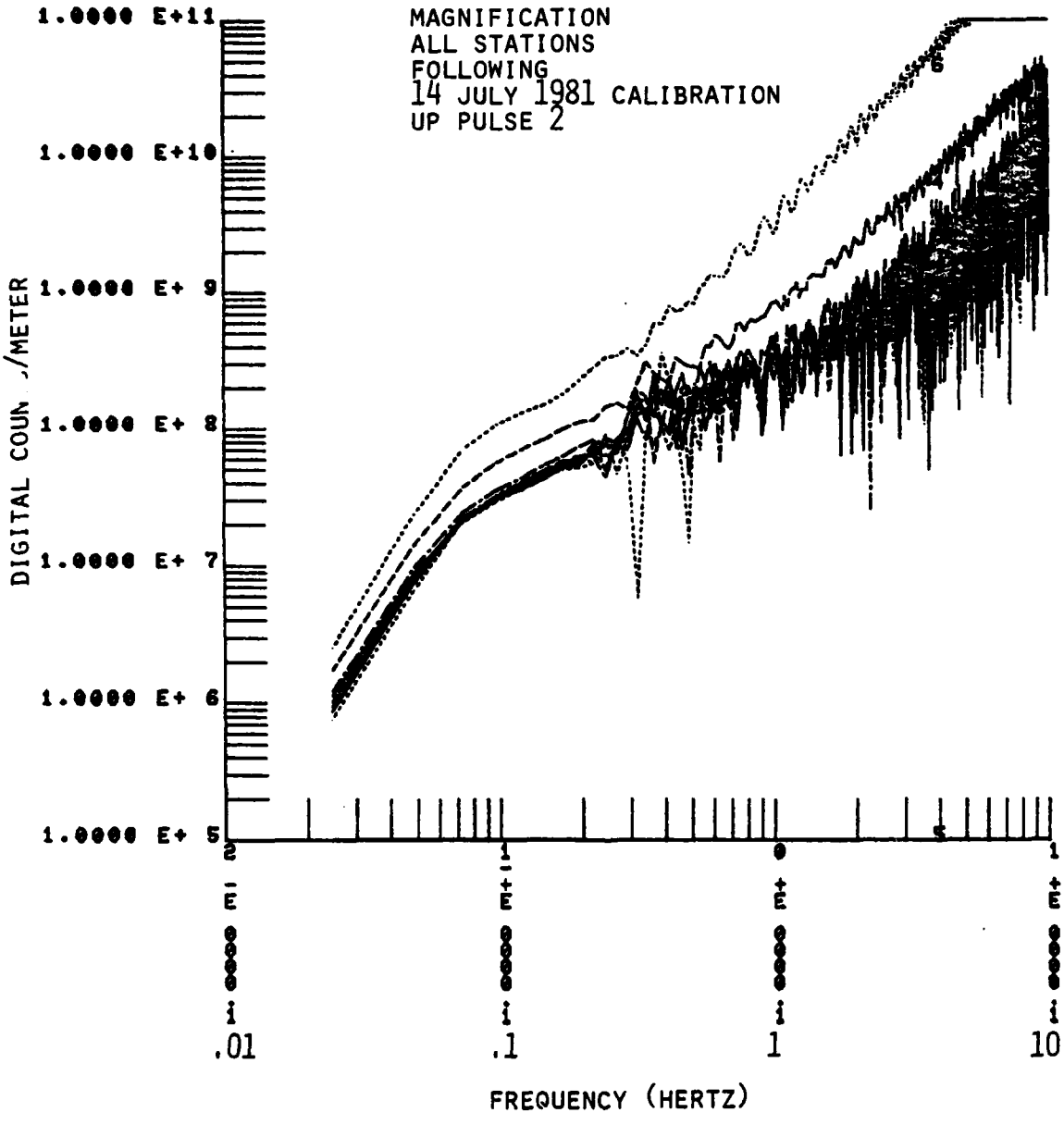

Figure 4-50. Magnification curve - all components - after 14 July 1981. Calibration Pulse 2

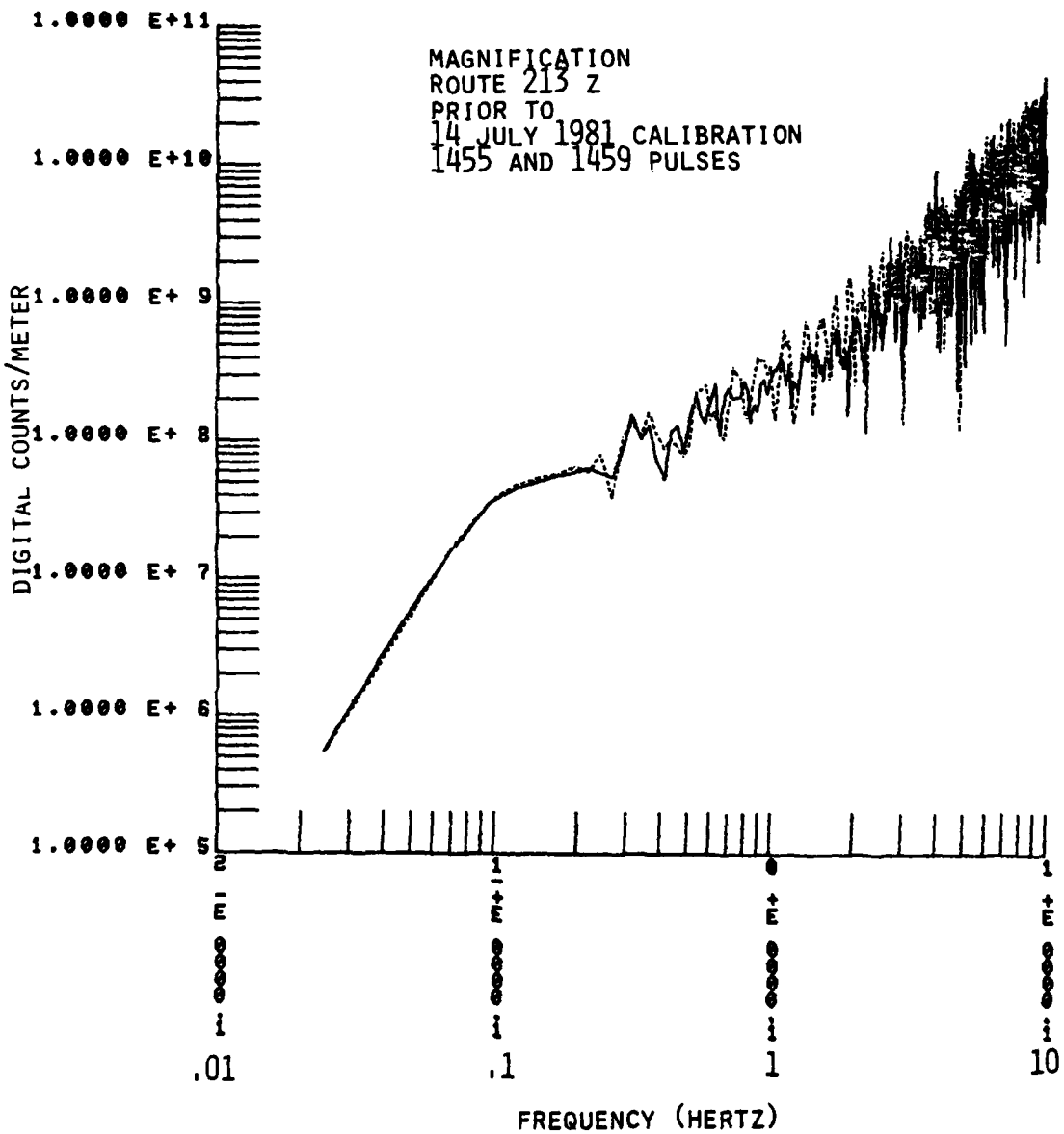

Figure 4-51. Magnification curves - 213 Z - results from two pulses superimposed.

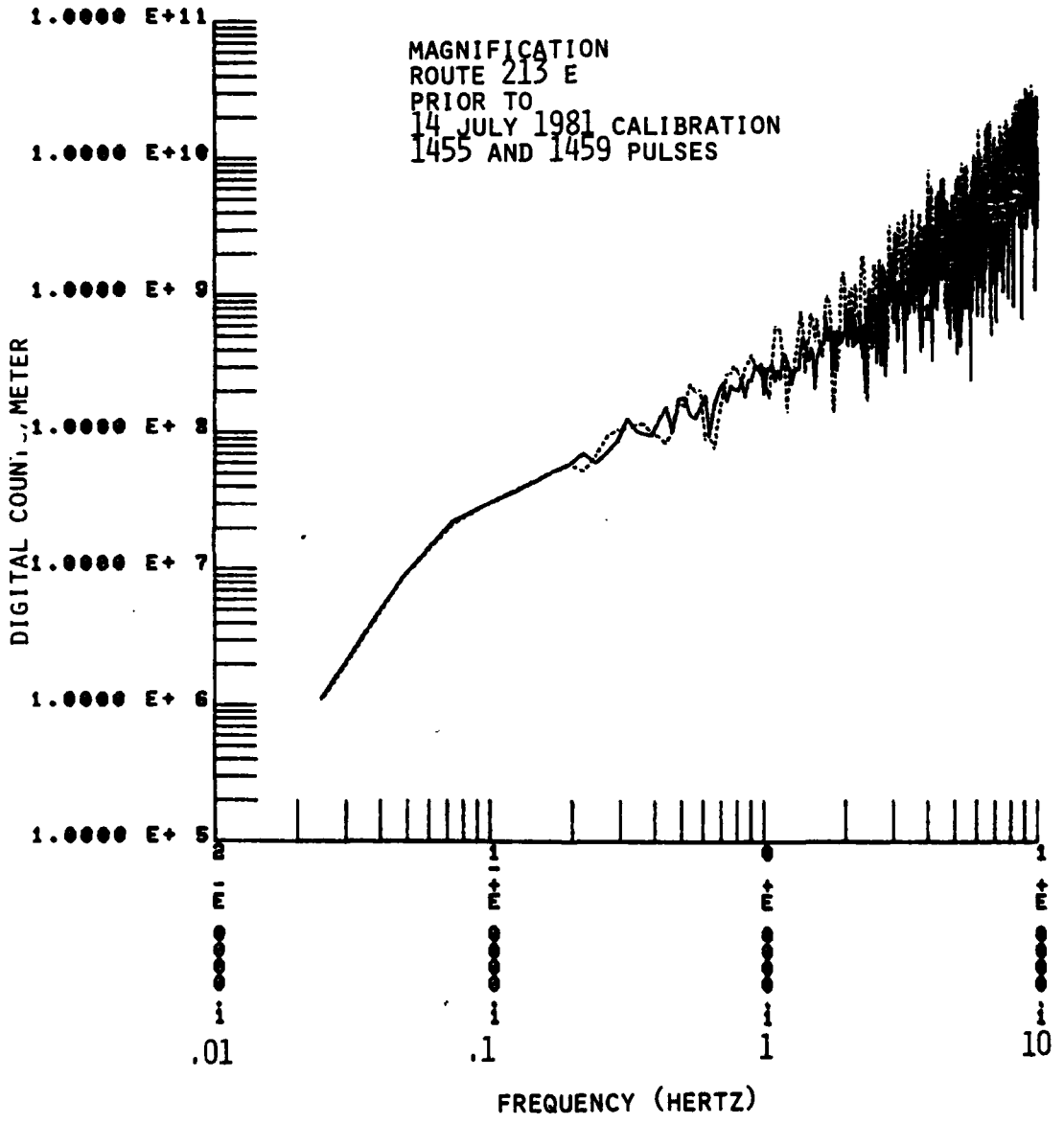

Figure 4-52. Magnification curves - 213 E - results from two pulses superimposed.

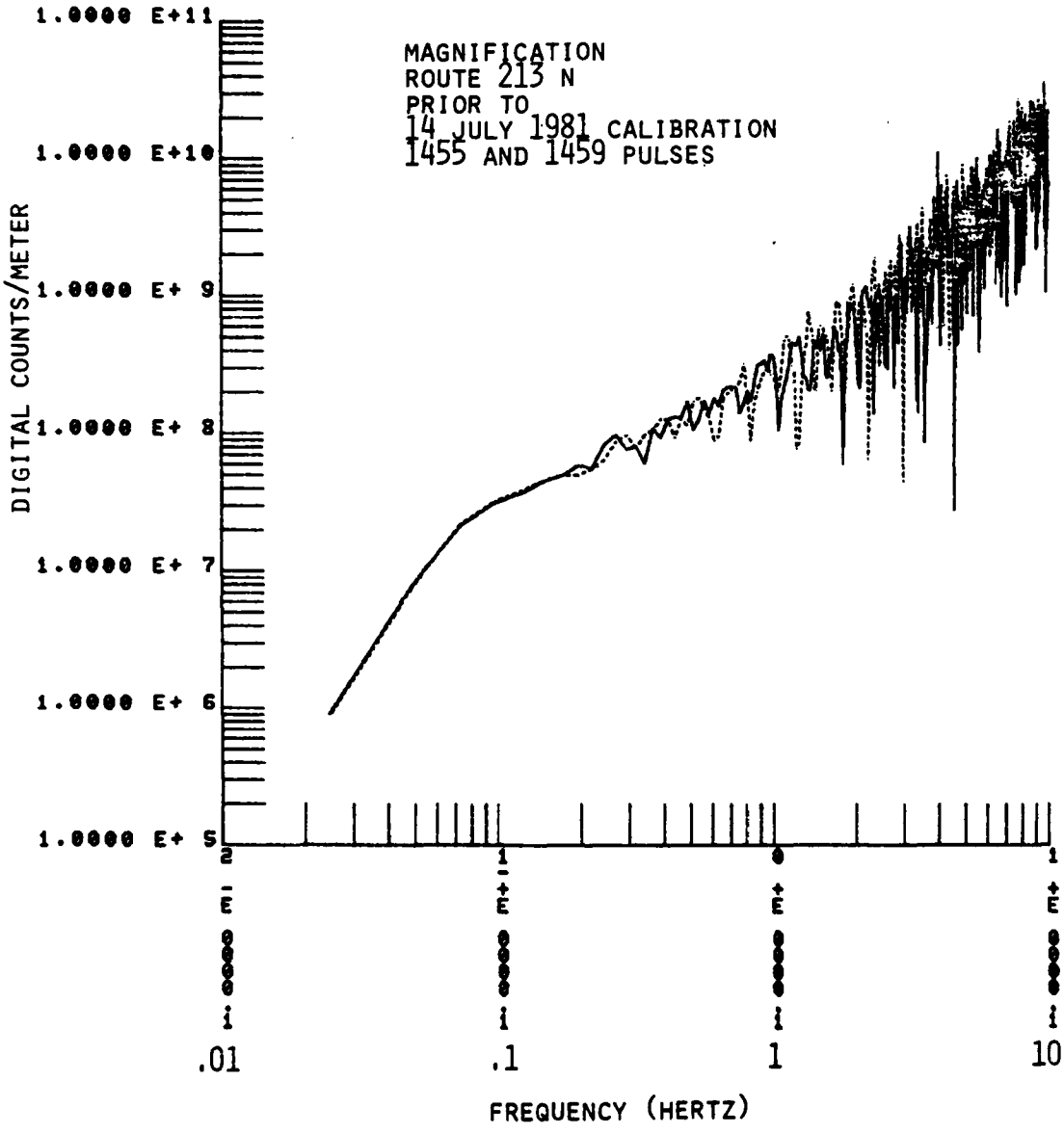

Figure 4-53. Magnification curves - 213 N - results from two pulses superimposed.

Unclassified

SECURITY CLASSIFICATION OF THIS PAGE (When Data Entered)

REPORT DOCUMENTATION PAGE

READ INSTRUCTIONS BEFORE COMPLETING FORM

1. REPORT NUMBER: 2	2. GOVT ACCESSION NO.
3. RECIPIENT'S CATALOG NUMBER	
4. TITLE (and Subtitle): The Use of Intermediate and Long Period Seismic Waves for Discrimination and Yield Determination	5. TYPE OF REPORT & PERIOD COVERED: Annual Technical 1 Oct. 1980-30 Sept. 1981
	6. PERFORMING ORG. REPORT NUMBER: 05-80-01
7. AUTHOR(s): Dr. Paul W. Pomeroy	8. CONTRACT OR GRANT NUMBER(s): F49620-80-C-0021
9. PERFORMING ORGANIZATION NAME AND ADDRESS: Rondout Associates, Incorporated, P.O. Box 224, Stone Ridge, New York 12484	10. PROGRAM ELEMENT, PROJECT, TASK AREA & WORK UNIT NUMBERS: Element 61101 E, Code 0D60, ARPA Order 3291-32
11. CONTROLLING OFFICE NAME AND ADDRESS: Air Force Office of Scientific Research, Building 410, Bolling Air Force Base, D.C. 20332	12. REPORT DATE: 1 November 1981
	13. NUMBER OF PAGES
14. MONITORING AGENCY NAME & ADDRESS (if different from Controlling Office): DCASMA, Bridgeport, 550 South Main Street, Stratford, CT 06497	15. SECURITY CLASS. (of this report): Unclassified
	15a. DECLASSIFICATION/DOWNGRADING SCHEDULE

16. DISTRIBUTION STATEMENT (of this Report)

Approved for public release; distribution unlimited.

17. DISTRIBUTION STATEMENT (of the abstract entered in Block 20, if different from Report)

N.A.

18. SUPPLEMENTARY NOTES

N.A.

19. KEY WORDS (Continue on reverse side if necessary and identify by block number)

Lg waves	HARZER
Catskill Seismic Array	seismic noise characteristics
yield determination	array calibration

20. ABSTRACT (Continue on reverse side if necessary and identify by block number)

This report, which is presented in four parts, deals with the following subjects:

1. The use of Lg to determine yield for U.S. explosions as recorded by WWSSN stations in the United States.

2. Analyses of seismic data from the HARZER nuclear explosion as recorded at the Catskill Seismic Array (CSA) in Stone Ridge, New York.

DD FORM 1 JAN 73 1473

Unclassified

SECURITY CLASSIFICATION OF THIS PAGE (When Data Entered)

3. Seismic noise characteristics at the Catskill Seismic Array and

4. The calibration and response of the Catskill Seismic Array.